RI 8360

Bureau of Mines Report of Investigations/1979

The Flammability of Coal Dust-Air Mixtures

Lean Limits, Flame Temperatures, Ignition Energies, and Particle Size Effects

UNITED STATES DEPARTMENT OF THE INTERIOR

50272-101

REPORT DOCUMENTATION PAGE	1. REPORT NO. BuMines RI 8360	2.	3. Recipient's Accession No. PB299521

4. Title and Subtitle	5. Report Date
The Flammability of Coal Dust-Air Mixtures. Lean Limits, Flame Temperatures, Ignition Energies, and Particle Size Effects	1979
	6.
7. Author(s) Martin Hertzberg, Kenneth L. Cashdollar, and John J. Opferman	8. Performing Organization Rept. No.
9. Performing Organization Name and Address Pittsburgh Mining and Safety Research Center Bureau of Mines, USDI 4800 Forbes Avenue Pittsburgh, PA 15213	10. Project/Task/Work Unit No. 11. Contract(C) or Grant(G) No. (C) (G)
12. Sponsoring Organization Name and Address Bureau of Mines, USDI 2401 E Street, NW Washington, D.C. 20241	13. Type of Report & Period Covered Report of Investigations 14.

15. Supplementary Notes

16. Abstract (Limit: 200 words)

A comprehensive study of the flammability behavior of air-dispersed coal dust was made using an 8-liter Bureau of Mines system which included the following: (1) An optical probe to continuously monitor the dust concentration; (2) measurements of ignition energy requirements; (3) the use of several narrow size distributions ranging from 3 to 65 μm average diameter; (4) measurements of the extent of flame propagation based on pressure attained at constant volume, residual O_2 content after combustion, and flame and dust surface temperatures. The measured lean limit for near-horizontal propagation of Pittsburgh coal dust was about 135 mg/l (milligrams per liter), virtually independent of particle size. Required ignition energies were hundreds of joules and measured limit flame tempera-

17. Document Analysis a. Descriptors

b. Identifiers/Open-Ended Terms

c. COSATI Field/Group

18. Availability Statement	19. Security Class (This Report)	21.
Release unlimited by NTIS.	20. Security Class (This Page)	22. Price PC A05 MF A01

(See ANSI–Z39.18) See Instructions on Reverse OPTIONAL FORM 272 (4–77) (Formerly NTIS–35) Department of Commerce

Report of Investigations 8360

The Flammability of Coal Dust-Air Mixtures

Lean Limits, Flame Temperatures, Ignition Energies, and Particle Size Effects

By Martin Hertzberg, Kenneth L. Cashdollar,
and John J. Opferman

UNITED STATES DEPARTMENT OF THE INTERIOR
Cecil D. Andrus, Secretary

BUREAU OF MINES
Lindsay D. Norman, Acting Director

This publication has been cataloged as follows:

Hertzberg, Martin

The flammability of coal dust-air mixtures: lean limits, flame temperatures, ignition energies, and particle size effects / by Martin Hertzberg, Kenneth L. Cashdollar, and John J. Opferman. [Washington] : U.S. Dept. of the Interior, Bureau of Mines, 1979.

70 p. : ill., diagrs., maps ; 27 cm. (Report of investigations - Bureau of Mines ; 8360)

Bibliography: p. 67-70.

1. Dust explosion. 2. Mine dusts. 3. Fire-testing. 4. Coal mines and mining - Dust control. I. Cashdollar, Kenneth L., joint author. II. Opferman, John J., joint author. III. United States. Bureau of Mines. IV. Title. V. Series: United States. Bureau of Mines. Report of investigations - Bureau of Mines ; 8360.

TN23.U7 no. 8360 622.06173

U.S. Dept. of the Int. Library

CONTENTS

Page

Abstract.......... 1
Acknowledgments.......... 1
Introduction.......... 2
Apparatus and experimental method.......... 4
Flammability data.......... 17
    Ignition energy requirements.......... 17
    Lean-limit measurements.......... 22
    Dispersion-agglomeration effects: Lean-limit opacities.......... 31
    Pressure development.......... 33
    Correlation of peak pressure ratios with residual oxygen contents.. 36
    Flame temperatures.......... 37
    Inerting requirements.......... 42
    Sampling data and photomicrographs.......... 44
    High-speed motion pictures.......... 45
Discussion and interpretation.......... 51
Conclusions and recommendations.......... 64
References.......... 67

ILLUSTRATIONS

1. Modified Hartmann chamber used to study the flammability behavior of air-dispersed dusts.......... 5
2. Vertical cross section of the modified Hartmann 8-liter flammability chamber.......... 5
3. Dispersion of Purple K dust in the 8-liter vessel measured with the optical dust probe at a height of 18.5 cm.......... 8
4. Dispersion of Pocahontas seam coal dust in the 8-liter vessel measured with optical dust probes at two different heights, H.......... 9
5. Dispersion of Pittsburgh seam coal dust in the 8-liter vessel measured with optical dust probes at three heights, H.......... 9
6. Functional block diagram of experimental procedure and measurements 11
7. Flammability chamber and instrumentation console.......... 12
8. Actual recorder traces of absolute pressure and optical dust probe transmission for four runs with different concentrations of 6.6-μm Pittsburgh coal dust.......... 13
9. Six-channel infrared pyrometer used to measure temperatures of dust explosions.......... 15
10. Circuit diagram for two channels of the six-channel, infrared pyrometer.......... 17
11. Effect of ignition energy for 6.6-μm Pittsburgh coal dust; pressure ratio versus concentration.......... 18
12. Apparent lean limit of flammability for 6.6-μm Pittsburgh coal dust as a function of ignition energy.......... 19
13. Flammability data for a narrow size distribution of Pittsburgh coal dust with $\bar{d}_s$ = 2.7 μm.......... 24
14. Dust probe transmission measurements (at ignition) as a function of nominal dust concentration for 2.7-μm Pittsburgh coal.......... 24

ILLUSTRATIONS--Continued

Page

15. Flammability data for a narrow size distribution of Pittsburgh coal dust with $\bar{d}_s$ = 3.2 µm.. 25
16. Dust probe transmission measurements (at ignition) as a function of nominal dust concentration for 3.2-µm Pittsburgh coal............ 25
17. Flammability data for a narrow size distribution of Pittsburgh coal dust with $\bar{d}_s$ = 6.6 µm.. 26
18. Dust probe transmission measurements (at ignition) as a function of nominal dust concentration for 6.6-µm Pittsburgh coal............ 26
19. Flammability data for a narrow size distribution of Pittsburgh coal dust with $\bar{d}_s$ = 15 µm.. 27
20. Dust probe transmission measurements (at ignition) as a function of nominal dust concentration for 15-µm Pittsburgh coal............ 27
21. Flammability data for a broad size distribution of Pittsburgh coal dust with $\bar{d}_s$ = 21 µm.. 27
22. Dust probe transmission measurements (at ignition) as a function of nominal dust concentration for 21-µm Pittsburgh coal............ 27
23. Flammability data for a narrow size distribution of Pittsburgh coal dust with $\bar{d}_s$ = 22 µm.. 28
24. Dust probe transmission measurements (at ignition) as a function of nominal dust concentration for 22-µm Pittsburgh coal............ 28
25. Flammability data for a narrow size distribution of Pittsburgh coal dust with $\bar{d}_s$ = 34 µm.. 28
26. Dust probe transmission measurements (at ignition) as a function of nominal dust concentration for 34-µm Pittsburgh coal............ 28
27. Flammability data for a narrow size distribution of Pittsburgh coal dust with $\bar{d}_s$ = 51 µm.. 29
28. Dust probe transmission measurements (at ignition) as a function of nominal dust concentration for 51-µm Pittsburgh coal............ 29
29. Flammability data for a narrow size distribution of Pittsburgh coal dust with $\bar{d}_s$ = 65 µm.. 29
30. Dust probe transmission measurements (at ignition) as a function of nominal dust concentration; theoretical lines are based on $\bar{d}_s$ = 65 µm, Q = 1.5, ρ = 1.3 g/cm³, and two agglomeration factors α.. 29
31. Composite curves of optical probe transmission for the nine coal dust sizes studied.. 30
32. Optical probe transmission as a function of reciprocal of particle diameter for a fixed concentration of 150 mg/l.................. 30
33. Optical probe transmission as a function of reciprocal of particle diameter for a fixed concentration of 400 mg/l.................. 32
34. Explosion pressure growth curves for eight different concentrations of Pittsburgh coal with $\bar{d}_s$ = 2.7 µm............................ 33
35. Explosion pressure growth curves for eight different concentrations of Pittsburgh coal with $\bar{d}_s$ = 22 µm............................ 33
36. Correlation between peak pressure ratio and oxygen consumption for all the coal dust sizes and concentrations studied.............. 37
37. Infrared spectrum of a 2,000 K methane-air flame at 2 atm pressure 38

ILLUSTRATIONS--Continued

Page

38. Infrared radiation from a $\overline{d}_s$ = 6.6 μm Pittsburgh coal dust explosion measured at six wavelengths by the infrared pyrometer....... 40
39. Peak gas and dust-surface explosion temperatures as a function of dust concentration for 6.6-μm coal dust, obtained with the six-channel, infrared pyrometer.................................... 40
40. Flammability data for Pittsburgh coal dust inerted to a 40 percent incombustible content with rock dust, $KHCO_3$, or NaCl............ 42
41. Flammability data for Pittsburgh coal dust inerted to a 50 or 60 percent incombustible content with rock dust, $KHCO_3$, or NaCl...... 42
42. Scanning electron microscope photographs of unburned and burned Pittsburgh coal dust.. 46
43. Frames from a high-speed motion picture of a coal dust explosion at a dust concentration of 150 mg/l in the 8-liter flammability chamber.. 47
44. Frames from a high-speed motion picture of a coal dust explosion at a dust concentration of 300 mg/l in the 8-liter flammability chamber.. 50

TABLES

1. Size distributions of coal used for lean flammability limit studies 23
2. Summary of lean-limit measurements.................................. 23
3. Pressure development, residual O_2, and calculated burning velocities for Pittsburgh coal dust with $\overline{d}_s$ = 2.7 μm....................... 34
4. Pressure development, residual O_2, and calculated burning velocities for Pittsburgh coal dust with $\overline{d}_s$ = 22 μm........................ 34
5. Effect of ignition energy and match head configuration on pressure development at a fixed concentration of 150 mg/l................. 35
6. Effect of ignition energy on the pressure development at a fixed concentration of 175 mg/l... 36
7. Lean-limit coal dust concentrations for three inerting agents...... 43
8. Proximate and ultimate analyses of post-explosion dust-residues compared with the original coal.................................. 44
9. Evaluation of previous lean-limit measurements..................... 51

THE FLAMMABILITY OF COAL DUST-AIR MIXTURES

Lean Limits, Flame Temperatures, Ignition Energies, and Particle Size Effects

by

Martin Hertzberg,[1] Kenneth L. Cashdollar,[2] and John J. Opferman[3]

ABSTRACT

A comprehensive study of the flammability behavior of air-dispersed coal dust was made using an 8-liter Bureau of Mines system which included the following: (1) An optical probe to continuously monitor the dust concentration; (2) measurements of ignition energy requirements; (3) the use of several narrow size distributions ranging from 3 to 65 µm in average diameter; (4) measurements of the extent of flame propagation based on pressure attained at constant volume, residual O_2 content after combustion, and flame and dust surface temperatures.

The measured lean limit for near-horizontal propagation of Pittsburgh coal dust was about 135 mg/l (milligrams per liter), virtually independent of particle size. Required ignition energies were hundreds of joules and measured limit flame temperatures were 1,450 to 1,600° K. Data on inerting requirements with $KHCO_3$, rock dust, and NaCl gave approximately the same results as full-scale explosion tests. The good agreement suggests that the cause of earlier discrepancies between small-scale laboratory data and full-scale mine experiments may not have been the difference in size, but were rather a problem of proper care in isolating and controlling the significant experimental variables and in consistently defining the extent of flame propagation at the limits.

ACKNOWLEDGMENTS

The authors wish to acknowledge the important contributions of I. Liebman and R. S. Conti that were made during the early studies of dust dispersion effectiveness and that led to the redesign of the 8-liter apparatus; and to acknowledge R. B. Lieber, T. Weldon, and other personnel (all of the Pittsburgh Mining and Safety Research Center) for their valuable contributions in the collection and analysis of the data.

[1] Supervisory research chemist.
[2] Physicist.
[3] Electronics technician.
All authors are with the Pittsburgh Mining and Safety Research Center, Bureau of Mines, Pittsburgh, Pa.

INTRODUCTION

An accurate knowledge of the flammability behavior of substances is essential for a realistic appraisal of the fire and explosion hazards involved in their use. This concern has motivated numerous experimental and theoretical studies of the flammability limits of natural substances or manufactured chemicals. These chemical substances are of practical importance to mining and manufacturing, in trade and transportation, to defense and space exploration, in habitats, and in powerplants. The results of such studies have been collected, reviewed, and summarized in a series of Bureau of Mines Bulletins (8, 40).[4] The substances considered in those Bulletins were homogeneous mixtures of gases, and for such mixtures our state of knowledge is reasonably satisfactory. The data are sufficiently accurate and reproducible to generate a consensus among scientists concerning their validity. There remain some subtle differences that relate to the direction of flame propagation, the criteria to be chosen for defining the limit conditions, and the actual cause of the existence of such limits (6, 19). However, few would quarrel with the overwhelming weight of experimental data for those substances that have been studied in detail. For example, for methane in air, the lean limit for upward flame propagation is 5.0 percent methane at standard conditions, and that value serves as a basis for internationally accepted regulations for the mining industry (38).

By contrast, for heterogeneous mixtures of dusts dispersed in air, there appears to be no such consensus. The data are often quite different from one apparatus to another. Even within a given apparatus, there can be a lack of reproducibility from day to day or from one run to the next. For example, there is currently no accepted value for the lean-limit concentration for air-dispersed Pittsburgh pulverized coal dust (or coal of similar rank). Values quoted in the early literature are as low as 5 mg/l (15), whereas some recent data suggest values as high as 300 mg/l (27). Intermediate values that have been reported are: 30 to 50 (34), 35 (15), 40 (24), 50 to 60 (10, 17, 30), 50 (16), 50 to 60 (9), 55 (17), 60 (32), 60 to 100 (3-4), 50 to 150 (18), 85 to 125 (39), 100 to 140 (36-37), 140 to 180 (2), and 240 to 310 mg/l (27). Clearly, there appears to be no agreement concerning which of these is the correct value.

The main purpose of this report is to present a new and independent set of measurements for the lean-limit concentrations, including their dependence on particle size and ignition energy.

But what reason is there to believe that the uncertainties will be resolved by still another set of measurements? The differences referred to above clearly imply that there are enormous experimental difficulties in obtaining accurate and reproducible measurements. A skeptic would justifiably question whether any new data could realistically resolve the many uncertainties and contradictions; after all, any given set of measurements will necessarily differ from most of the data already reported in the literature. The

---

[4]Underlined numbers in parentheses refer to items in the list of references at the end of this report.

experimental methods and data of previous researchers need to be properly reanalyzed and reevaluated, otherwise it is unlikely that any new data will improve the chances at arriving at a valid consensus. Such a reevaluation will be attempted as part of this report.

The data reported here were obtained with an 8-liter apparatus and an improved method that insured reliability and reproducibility. The modifications in apparatus and improvements in method were as follows:

1. An optical dust concentration probe (26) was used as an integral part of the dust-dispersion chamber. The probe was used to continuously monitor the dust concentration by measuring the opacity within the explosion chamber. In many previous studies using air-dispersed dusts, the concentration was usually calculated from the total mass of dust dispersed into the total chamber volume without any detailed measurements of the spatial or temporal uniformity of the air-dispersion process. This assumption of spatial uniformity is known to be unrealistic, especially during the early stages of the dispersion process (12). Exploratory measurements were made with the optical dust probe to determine the uniformity and effectiveness of air-dispersion in the 8-liter vessel, and those measurements did confirm that the assumption of uniform and efficient dispersion could be grossly inaccurate. These exploratory measurements led to a redesign of the dispersion chamber and to an improvement in the dispersion method. Measurements with dust probes at various heights and radial positions were made to determine the time at which good spatial uniformity was obtained. The ignition source was not energized until this time was reached. In all flammability experiments to be reported here, a dust probe continuously monitored the concentration from the instant of dispersion to the instant of ignition. The spatial uniformity of the dispersion, as measured by the optical dust probes, indicated that the actual concentrations were close to the nominal concentrations.

2. The question of a realistic choice of ignition energy for limit measurements was explored in depth. While spark energies in the 100-millijoule range are adequate for homogeneous gases, it was generally agreed that such energies are far too low for heterogeneous dusts. The present studies indicate that required energies are in the range of hundreds of joules, far higher than the values generally anticipated or used in most previous laboratory-scale studies.

3. Careful control was maintained on the particle size distributions of the dust used. Narrow size distributions of centrifugally classified fines or sieve-classified coarse dusts were used, and the results were compared with data obtained from a very broad distribution. Nine size distributions were studied, from centrifugally classified fines with an average particle diameter of 2.7 μm, to sieve-classified coarse dust of particle diameter of 65 μm.

4. The "quality" or extent of flame propagation was carefully monitored. In the data previously cited, there were substantial differences in the way various researchers defined the limit criteria. For this report, limit criteria were defined in terms of (1) the pressure attained in the constant-volume explosion chamber and its time-dependence, and (2) the residual oxygen concentration after flame propagation was completed. Two additional criteria studied were (1) the temperature of the gas flame and the dust particles, and (2) the shape and continuity of the combustion wave as recorded by high-speed motion pictures. Generally, these criteria correlated well with one another.

These improvements will be described in more detail in the various sections of this report. In sum, however, they provided for a careful control of the significant experimental variables and thus allowed for a fuller appreciation of their significance.

APPARATUS AND EXPERIMENTAL METHOD

The flammability chamber is a somewhat larger version (7.8 liters) of the originally designed Hartmann apparatus (10, 12), which is commonly used for dust explosibility studies and has gained general acceptance (31). A photograph of the chamber is shown in figure 1 and a sketch of the chamber and the air-dispersion tank is shown in figure 2. The vessel had previously been used for various dust- and gas-explosion studies (21, 30); however, after preliminary tests with the optical probe it was found necessary to modify the interior shape to improve the effectiveness of dust dispersion.

The procedure for dispersing dust was to first uniformly spread a known mass of dust around the dispersion cone in the dust cup at the bottom of the chamber. Pressurized air from the reserve-air tank was then ejected radially from the disperser cone to lift the dust. In previous studies with this type of apparatus, results were reported in terms of the nominal concentration--the total mass of dust divided by the chamber volume. However, it was generally realized that the dispersion was probably not uniform (10, 12). In these earlier studies of minimum explosive concentration, a continuous ignition source was continuously activated during the dust dispersion process.

In the present studies, optical dust probes and high-speed movies were used to measure the uniformity of the dust cloud and the effectiveness of dispersion. The optical dust probe (consisting of a light-emitting diode and a silicon photodetector) measures the transmission of light through a 3.8-cm-long path in the dust cloud (26). The probe windows were kept free of dust with narrow jets of air whose total flow was small compared with the total flow of air in the dispersion pulse. Window transmissions were maintained at more than 95 percent even for the heaviest dust loadings. The probe volume of 33 cm^3 occupies only 0.4 percent of the chamber volume. Preliminary measurements with one or two probes at several heights and radial positions were used to redesign the chamber geometry so that it contained a streamlining insert. The original interior wall shape was cylindrical, 19.5 cm interior diameter, and 33.5 cm high, with a dispersion cup in the bottom plate. The redesign consisted of an inverted cone-shaped insert (the cross-hatched area in fig. 2) which was added to the bottom half of the chamber to provide a smooth contour

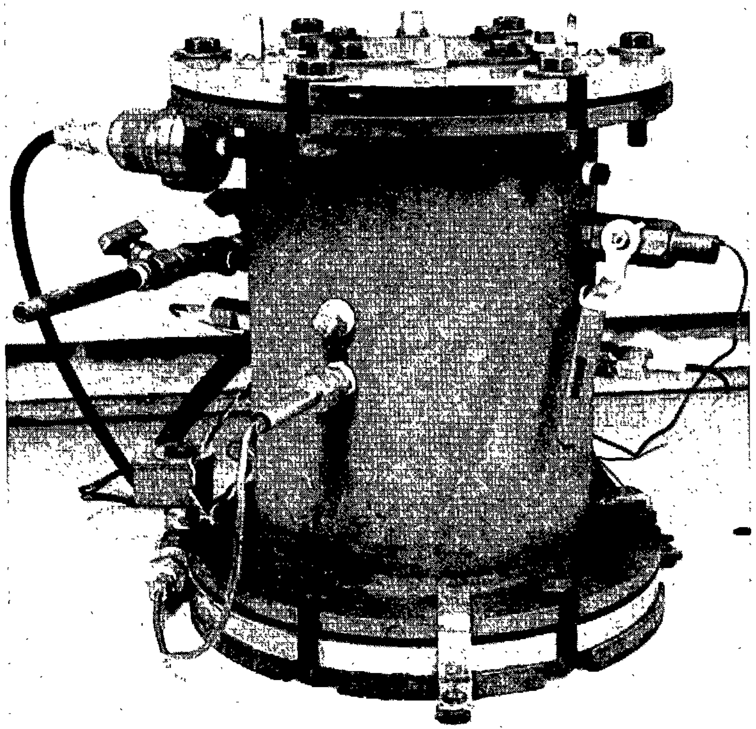

FIGURE 1. - Modified Hartmann chamber used to study the flammability behavior of air-dispersed dusts.

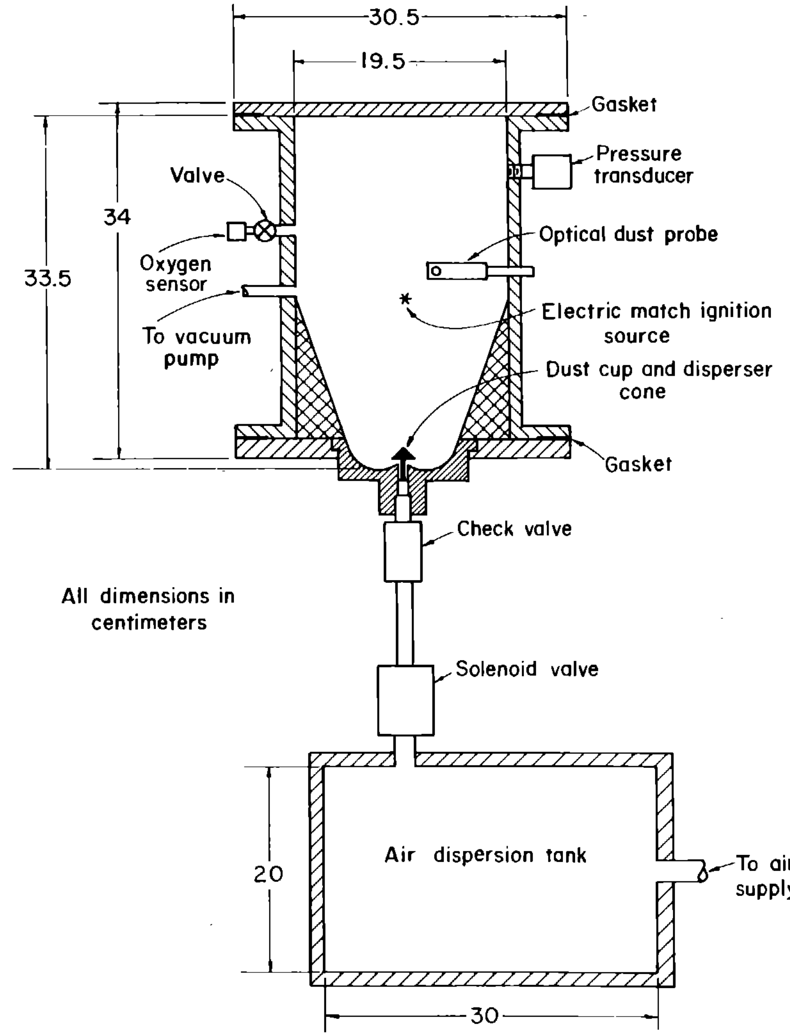

FIGURE 2. - Vertical cross section of the modified Hartmann 8-liter flammability chamber.

from the dispersion cup to the side walls. This eliminated the ledge in the bottom plate and the dead-air space in the peripheral regions above it. Dust was previously observed to settle and accumulate on the ledge and thus impeded effective dispersion. This insert reduced the chamber volume from 9.3 liters to 7.8 liters, but significantly improved the effectiveness and reproducibility of the dust dispersion. With the improved chamber geometry the dust dispersion uniformity was studied as a function of time. During the dispersion air pulse, the optical probes showed a somewhat higher dust concentration in the upper half of the chamber due to the continuous dilution of dust in the bottom of the chamber by inflowing air. Shortly after the end of the dispersion pulse, however, the cloud becomes fairly uniform at the several heights studied. Radial uniformity of the dust cloud was also seen in high-speed motion pictures as the dust dispersion was observed from the top of the chamber through a 2.5-cm-thick plastic cover plate. With this redesigned chamber, the opacity data showed that spatial uniformity in concentration was within about 15 percent once the dispersion transient was over. This 15-percent value also characterized the repeatability of the dust dispersion from run to run. This spatial uniformity and repeatability of the dust dispersions justified the use of the nominal concentration values for the flammability data of this report.

During most of the flammability tests a single probe was used and located at a height of 18.5 cm above the cup, 3 cm from the chamber axis. The ignition source was located along the axis at a height of 17 cm. The dust dispersion method selected for these flammability studies was to first partially evacuate the chamber to about 0.2 to 0.3 atm. The dust was dispersed with pressurized air from the tank reservoir at 6 atm (atmospheres), with a 0.2-sec pulse duration. The chamber pressure reached about 1 atm by the end of the pulse; hence, the mass of air in the dispersion pulse was a factor of 3 to 5 larger than the initial mass in the chamber.

The opacity readings became fairly constant by about 0.1 sec after the end of the dispersion pulse, and remained fairly constant for at least several tenths of a second. For the flammability studies, the ignition source was activated at 0.1 sec after the end of the dispersion pulse, and the transmission reading at that time was used to characterize the dust concentration. For each type and size of dust studied, a Coulter-Counter[5] size analysis was obtained and a mean particle size was calculated from the Coulter size distribution. The mean diameter used to characterize the dusts was the surface-area weighted ($\bar{d}_s$) or volume-to-surface mean diameter ($\bar{d}_{32}$), which is defined as

$$\bar{d}_s = d_{32} = \frac{\Sigma d^3 N(d)\Delta d}{\Sigma d^2 N(d)\Delta d}, \tag{1}$$

where N(d) is the number of particles per size interval Δd, and d is the diameter in each size interval. Now the measured transmission of the dust probe can be used to infer an effective particle size for conditions where dispersion is sufficiently uniform that the actual dust concentration can be

[5]Reference to trade names or manufacturers is made for identification only and does not imply endorsement by the Bureau of Mines.

considered equal to the nominal concentration. The Bouguer-Beer-Lambert law for the transmission of light through a homogeneously dispersed mixture of uniform spherical particles is

$$T = \frac{I}{I_0} = \exp\ (-QAn\ell) = \exp\left(-\frac{3}{2}\ \frac{QC_m\ell}{\rho d}\right), \tag{2}$$

where T is the light transmission or the ratio of transmitted intensity I to incident intensity I_0, Q is a dimensionless extinction coefficient, A is the cross sectional area of each spherical particle of diameter d, ℓ is the path length, n is the number density of particles, C_m is the mass concentration of dust, and ρ is the density of the solid particle.

For particle clouds in which all particles do not have identical diameters, d is replaced by the surface-area-weighted mean diameter $\bar{d}_s$. Similarly, Q is replaced by $\bar{Q}$ which is defined as

$$\bar{Q} = \frac{\Sigma Q(d)d^2N(d)\Delta d}{\Sigma d^2N(d)\Delta d}\ . \tag{3}$$

The extinction coefficient Q includes loss of light due to both absorption and scattering. Theoretical values of Q were calculated from Mie theory based on the wavelength of light of the dust probe (λ = 0.95 μm), the complex refractive index of coal (1.8-0.1i), and various size distributions of the dust. These calculations showed that Q decreased monotonically from a value of 2.5 at $\bar{d}_s$ = 3 μm, to a value of 2.3 at $\bar{d}_s$ = 10 μm, to a value of 2.1 at 20 μm for dust distributions similar to those studied in this report. For $\bar{d}_s \gg \lambda$, Q asymptotically approaches 2.0. However, these calculations are for the ideal, perfectly collimated case such as a laser light source and a far field detector which does not collect any of the scattered light. If all of the scattered light reached the detector and only the light absorbed by the particles would be lost from the beam, then the coefficient Q would be half the above values, approaching a value of 1.0 for $d \gg \lambda$. However, the optical dust probe used in this report collects part of the scattered light and therefore has an effective value of the coefficient Q that is intermediate between these extremes. Based upon several independent studies of the probe's characteristics in comparison with a laser light source and a far field detector with a narrow half-angle view field of 0.3°, the effective extinction coefficient for the probe was determined to be Q_{eff} = 1.5 ± 0.1. Substituting this value into equation 2, setting ℓ = 3.8 cm and ρ = 1.34 g/cm³, for Pittsburgh coal gives

$$\%T = 100\ \exp\left[-6.4\times 10^{-2}\ \frac{C_m\ (mg/1)}{\bar{d}_s\ (\mu m)}\right], \tag{4}$$

where %T is now the percent transmission. The effective diameter measured by the probe was generally observed to be at least equal to or larger than the Coulter diameter. It was significantly larger if the particle tended to agglomerate. Thus,

$$\bar{d}_s\ (\text{effective}) = \alpha\bar{d}_s\ (\text{Coulter}), \tag{5}$$

where α is an agglomeration factor ($\alpha \geq 1$).

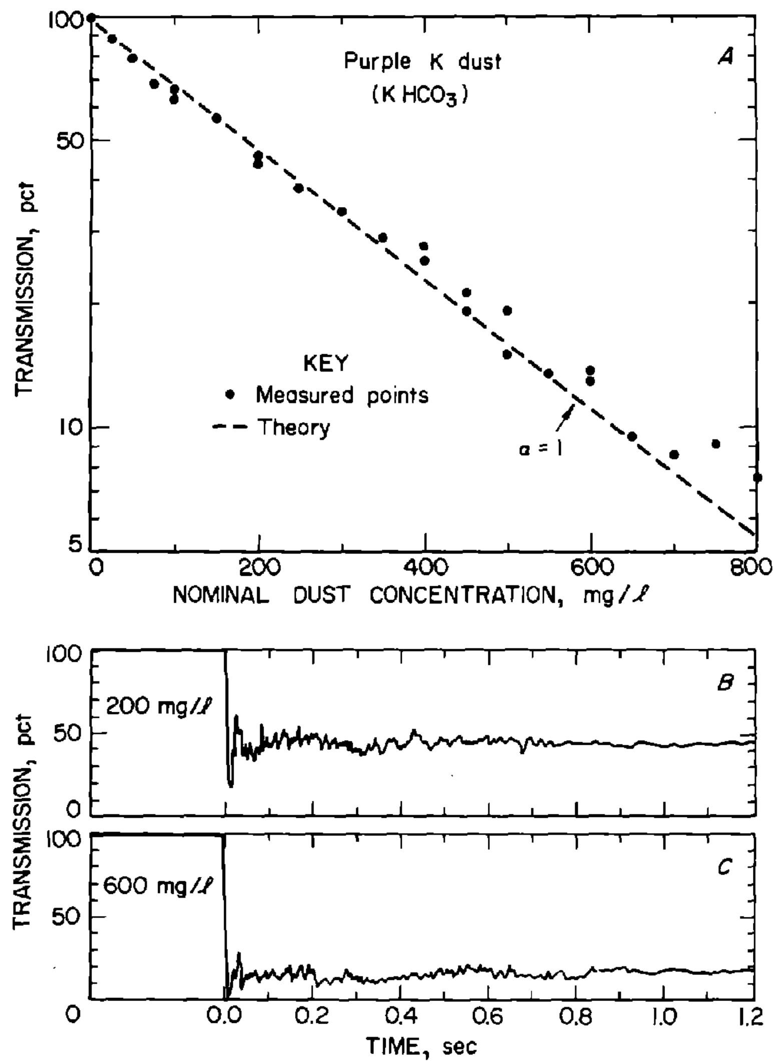

FIGURE 3. - Dispersion of Purple K dust in the 8-liter vessel measured with the optical dust probe at a height of 18.5 cm. *A*, Probe transmission versus concentration with theoretical line for $\bar{d}_s$ = 10.8 μm, Q = 1.5, ρ = 2.17 g/cm^3, and α = 1; *B-C*, actual probe transmission traces for two concentrations.

Some typical variations in this agglomeration factor are illustrated in figures 3-5. The optical probe transmission data are plotted as a function of the nominal dust concentration for three types of dust: Purple K (free-flowing $KHCO_3$), Pocahontas seam coal dust, and Pittsburgh seam coal dust. The transmission data points shown were those measured at 0.1 sec after the end of the 0.2-sec dispersion pulse, at which time the dust was uniformly dispersed in space. However, the microscopic effectiveness of dispersion, as measured by the agglomeration factor α, is clearly different for the three types of dust. The dashed lines show the predicted transmission values, based on equation 2, for various agglomeration factors. Figure 3A shows that free-flowing $KHCO_3$ displays the same effective diameter when dispersed in air as when it is dispersed for its Coulter analysis in isopropyl alcohol. Thus, for Purple K, which is specially treated to be free-flowing, the data show virtually perfect dispersion at concentrations as high as 800 mg/l. There appears to be little or no agglomeration (α = 1), although a careful inspection of the data points shows some slight upward curvature in the semilog plot. The slight upward curvature is indicative of the tendency to agglomerate at high dust loading.

Also shown in figure 3 are the actual recorder traces for the dust probe at two different concentrations. These traces indicate that a steady-state concentration is attained by the end of the 0.2-sec dispersion pulse, and this steady-state condition lasts for at least 1 sec. Zero time on the scales coincides with the beginning of the dispersion pulse.

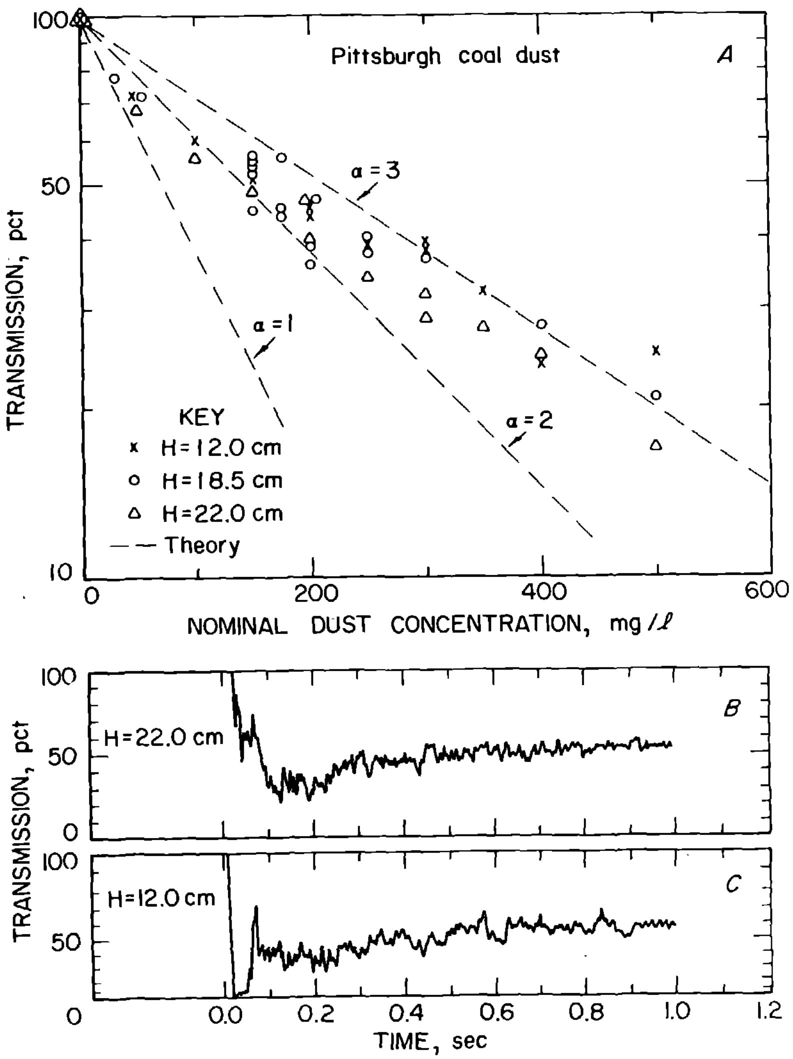

FIGURE 5. - Dispersion of Pittsburgh seam coal dust in the 8-liter vessel measured with optical dust probes at three heights, H. *A*, Transmission versus concentration with theoretical lines for $\bar{d}_s$ = 6.6 μm, Q = 1.5, ρ = 1.34 g/cm³; and three agglomeration factors, *α*; *B-C*, simultaneous probe transmission traces at two heights for a concentration of 200 mg/l.

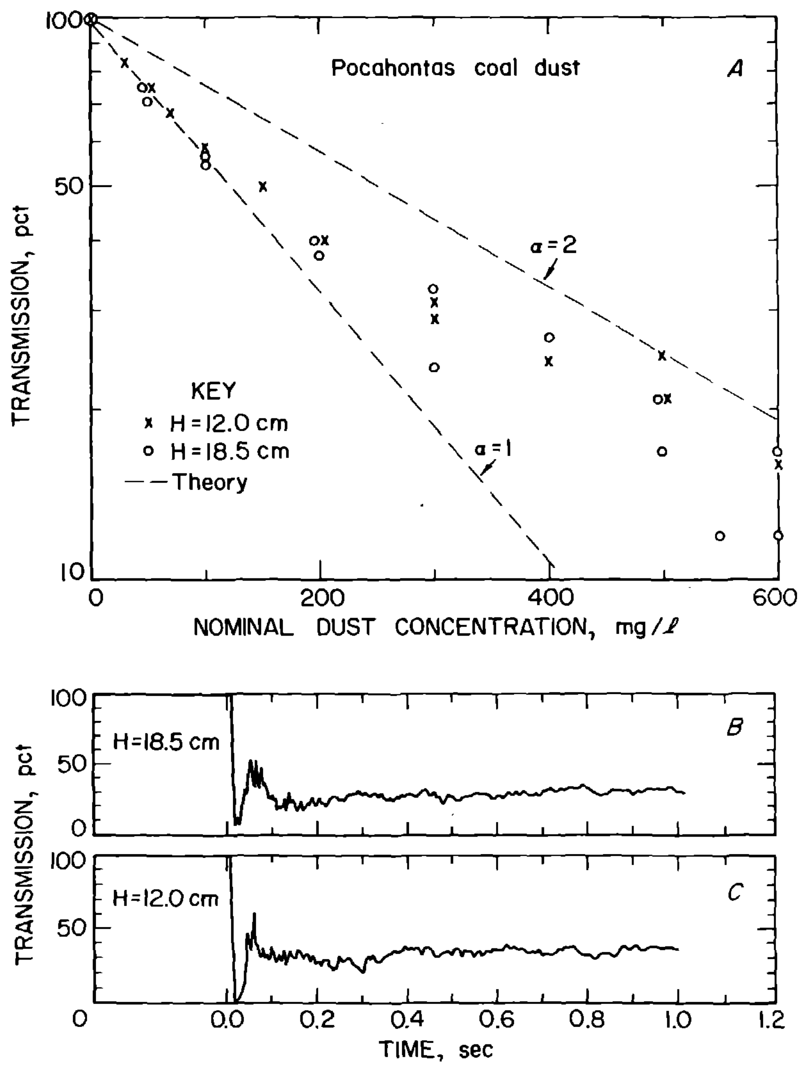

FIGURE 4. - Dispersion of *Pocahontas* seam coal dust in the 8-liter vessel measured with optical dust probes at two different heights, H. *A*, Probe transmission versus concentration with theoretical lines for $\bar{d}_s$ = 11.7 μm, Q = 1.5, ρ = 1.32 g/cm³, and two agglomeration factors, *α*; *B-C*, actual probe transmission traces at two heights for a concentration of 300 mg/l.

The data shown in figure 4 is for a Pocahontas seam coal with $\overline{d}_s$ (Coulter) = 11.7 μm. The data points that are shown are for two probes that measured the opacity at heights of 12 and 18.5 cm above the dispersion cup. These distances correspond approximately to 1/3 and 2/3 of the way up the chamber axis toward the top plate. The lack of any systematic difference in the opacity readings is indicative of the spatial homogeneity of the dust dispersion. The comparison of the data with the theory indicates little agglomeration of the Pocahontas coal at concentrations of 200 mg/l and below, but significant agglomeration to about α = 1.7 at concentrations of 600 mg/l. This trend, which was barely discernible for the Purple K, is now quite significant for coal. Also shown in figure 4 are the recorder traces for the dust probes viewing the dispersion at the two different heights. Note that the lower probe becomes essentially opaque at 0.02 sec while the upper probe shows a minimum transmission of 10 percent during this dispersion transient. This suggests that the dust is initially lifted en masse, and passes through the central regions as a very dense cloud before it begins to disperse uniformly throughout the chamber. The final steady-state transmissions, after the initial dispersion transient is over, are the same at the two heights, however. At concentrations as low as 200 mg/l, the final opacities at both heights are virtually identical to those predicted by equation 2.

The data shown in figure 5 is for Pittsburgh seam coal with $\overline{d}_s$ (Coulter) = 6.6 μm. The data points shown are for measurements at three heights near the axis of the chamber. These heights are roughly 1/3, 1/2, and 2/3 of the way from the bottom to the top. Clearly, the final steady-state opacities were independent of height, indicating good spatial homogeneity. The data points are again compared with theoretical dashed lines from equation 2, and the comparison now indicates a much larger degree of agglomeration, with the higher concentrations approaching α = 3. The larger degree of agglomeration in this case is partly attributable to the fact that the particle size is smaller than the previous case, and partly caused by the intrinsic nature of Pittsburgh seam coal to agglomerate more than Pocahontas seam coal. Also shown in figure 5 are the simultaneous probe traces at the lowest and uppermost heights. Note again, the zero transmission in the lower probe at 0.02 to 0.03 sec after the onset of the air-dispersion pulse. This is characteristic of the dust being lifted en masse during the early stage. Note, however, that this dense cloud is significantly diluted to near its steady-state concentration when its presence is detected at the uppermost probe at 0.13 sec after the onset of the air-pulse.

A functional block diagram of the overall experimental time-sequence is shown in figure 6. The figure is self-explanatory and indicates which measurements were normal or routine and which were added for various purposes. The figure also shows when the various measurements were made or recorded during the main time sequence of a given experiment.

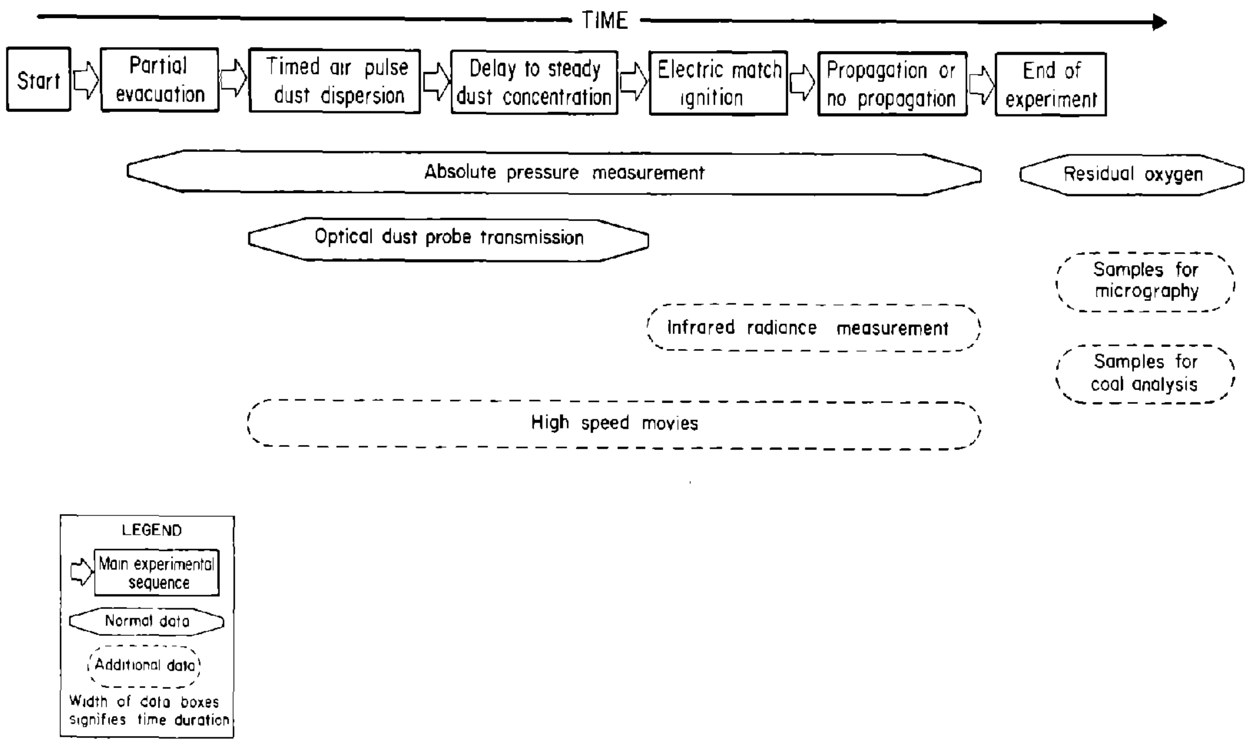

FIGURE 6. - Functional block diagram of experimental procedure and measurements.

The entire apparatus, including the instrumentation console, is shown in figure 7. The instrumentation rack contains the recording apparatus and the control and timing circuits. Pressures were measured with a Viatran Model 218 pressure transducer. The listed speed of response of the pressure sensor is 1 msec (millisecond) for 90 percent of the full-scale reading. The data was recorded with a Brush Model 260 strip chart recorder whose measured response speed was 20 msec for 90 percent of full-scale response. These response times were adequate for the time scale of the events that were recorded.

The data traces for a typical series of experimental runs are displayed in figure 8. The pressure and dust opacity histories are shown for four different concentrations of 6.6 μm Pittsburgh coal. The processes occurring during the course of any given run are indicated in figures 8A and 8C. The explosion chamber, containing a measured amount of the coal dust, is initially evacuated to a pressure of approximately 1/3 atm. The dust dispersion pulse lasts for about 0.2 sec and raises the chamber pressure to about 1 atm. There is then a 0.1-sec delay to allow the dust to disperse more evenly throughout the chamber before the ignition source is energized. The probe transmission measurement used to characterize the concentration is taken as the value just prior to ignition. After the ignition source is activated, the resultant ignition luminosity and dust flame radiation saturate the detector of the optical probe. Transmission measurements are no longer possible since these sources of radiance are much larger than the radiance of the light-emitting diode in the optical probe.

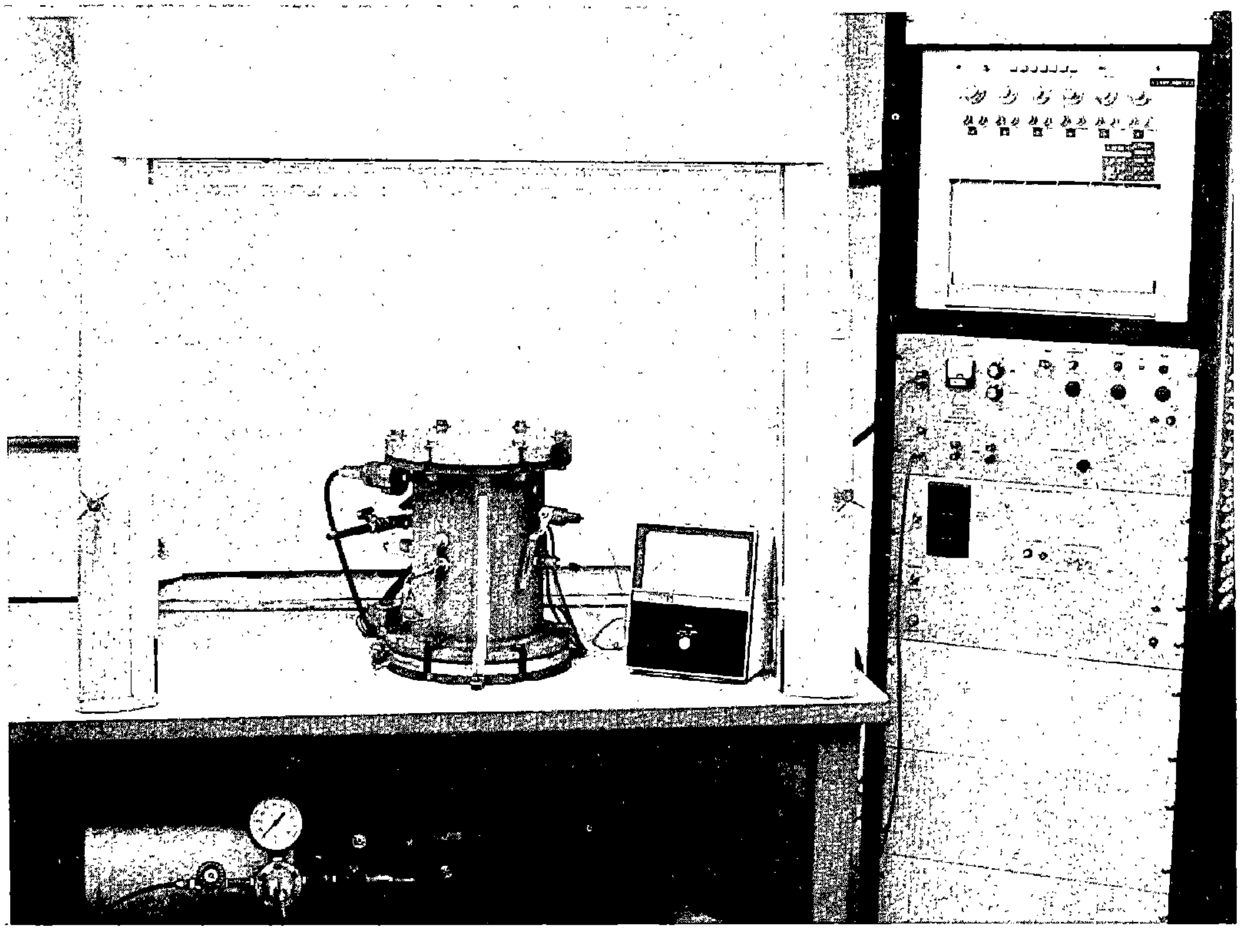

FIGURE 7. - Flammability chamber and instrumentation console.

In figure 8A, only the electric match ignitor luminosity is involved and it can be seen to decay rapidly. The probe transmission signal then recovers to the value it displayed prior to ignition. This recovery demonstrates the effectiveness and uniformity of dust dispersion and indicates that the uniformity is unaffected by the ignition source. The steady-state transmission signal of 54 percent remains constant for at least an additional second. The slight pressure rise seen in figure 8A is caused mainly by the match ignitors and hence that concentration of 100 mg/l is well below the lean limit of flammability.

In figure 8B, the nominal concentration of 125 mg/l is very close to the lean flammability limit for upward propagation. The maximum pressure (about 2 atm) is close to the value taken to be the criteria for upward flame propagation. These criteria will be discussed in more detail shortly.

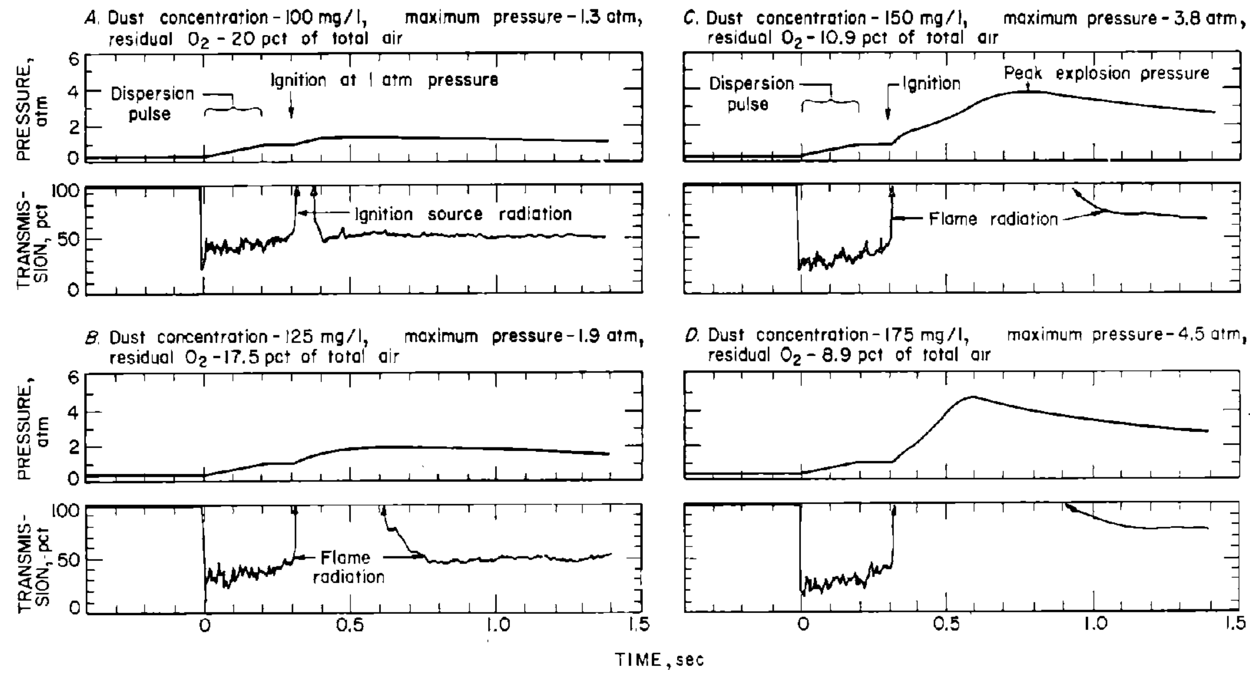

FIGURE 8. - Actual recorder traces of absolute pressure and optical dust probe transmission for four runs with different concentrations of 6.6-μm Pittsburgh coal dust.

Figures 8C-8D are cases where the dust concentrations were significantly above the lean-limit values, as can be seen from their large pressure rises. For these cases of significant and strong flame propagation through the dispersed dust, peak explosion pressures of 3.8 and 4.5 atm were attained. The output signals from the dust probe detector saturate immediately at ignition and remain saturated until combustion products cool and lose their luminosity. For cases 8C-8D, the probe signals recover to higher transmission levels than those observed prior to ignition. This is not surprising in view of the marked changes in the nature of the coal particles themselves and in the flow structure to be expected during the propagation of a combustion wave through the dust cloud.

The residual oxygen concentration for each experiment is also shown in figure 8. Residual oxygen contents were measured with an IBC Model 170 oxygen analyzer which uses a polarographic method to measure the partial pressure of O_2. The analyzer was calibrated initially with the chamber containing ambient air at atmospheric pressure (20.9 percent O_2). The sensor was then isolated from the explosion chamber during the actual flammability tests. After the explosion test was over and the product gases cooled to ambient temperatures, a ball valve connecting the chamber to the probe was opened. Data indicated that it required several minutes for mixing between the small dead-volume near the sensor and the main chamber volume containing combustion products. The intrinsic time response of the sensor is 20 sec for 95 percent of full-scale response. Hence, the sensor reading after the mixing delay was close to the final O_2 reading. A small pressure correction was then accounted by opening a valve on the opposite side of the chamber. This allowed the final probe reading to be made quickly at atmospheric pressure before any dilution by the outside air.

As seen from figure 8, the peak explosion pressure correlates well with the percentage of oxygen consumed. Their correlation, for all the data obtained in this study, will be presented in detail in the following section. For example, a measured peak pressure ratio of 2.0 corresponds on the average to the consumption of about 20 percent of the initial O_2 content of the explosion chamber. If referenced to the ignition point at H = 17 cm, the consumption of 20 percent of the mixture would correspond in the ideal case to propagation in the upward direction at a cone half-angle of about 30° from the vertical. Such a situation would correspond approximately to the conventional upward flame propagation limit, where only a fraction of the flammable mixture in the chamber is consumed. Now, for a measured peak pressure ratio of 3.0, about 40 percent of the initial O_2 content of the chamber is consumed. If referenced to the ignition point, this would correspond in the ideal case to propagation at a cone half-angle of about 50° from the vertical. Such a situation would correspond approximately to the conventional horizontal flame propagation limit where almost half of the flammable mixture would be consumed. This correspondence to upward and horizontal propagation is for the ideal premixed case where there is uniform propagation starting at the ignition source. It is realized that the real case is much more complicated and that the high-speed movies described later show patchy and streaked propagation, especially near the lean limit. Therefore, "upward" and "horizontal" are shown in quotes to denote that this correspondence is for the ideal case.

Thus, flammability limit criteria are set in terms of the peak explosion pressure ratio and this correlates well with both the fraction of mixture consumed and the predominant direction of flame propagation. The peak explosion pressure ratio, P.R., is defined as

$$\text{P.R.} = \frac{P_{max} - \Delta P\ (\text{matches})}{P_{initial}}, \tag{6}$$

where P_{max} is the maximum explosion pressure during an experiment, ΔP (matches) is the pressure rise due to the electric match ignition source by itself, and $P_{initial}$ is the pressure prior to ignition (~1 atm). Either the peak pressure ratio or the fraction of O_2 consumed are equivalent measures of the "quality" or extent of flame propagation. As will be seen subsequently, either parameter also correlates well with an independent measure of the "quality" of flame propagation: the flame or explosion temperatures calculated from the observed infrared radiance.

The gas flame and dust surface temperatures were measured with a Bureau of Mines multichannel infrared radiation pyrometer (7) which measured the dust explosion radiance simultaneously at six independent wavelengths: 1.57, 2.30, 3.46, 4.40, 4.67, and 5.19 μm. The development of this six-channel pyrometer was the outgrowth of earlier studies with a rapid scan spectrometer (21).

The radiation emitted from an object is a function of the wavelength observed, the emissivity of the object at that wavelength, and the temperature of the object. The theoretical equation describing this radiation is Planck's Law.

$$H(\lambda, \varepsilon, T) = \varepsilon \frac{2\pi hc^2}{\lambda^5} \left[\exp(hc/\lambda kT) - 1\right]^{-1}, \quad (7)$$

where H is the radiant power emitted per unit area per unit wavelength interval, ε is the emissivity, h is Planck's constant, λ is the wavelength of light observed, c is the speed of light, and k is Boltzmann's constant. Four of the wavelengths (1.57, 2.30, 3.46, and 5.19 μm) are used to characterize the Planck continuum emission from the surfaces of the hot, reacting coal dust particles in the flame or explosion. These wavelengths were chosen to avoid the discrete emission bands of product gases. The remaining two wavelengths (4.40 and 4.67 μm) were chosen to be representative of the emission band of the CO_2 product gas within the explosion fireball. This latter band has been previously used to obtain accurate flame temperature from gas explosions (20).

The relation between the measured voltage output of the pyrometer and the radiation from the flame is $H_\lambda = \frac{b_\lambda V_\lambda}{a}$, where H_λ is the radiation at each wavelength, a is a scale factor independent of wavelength, b_λ is the sensitivity factor for each wavelength, and V_λ is the measured voltage at each wavelength. The sensitivity factor, b_λ, for each channel or wavelength is determined by calibration with a Planck blackbody standard radiation source of known temperature and unit emissivity. The scale factor, a, is dependent on factors such as the fraction of the view field filled by the fireball and the attenuation caused by dust coating on the windows; but these factors are wavelength independent.

A sketch of the pyrometer and the experimental arrangement used in these studies is shown in figure 9. Calibration with the blackbody standard is done

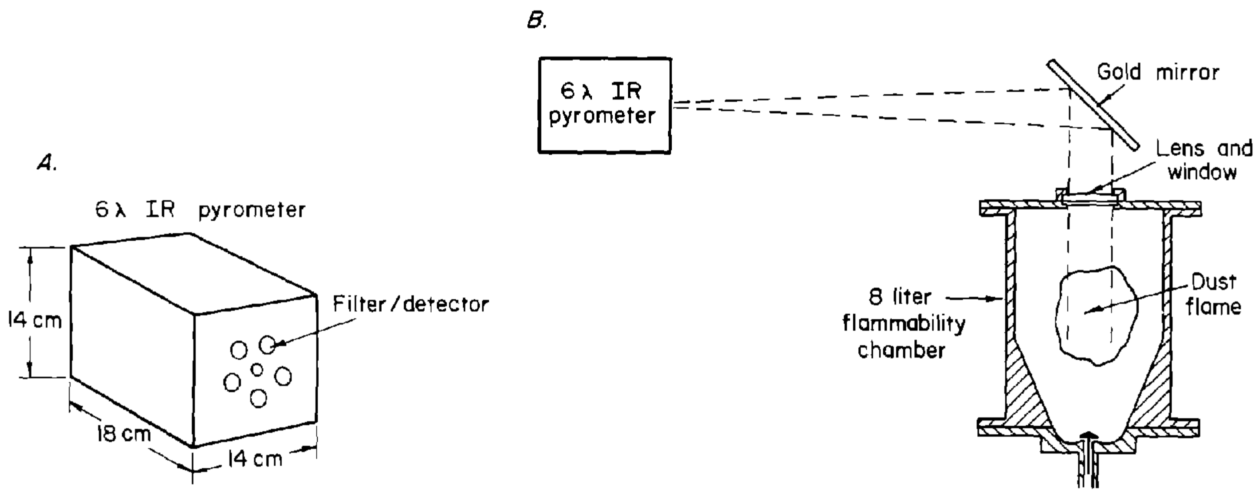

FIGURE 9. - Six-channel infrared pyrometer used to measure temperatures of dust explosions. *A*, Pyrometer detector-amplifier box; *B*, optical configuration of pyrometer and flammability chamber.

with the same lens, window, and mirror configuration depicted in figure 9B. The blackbody standard was manufactured by Land Pyrometers Ltd., and is a type MT with a 31-cm-diam spherical cavity and a 7.4-cm-diam aperture. Calibration was checked with the blackbody source over a temperature range of 1,000 to 1,500 °K. The linear response of the pyrometer permitted extrapolation of this calibration to higher temperatures.

The pyrometer housing consisted of a 14- by 14- by 18-cm aluminum box, depicted in figure 9A, that contained the filters, detectors, and amplifiers. The infrared, interference filters restrict the wavelength of the radiation reaching each detector. The detectors are lead selenide (PbSe) photoconductive devices, each in a bridge configuration that responds linearly to the incident radiation within the wavelength band of each filter. As shown in figure 9B, radiation from the dust flame passes through a sapphire window (0.3 cm thick and 7.6 cm in diam) and an arsenic trisulfide lens (76 cm focal length and 7.6 cm diam) that focuses the radiation onto the detectors. A front surface gold mirror deflects the radiation from its upward direction into the horizontal view field of the pyrometer. The aperture of the window-lens combination is 6.4 cm and this provides a 4.8° view field that is virtually common for each of the six detectors in the pyrometer. Five of the detectors and their respective filters are arranged in a 5-cm-diam circle in the faceplate of the housing, with the sixth detector and its filter in the center of the circle.

A circuit diagram for two representative channels is shown in figure 10. All six channels have essentially similar circuits with some variations in the bridge resistors and amplifier gains. Each bridge circuit is composed of two Optoelectronics OE-10, lead selenide (PbSe) photoconductive detectors, two fixed resistors, and one potentiometer. One of the detectors in each bridge is always dark and provides temperature compensation for the detector that actually views the infrared radiation. This compensation is necessary because the dark resistance of the lead selenide detector changes with ambient temperature. Although the detectors are "matched pairs," the compensation is not perfect, and a potentiometer in each bridge circuit is used for final balancing of the dark resistances. When the pyrometer receives infrared radiation, the resistance of the exposed PbSe detector decreases and unbalances the bridge. The signal is amplified in two stages by a Burr-Brown Model 3670 instrumentation amplifier and a Model 3500C operational amplifier. The final output signal is linearly proportional to the radiation incident on the detector. The intrinsic time response of the PbSe detectors is about 2 μsec (microseconds), but the time response of the pyrometer is limited to about 20 to 30 μsec by the frequency response of the amplifiers.

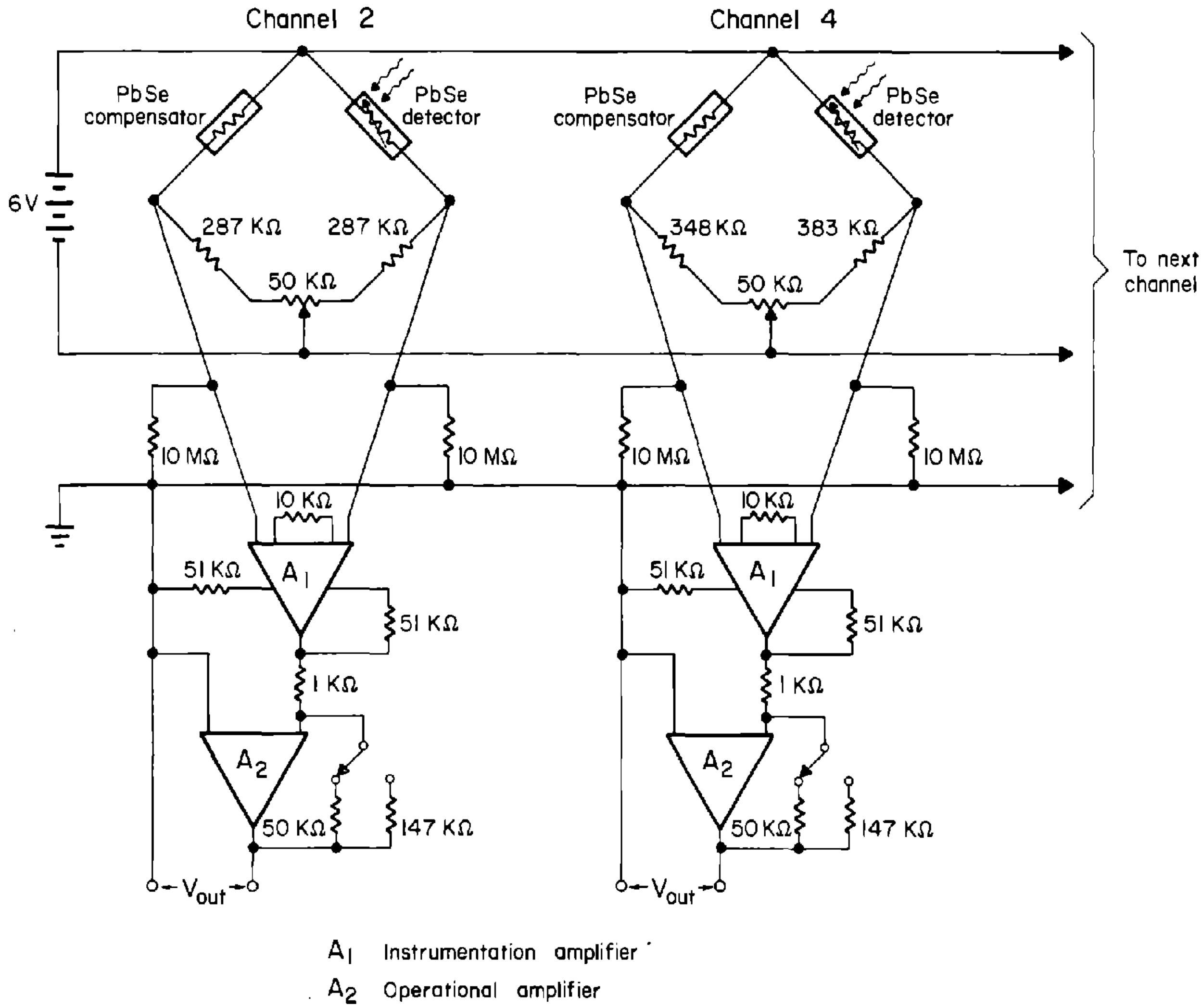

FIGURE 10. - Circuit diagram for two channels of the six-channel, infrared pyrometer.

FLAMMABILITY DATA

Ignition Energy Requirements

A series of experiments was performed to determine the ignition energies required for true limit measurements in such phase-heterogeneous mixtures. This question has never been adequately resolved in prior research. Preliminary experiments were performed with a capacitive discharge and a continuous transformer discharge. As can be seen in figure 11, those sources were not sufficiently energetic to give reliable ignitions as the lean limits were approached. While they are adequate for premixed gases, the data for coal dust-air mixtures indicated that typical electric discharges were not energetic enough to overcome the enormously larger energy losses that are present near the limits of flammability of the dust. This became obvious when a small quantity of guncotton, attached to the ignition electrodes, markedly reduced the minimum concentration that could be ignited. When it was felt that the

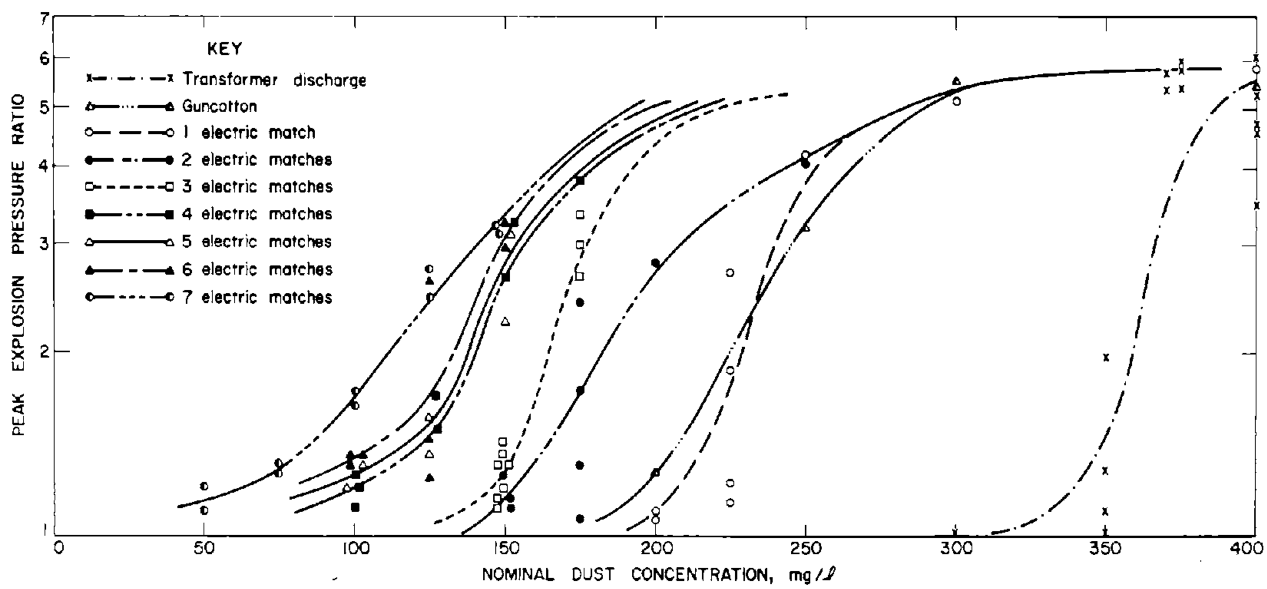

FIGURE 11. - Effect of ignition energy for 6.6-μm Pittsburgh coal dust; pressure ratio versus concentration.

temperature of the guncotton source might be too low, some ammonium perchlorate was tried. It was found that both of the ignition sources deposited their energy too slowly to be efficient ignitors. Eventually, a high-temperature electric match, Atlas M103, was found to be sufficiently energetic and rapid to serve as a reliable ignition source.

The results of these preliminary experiments are summarized in figure 11. The measured peak explosion pressure ratios from various ignition experiments are plotted as a function of dust concentration for a Pittsburgh seam dust with an average diameter of $d = 7$ μm. The explosion pressure ratio shown in figure 11 is defined as the ratio of the peak explosion pressure measured during any given run to the peak value measured from the ignition source by itself in the absence of dust. For most of the experiments, the latter was close to 1 atm, which was the initial pressure after dispersion and prior to activation of the ignitor. For one match, the additional contribution from the ignitor was from 0.04 to 0.05 atm. Thus, for example, in the experiments that used seven matches, the peak pressure value measured from the ignition source alone was 1.3 atm. Hence, the measured peak explosion pressure ratios were calculated relative to this higher value of the "initial" pressure. This pressure ratio differs only slightly from that of equation 6.

The data in figure 11 clearly shows that the required ignition energies are far higher than the values typically available in spark discharges. The transformer used to obtain the spark discharges had a rated output of 60 ma (milliamperes) at 15,000 volts. The apparent output electrical energy for a 0.3-sec spark duration would thus be about 270 joules. However, the data show that only a small fraction of this input electrical energy can actually contribute to the ignition process in the dust-air mixture. For example, the measured pressure rise from the spark alone is less than 0.006 atm. This gives an upper limit of about 5 joules for the "effective" or $V\Delta p$ ignition energy, where V is the chamber volume and Δp is the pressure rise from the ignition source by itself.

For this transformer-discharge source, the large increase in the measured peak explosion pressure ratio occurs in the range of 360 mg/1. Now, if one were satisfied that such a source were sufficiently energetic (as it would be for a premixed gas), it could erroneously be concluded that the lean-limit concentration was in that range. However, the data for the guncotton source (70 mg wrapped around one of the electrodes) clearly indicate that 360 mg/1 is far too high. For the guncotton source, the large increase in the peak explosion pressure ratio occurs near 230 mg/1. Nearly the same value is obtained with one electric match as with the guncotton source. However, even these are clearly not sufficiently energetic. It is not until four to seven electric matches are used that the large increase in peak explosion pressure ratio appears to become nearly invariant at a concentration near 140 mg/1. The $V\Delta p$ energy deposited by the guncotton alone is about 90 joules, but the rate of deposition is rather slow (about 0.5 sec). The pressure rise of 0.04 to 0.05 atm. per match gives a $V\Delta p$ energy of about 35 joules per match, and this energy is deposited quite rapidly (in about 0.05 sec). Too slow injection of ignition energy allows time for dissipative processes to occur and hence the rapid match source was chosen for subsequent experiments.

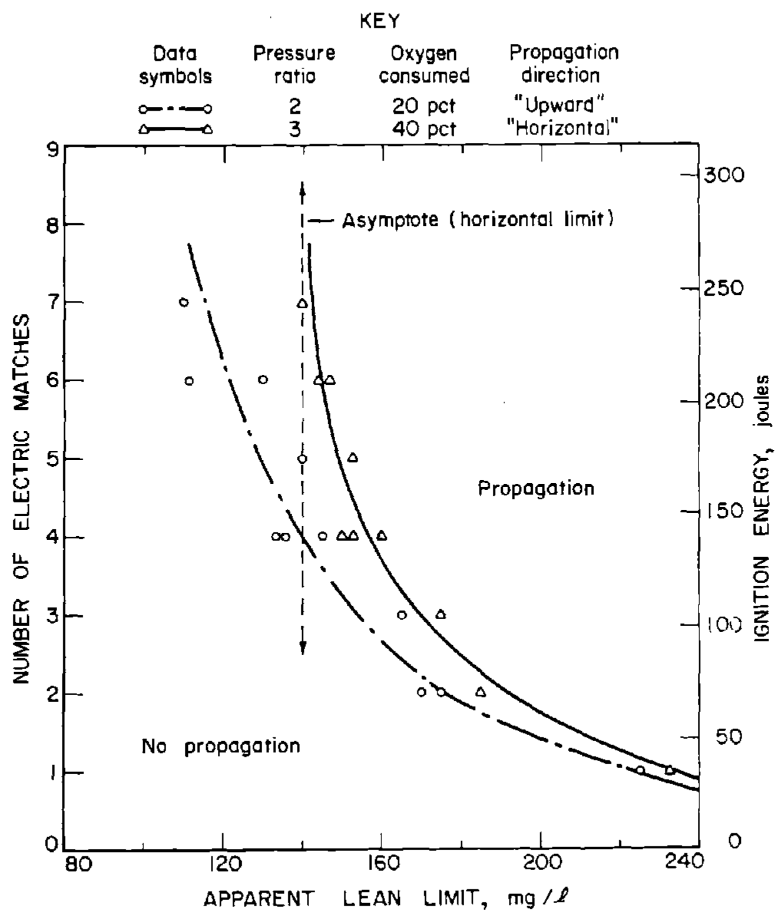

FIGURE 12. - Apparent lean limit of flammability for 6.6-μm Pittsburgh coal dust as a function of ignition energy.

The data from figure 11 for the electric match ignitions are replotted in figure 12, which also includes more recent measurements in which match head configurations were varied and the precise value of the initial O_2 content of the air was measured. The ignition energy is plotted against the apparent lean-limit concentration based on peak pressure ratio criteria of 2.0 and 3.0. The upper curve, for the more stringent criteria, appears to approach the vertical asymptotically at a concentration near 140 mg/1. This concentration is therefore considered to be the "true horizontal" limit, that is, the concentration that would be self-propagating in the absence of any limitations on ignition energy. All higher values are not true limits because they appear to be limited by the ignition energy available.

The lower curve is for the less stringent criteria that has been associated with the "upward" propagation direction. It does not yet appear to have reached its vertical asymptote even at seven matches; however, it is felt that this propagation criteria is too "soft" a condition for the system. Even though the peak pressure ratio is corrected for the pressure rise caused by the ignition source alone, there is always some additional combustion of the coal in the volume surrounding the ignition source flame even at concentrations well below the true limits. For low ignition energies, this is not significant relative to the total chamber volume. However, for very large ignition energy inputs, the volume around the ignition source becomes a significant fraction of the total chamber volume. In such cases, local combustion near the ignition source can readily generate a peak pressure ratio of 2.0, even though there may be virtually no propagation beyond the region of ignition. Thus, it is concluded that the less stringent criteria (P.R. = 2.0) is too "soft" a condition when high ignition energies are used in the small 7.8-liter apparatus used in these studies. If the total volume of the apparatus were much larger, it is confidently felt that even the less stringent criteria would display a true asymptotic limit.

It should be noted from figure 12, that the "true horizontal" limit concentration (obtained from the upper curve) is approximately the same as the limit value from the lower curve at an ignition energy of four matches. To avoid using very large numbers of matches (which would ideally require a much larger apparatus), a practical compromise was reached between the required ignition source energy and the propagation criteria. The standard ignition source for lean-limit measurements was chosen to be four electric matches and the propagation criteria was chosen to be a peak pressure ratio of 2, because this combination gave a lean-limit value close to the "true horizontal" limit, as shown in figure 12. As figure 12 illustrates, this compromise of using the lower ignition energy and a "softer" propagation criteria for the "horizontal" limit is equivalent to using a virtually infinite ignition energy and the "harder" criteria for the "horizontal" limit. In the data to be presented in the following sections, four matches are used as the "standard" ignitor and the "soft" criteria is used, but ascribed to the "horizontal" propagation.

In addition to the data shown in figure 12, which are for Pittsburgh coal dust with $\overline{d}_s = 7\ \mu m$, ignition energy requirements were measured for two other distributions ($\overline{d}_s = 3\ \mu m$ and $\overline{d}_s = 22\ \mu m$). The results were similar to those shown in figure 12.

The ignition energy scale in figure 12 is shown in both number of matches and in joules. The joule scale is the final result of a series of experiments that were conducted to determine the effective energy output of the various ignition sources used. One way to compare the ignition sources on an equal basis was to measure the actual energy deposited in the gas in terms of the pressure rise. This "effective" or $V\Delta p$ energy was based on the volume of the chamber, V, and the measured pressure rise, Δp, due to the ignition source. As indicated earlier, the 15-kv(kilovolt) transformer at a rated current of 60 ma and a discharge of 0.3 sec duration would produce an apparent energy in the secondary circuit of 270 joules. However, as also indicated earlier, the fraction of this energy that appears in the burned mixture, at a sufficiently high temperature to be effective in ignition, is undoubtedly much smaller. The measured pressure rise from the discharge was less than 0.006 atm, and therefore the $V\Delta p$ effective energy available to the gas was significantly less than 5 joules. The use of 70 mg of guncotton appeared to deposit more energy (about 90 joules) into the gas, but the recorder pressure trace for the guncotton ignitor by itself revealed a very slow rate of combustion, requiring as long as 0.5 sec for the pressure to rise to its maximum value of 0.12 atm above ambient.

A single ICI Atlas M103 electric match was then tried and it was found to be as effective as the guncotton. The rate of deposition of energy from the match was, however, much more rapid. The measured pressure pulse from the match, and the luminosity associated with its reaction (fig. 8A) indicated that the energy was deposited in about 50 msec. From the measured pressure rise of 0.04 to 0.05 atm per match, and the chamber volume of 7.8 liters, the calculated $V\Delta p$ effective energy was about 35 joules per match. This value was not inconsistent with the calculated combustion energy expected from the mass of the pyrotechnic and its approximate heat of combustion. Observations of the electric matches with high-speed motion pictures showed that the main luminosity was centered at the match position with an occasional small fragment of a match thrown out to other parts of the vessel.

It was thus decided to standardize on the electric matches as ignition sources, and a series of experiments were conducted to study their properties. The multichannel infrared pyrometer was used to measure their continuum radiation temperature. Two types of matches were available: The M100 with a measured continuum temperature of about 1,600 K, and the M103 with a measured continuum temperature of about 2,000 K. To avoid any possible ignition temperature limitations, the hotter M103 ignitor was chosen.

Calorimetric measurements were made of the energy deposited by the match ignitors. The result for the M103 was 170 joules per match in air and 60 joules per match when energized in nitrogen. The energy in terms of the measured $V\Delta p$ was in about the same ratio: 35 joules per match in air and about 10 joules per match in nitrogen. The pyrotechnic mixture (including coating and fuse wire) is fuel rich and the significant difference between air and nitrogen ignition is probably caused by the excess fuel combustion with the oxygen of the air in the chamber. Now the calorimeter measures the total energy that is generated by the combustion of the matches. However, in an actual ignition experiment some fraction of this total is lost by radiation to the chamber walls, or to the dust cloud far from the ignitor. This lost fraction is not available in the ignition volume near the source. In the calorimetric experiments there are no radiation losses. Thus, part of the difference between the calorimetric energy and the "prompt energy" may be due to the energy lost by radiation. However, the fraction lost would have to be 75 to 80 percent to account for the total difference, and this is probably too large a value to expect. At most, the radiant fraction could approach 50 percent. The remaining difference could be due to the presence of a slow, heat release contribution that is present in the calorimetric measurements but which is too slow to appear as prompt $V\Delta p$ energy. However, such a slow heat release contribution would not be effective in the ignition process either. It would be as ineffective as discharge energy dissipating as heat in the ignition electrodes. It is beyond the scope of these studies to consider these detailed questions of ignition dynamics. The data cited, together with the above reasoning, suggests that the $V\Delta p$ "prompt energy" measurement of 35 joules is probably close to the effective ignition energy available from each match in air. Thus, the four- to seven- match requirement indicates that ignition energies in the range of several hundred joules are necessary to obtain true limit measurements for such coal dust-air mixtures. This, then, is the origin of the energy scale shown in figure 12.

The data points shown in figure 12 include small variation in O_2 content of the air used and small differences in the configuration of the match heads. Although the data points do not distinguish between these variables, the small differences caused systematic variations. The O_2 content of the "air" used was as high as 21.5 and as low as 20.2. Preliminary data indicates that this small decrease in the initial O_2 content caused the lean limit to increase by almost 10 mg/l. In addition, the match head configurations could be varied by alining the match heads in a "facing" configuration or as a linear array. Later, preliminary data indicate that the "facing" configuration is more efficient in concentrating the combustion energy of the match heads into a single, small ignition volume. However, the lean-limit flammability data presented in this report were obtained earlier with the linear array of four matches.

Lean-Limit Measurements

The complete set of flammability data for various sizes of Pittsburgh seam coal dusts are shown in figures 13-30. The odd numbered figures show the measured peak pressure ratios (equation 6) and the percent of initial oxygen consumed by the explosions. Both parameters are measures of the extent of flame propagation. Both are plotted as a function of the nominal dust concentration, which is defined as the total mass of dispersed dust divided by the volume of the combustion chamber. As a measure of the effectiveness of the dust's dispersion, the even numbered figures show the simultaneously measured dust probe transmissions just prior to ignition.

All data are for Pittsburgh seam coal with standard ASTM volatility of 34.0 to 37.5 percent on a moisture-free basis and an ash content of 6 to 9 percent. The data from Coulter-Counter size analyses of the nine different particle size distributions are shown in table 1. The Coulter size analyses are made with the dusts dispersed in isopropyl alcohol and therefore serve as a basis for comparing the nine distributions in an unagglomerated state. When the same dusts are dispersed in air, they will agglomerate to a larger average particle size. The nine dusts range in surface mean diameter from 2.7 μm to 65 μm. The widths of the size distributions are indicated in the third column of the table. The quantity, d_{75}, is that diameter which contains 75 percent of the cumulative distribution function, whereas 25 percent of the distribution is less than the d_{25} value. The ratio d_{75}/d_{25} is thus a measure of the size distribution. Six of the distributions ($\bar{d}_s$ = 2.7, 3.2, 6.6, 15, 22, and 34 μm) were size-classified with a Donaldson centrifugal classifier and have rather narrow distributions. The $\bar{d}_s$ = 21 μm distribution is an unclassified pulverized coal with a broad distribution. The two largest sizes ($\bar{d}_s$ = 51 and 65 μm) were sieve-classified and also have narrow distribution widths; they also have lower ash contents of 5 and 2 percent respectively.

TABLE 1. - Size distributions of coal used for lean flammability limit studies[1]

Mean particle diameter $\bar{d}_s$ (surface-area-weighted), μm	Mean diameter, $\bar{d}_w$ (mass-weighted), μm	Distribution width $[d_{75}/d_{25}]_s$ (surface-area-weighted)
2.7	3.4	2.3
3.2	4.1	2.3
6.6	9.2	2.9
15	19	2.2
21 (broad)	38	6.0
22	31	2.3
34	41	1.7
51	55	1.2
65	70	1.3

[1] Data based on Coulter-Counter size analyses.

The data in figures 13-30 serve as a basis for the summary of the lean-limit measurements presented in table 2. As can be seen from the graphs, the onset of significant flammability is virtually independent of particle size in the range of sizes studied. The limit concentration or minimum explosive concentration averages to be 135 ± 8 mg/l. As indicated earlier, all measurements were made with an ignition source of four matches, which corresponds to an effective ignition energy of 140 joules. It is the "standard" ignitor, which is somewhat weaker than the energy needed to obtain a true asymptotic limit. However, this is compensated for in table 2 by using the "soft" limit criteria of a pressure ratio of 2.0, and ascribing that condition to the "horizontal" limit.

Also shown in table 2 is the measured optical density per unit length at the limit concentration. It is defined as $D = \frac{1}{\ell} \log_{10} (\frac{100}{T})$, where T is the percent transmission at the limit concentration and ℓ is the dust probe path length.

TABLE 2. - Summary of lean-limit measurements

Particle size $\bar{d}_s$, μm	Lean-limit concentration, mg/l	Oxygen consumed at limit, percent of total	Optical density at limit D, cm^{-1}	Agglomeration factor at the limit α
2.7	142	32	0.20	1.9
3.2	143	23	.15	2.1
6.6	130	16	.077	1.9
15	132	19	.046	1.4
21 (broad)	123	19	.038	1.1
22	137	26	.028	1.6
34	140	18	.021	1.4
51	126	22	.017	1.1
65	145	19	.012	1.4
Mean and standard deviation for all sizes...........	135 ± 8	22 ± 5	-	1.5 ± 0.4

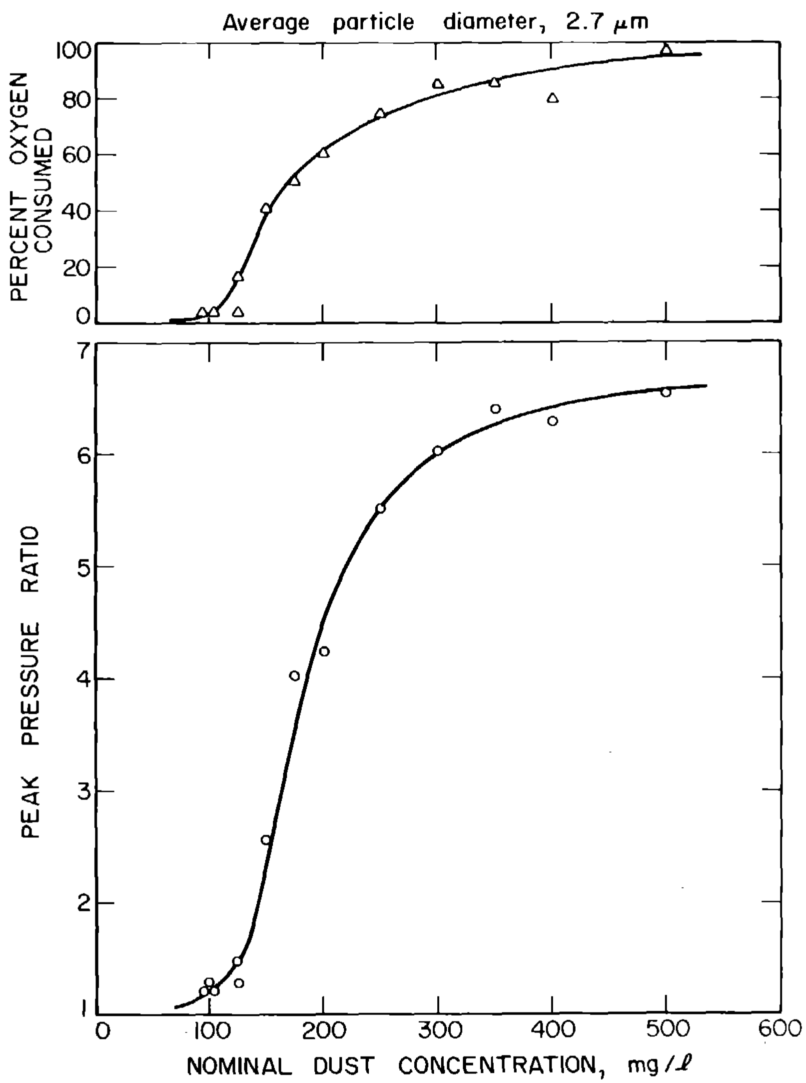

FIGURE 13. - Flammability data for a narrow size distribution of Pittsburgh coal dust with $\bar{d}_s$ = 2.7 μm; percent of initial oxygen consumed and peak pressure ratio as a function of dust concentration.

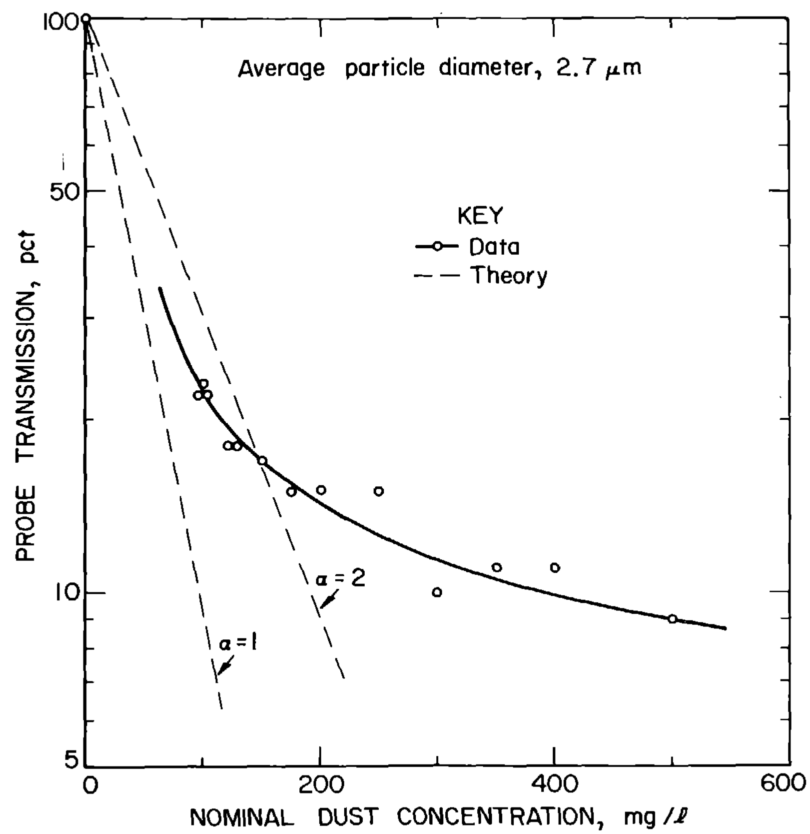

FIGURE 14. - Dust probe transmission measurements (at ignition) as a function of nominal dust concentration; theoretical lines are based on $\bar{d}_s$ = 2.7 μm, Q = 1.5, ρ = 1.3 g/cm³, and two agglomeration factors, α.

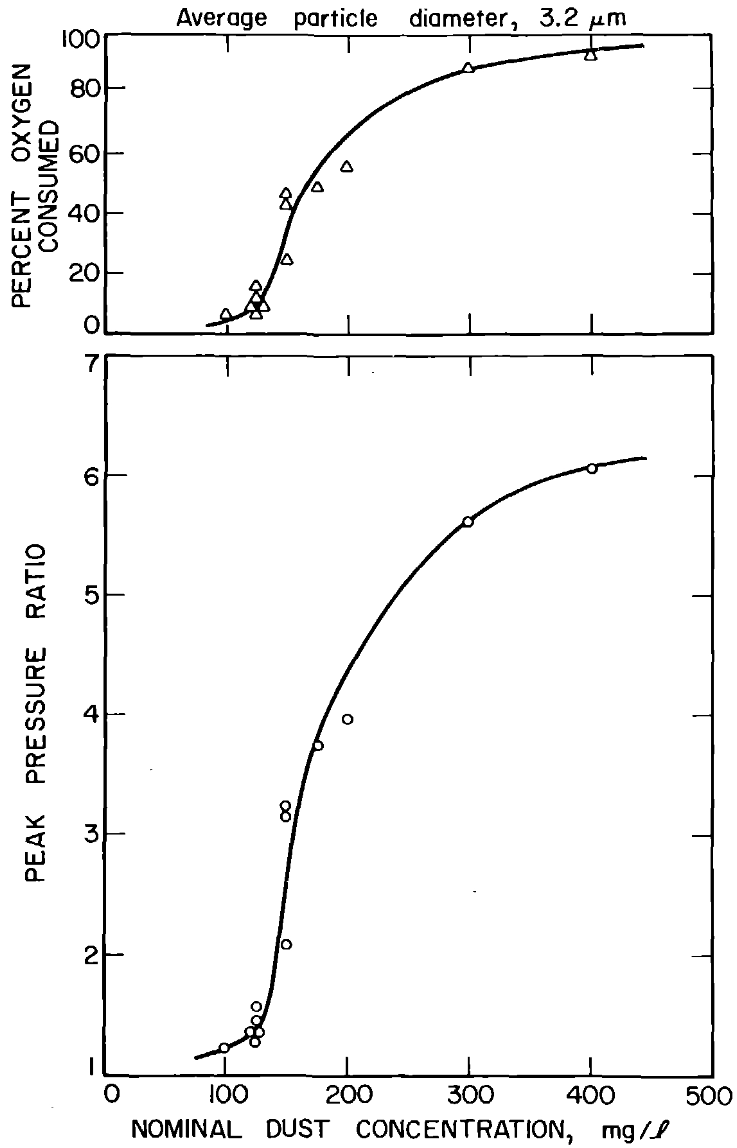

FIGURE 15. - Flammability data for a narrow size distribution of Pittsburgh coal dust with $\bar{d}_s$ = 3.2 μm.

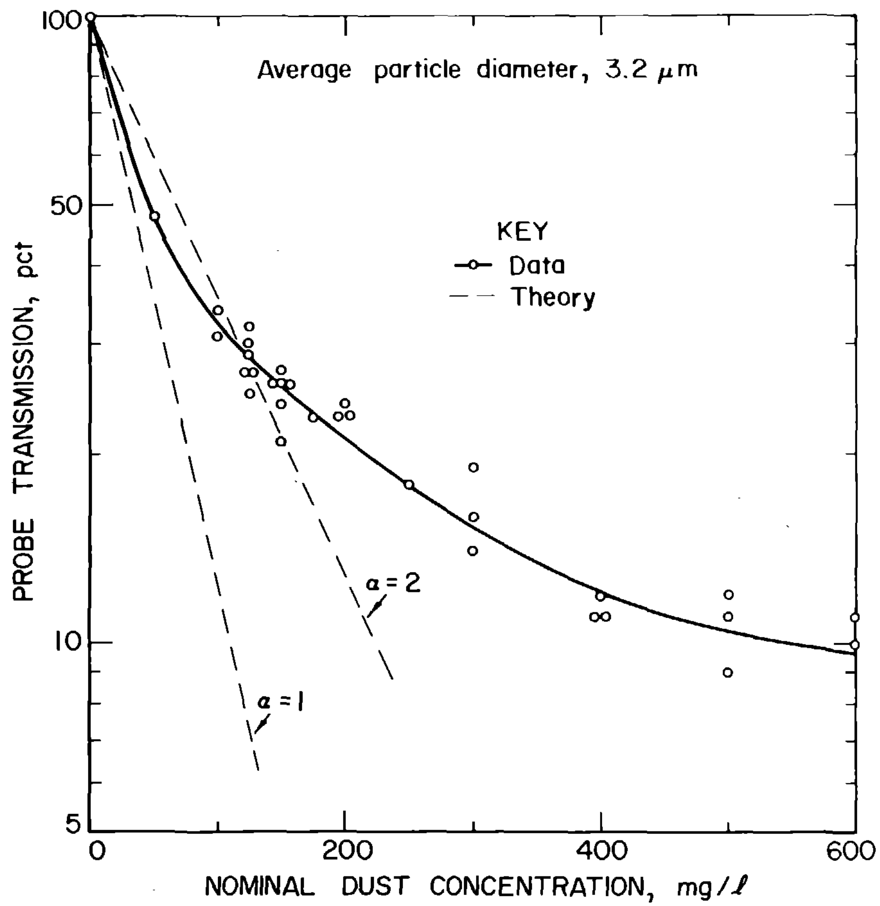

FIGURE 16. - Dust probe transmission measurements (at ignition) as a function of nominal dust concentration for 3.2-μm Pittsburgh coal.

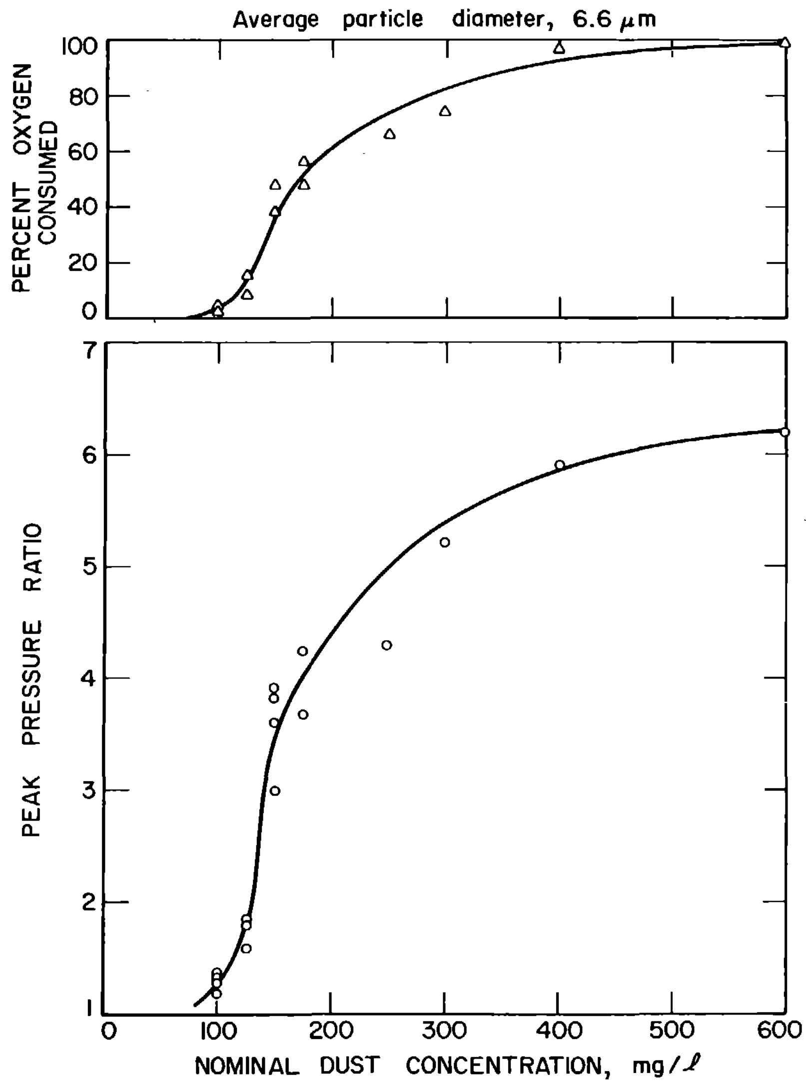

FIGURE 17. - Flammability data for a narrow size distribution of Pittsburgh coal dust with $\bar{d}_s = 6.6$ μm.

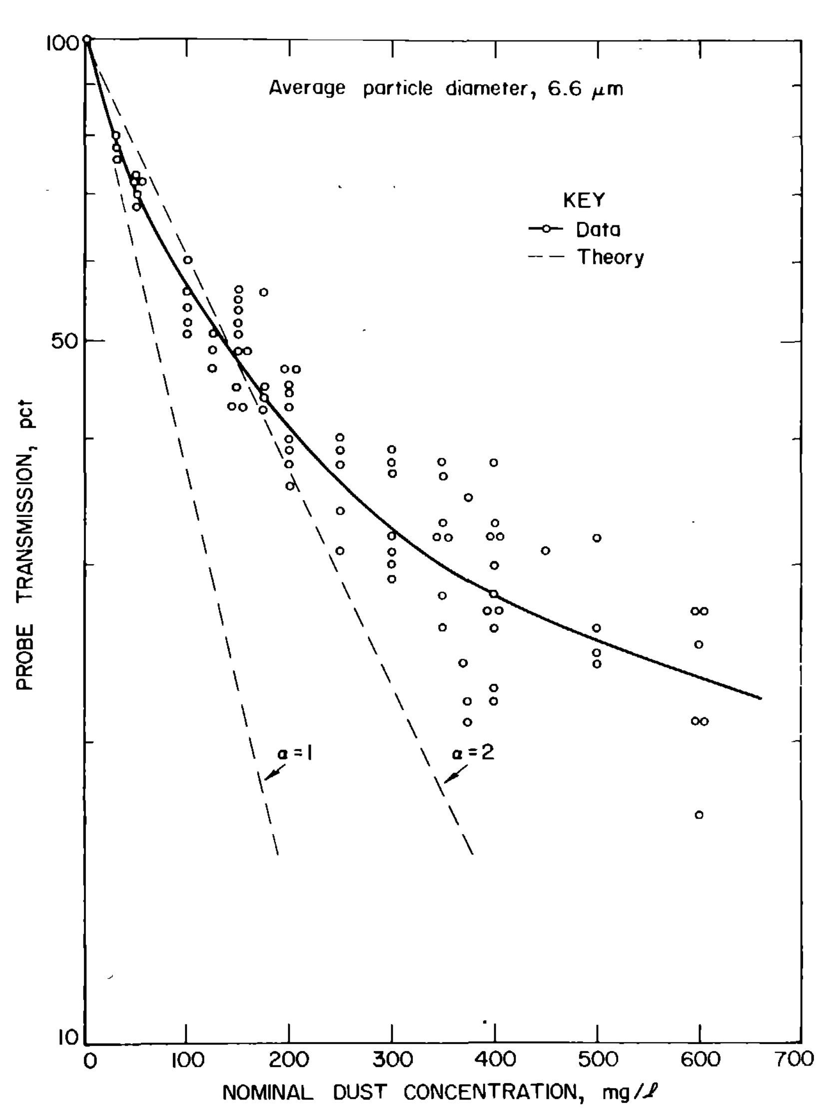

FIGURE 18. - Dust probe transmission measurements (at ignition) as a function of nominal dust concentration for 6.6-μm Pittsburgh coal.

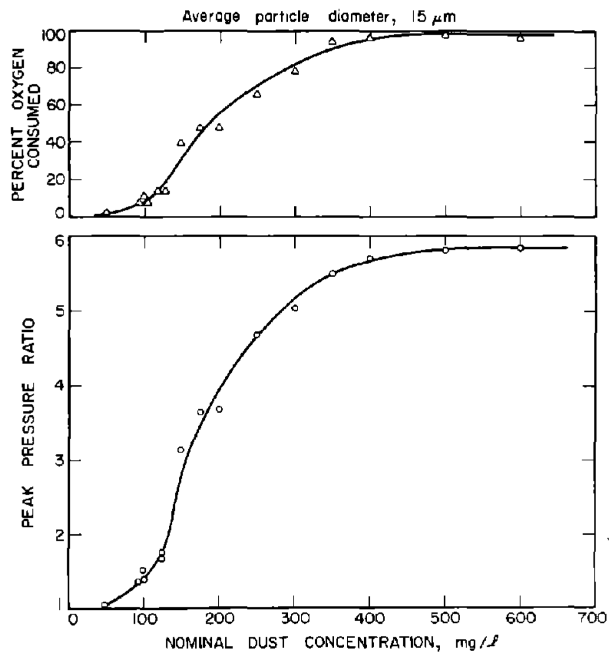

FIGURE 19. - Flammability data for a narrow size distribution of Pittsburgh coal dust with $\bar{d}_s$ = 15 μm.

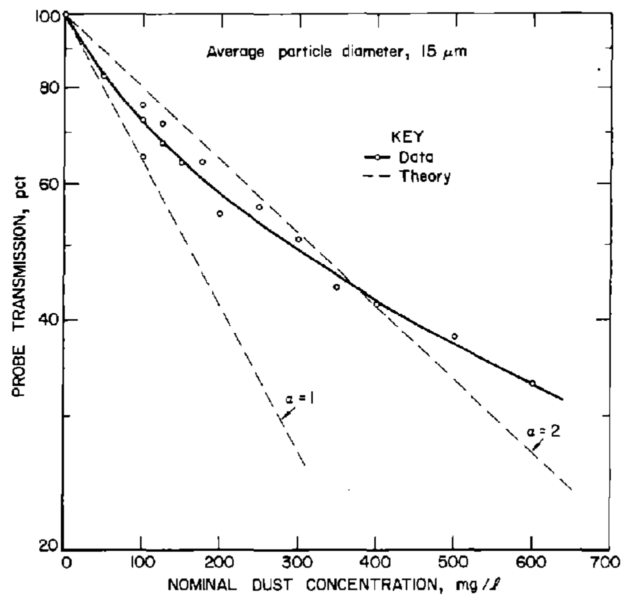

FIGURE 20. - Dust probe transmission measurements (at ignition) as a function of nominal dust concentration for 15-μm Pittsburgh coal.

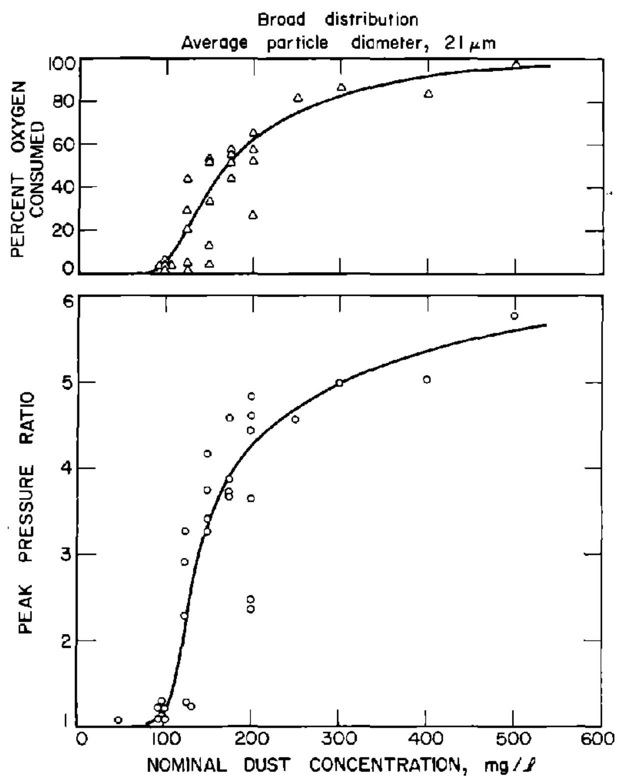

FIGURE 21. - Flammability data for a broad size distribution of Pittsburgh coal dust with $\bar{d}_s$ = 21 μm.

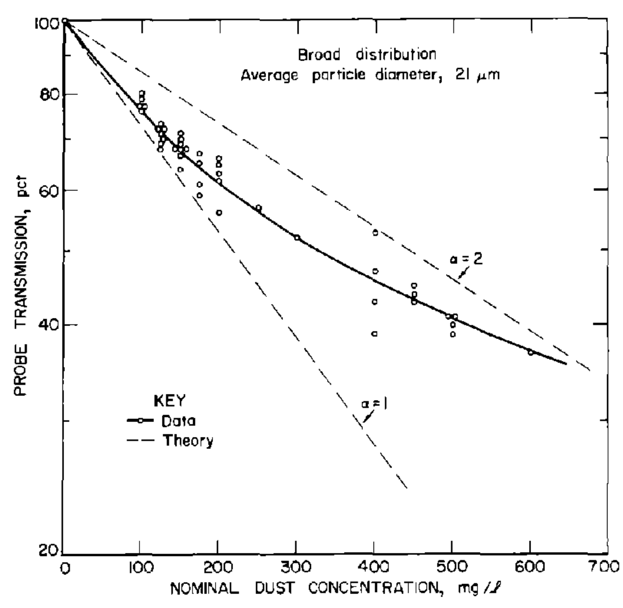

FIGURE 22. - Dust probe transmission measurements (at ignition) as a function of nominal dust concentration for 21-μm Pittsburgh coal.

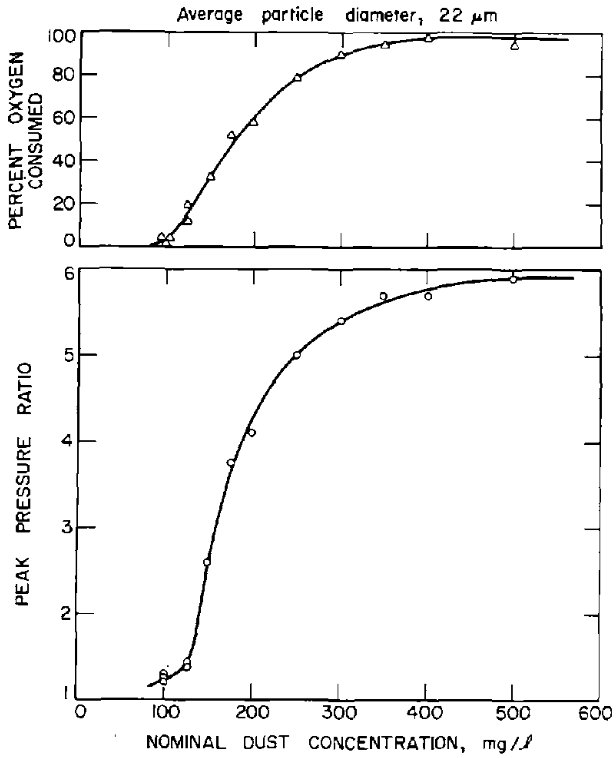

FIGURE 23. - Flammability data for a narrow size distribution of Pittsburgh coal dust with $\bar{d}_s = 22$ μm.

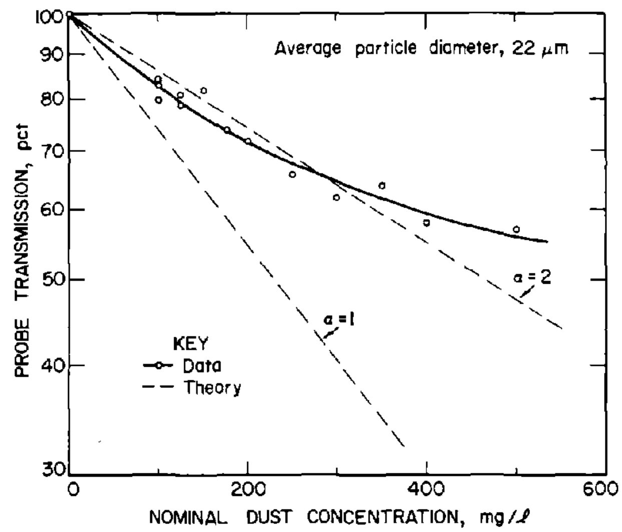

FIGURE 24. - Dust probe transmission measurements (at ignition) as a function of nominal dust concentration for 22-μm Pittsburgh coal.

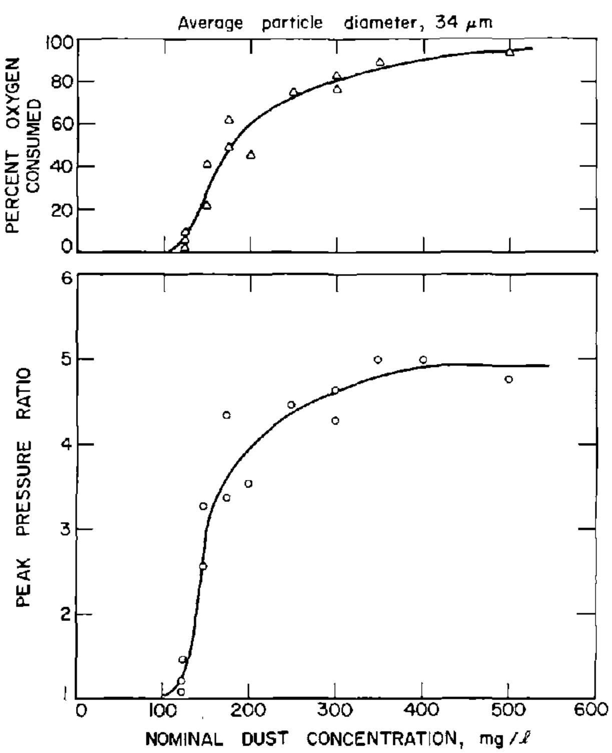

FIGURE 25. - Flammability data for a narrow size distribution of Pittsburgh coal dust with $\bar{d}_s = 34$ μm.

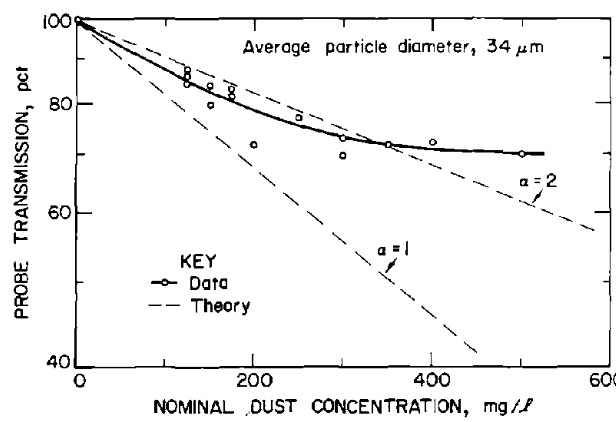

FIGURE 26. - Dust probe transmission measurements (at ignition) as a function of nominal dust concentration for 34-μm Pittsburgh coal.

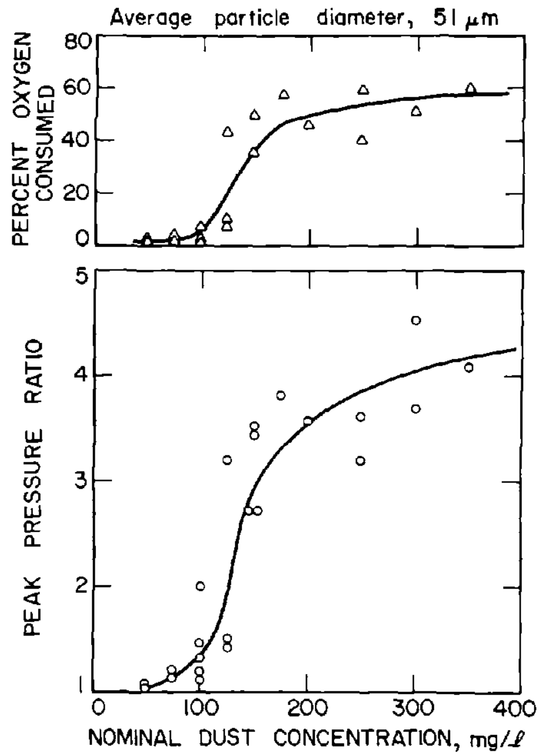

FIGURE 27. - Flammability data for a narrow size distribution of Pittsburgh coal dust with $\bar{d}_s = 51\ \mu m$.

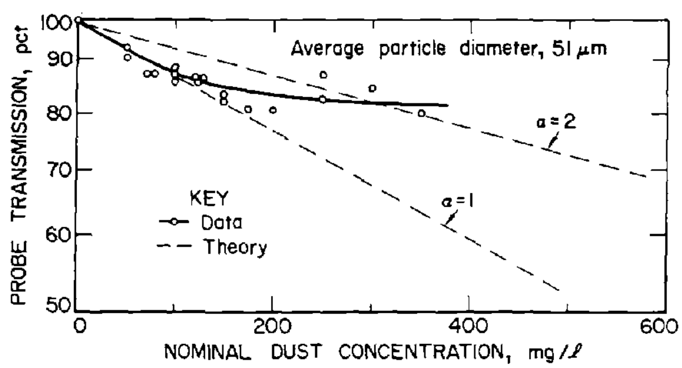

FIGURE 28. - Dust probe transmission measurements (at ignition) as a function of nominal dust concentration for 51-μm Pittsburgh coal.

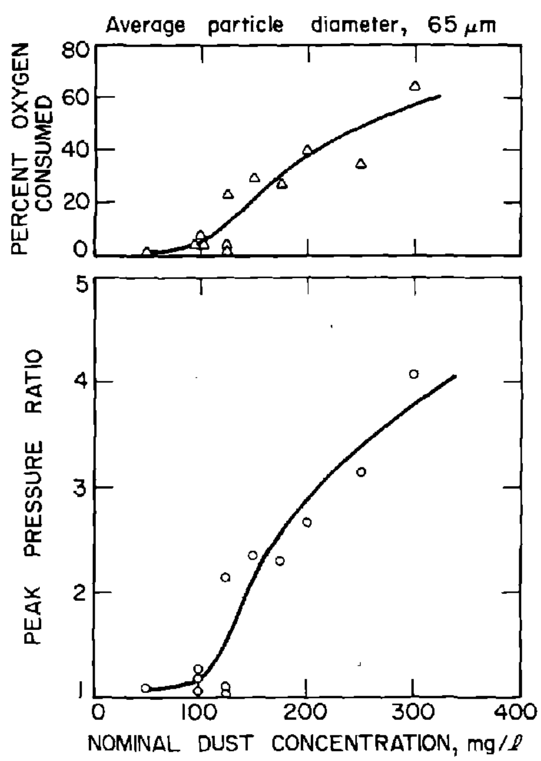

FIGURE 29. - Flammability data for a narrow size distribution of Pittsburgh coal dust with $\bar{d}_s = 65\ \mu m$.

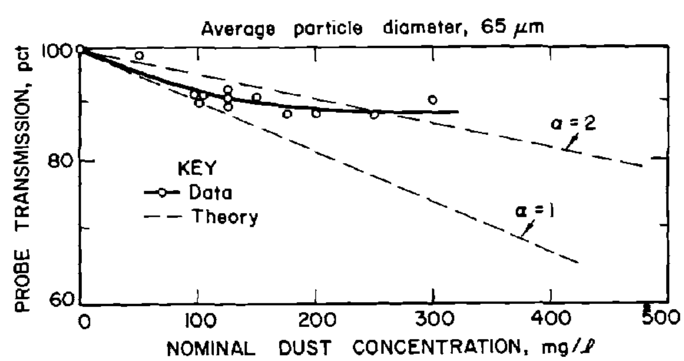

FIGURE 30. - Dust probe transmission measurements (at ignition) as a function of nominal dust concentration; theoretical lines are based on $\bar{d}_s = 65\ \mu m$, $Q = 1.5$, $\rho = 1.3\ g/cm^3$, and two agglomeration factors, α.

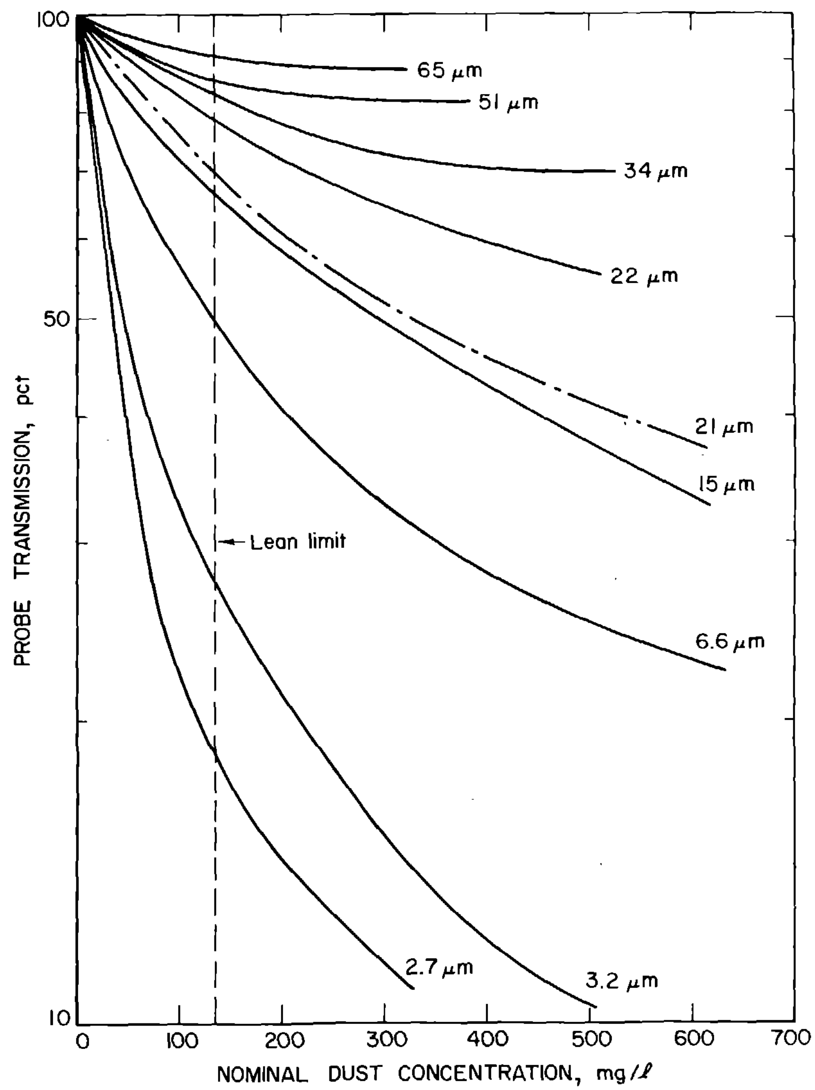

FIGURE 31. - Composite curves of optical probe transmission for the nine coal dust sizes studied. Intersections of the vertical dashed line with the transmission curves show the transmission values at the lean limit of flammability.

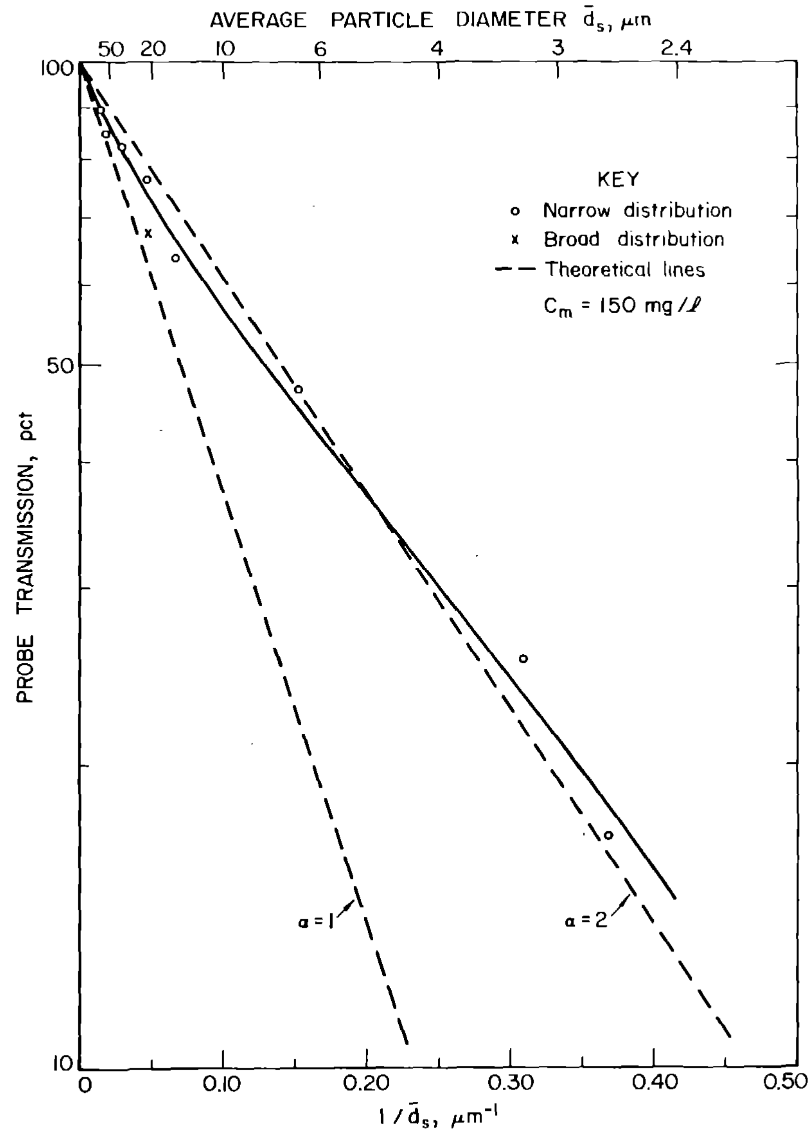

FIGURE 32. - Optical probe transmission as a function of reciprocal of particle diameter for a fixed concentration of 150 mg/1.

Dispersion-Agglomeration Effects: Lean-Limit Opacities

The effectiveness of the dust dispersion process (as measured by the dust probe) for all the sizes studied is illustrated in the semilog plots of figures 14, 16, 18, 20, 22, 24, 26, 28, and 30. The dashed, theoretical lines are calculated from equations 4 and 5. They show the expected transmission versus concentration for perfect dispersion at an effective diameter equal to the Coulter mean diameter ($\alpha = 1$) and at twice the Coulter diameter ($\alpha = 2$). The solid curves are the smoothed measured values and they show that, in reality, the dust agglomerates to a larger size with increasing dust concentration. The opacity measurement, by itself, cannot distinguish this agglomeration effect (ineffective dispersion on the microscopic scale) from ineffective dispersion on the macroscopic scale which may involve the inability of the air jet to lift the entire mass of dust contained in the cup. The smoothed data curves for all nine sizes studied are shown in figure 31. In the range of limit concentrations (123 to 145 mg/l), the measured agglomeration factors are generally between $\alpha = 1$ and $\alpha = 2$. This is illustrated most clearly in figure 32, where the probe transmissions for a fixed nominal concentration of 150 mg/l are plotted as a function of $1/\overline{d}_s$ (Coulter). The comparison with equation 4 is also shown for two cases: no agglomeration ($\alpha = 1$) and for an agglomeration factor of two ($\alpha = 2$). The results clearly indicate that the coarser dusts show less agglomeration than the finer dusts. The finer dusts, because of their larger surface area per unit mass, are more strongly influenced by surface adhesion forces and thus show a more marked tendency to disperse as agglomerates or to agglomerate by collisions after their initial dispersion.

Figure 33 shows similar data for a higher coal dust concentration (400 mg/l). As the particle diameters increase, the data curve approaches the $\alpha = 2$ dispersion line rather than the perfect dispersion line ($\alpha = 1$) which the data approached at the lower concentration. As before, the transmission measurement cannot distinguish between the effect of agglomeration (ineffecive microscopic dispersion) and inability of the air jet to lift the entire mass of dust from the dispersion cup (ineffective macroscopic dispersion). However, figures 28 and 30 (for 51 and 65 µm dust) show that the transmission remains constant or rises slightly as the dust concentration increases above 200 mg/l. It is unlikely that these large particles would agglomerate this much, and therefore it is concluded that the present air jet is unable to disperse the larger dust loadings from the disperser cup for these large-size coal dusts. The absence of surface forces may provide an opportunity for the air jets to channel through the dust pile lifting only some fraction of the dust placed in the bottom of the cup. The mass of deployed coal dust is more easily lifted en masse if strong surface forces are present that can transmit the air-drag impulse to the entire assembled mass. However, the presence of such strong surface forces make it less likely that the individual particles in the lifted mass will be separated from one another during the remainder of the dispersion process. This is the case for the finer dusts. On the other hand, for the coarser dusts, individual particles are more easily separated once the mass is airborne; however, the absence of strong surface forces makes it more difficult for the entire assembled mass to become airborne at high dust loadings.

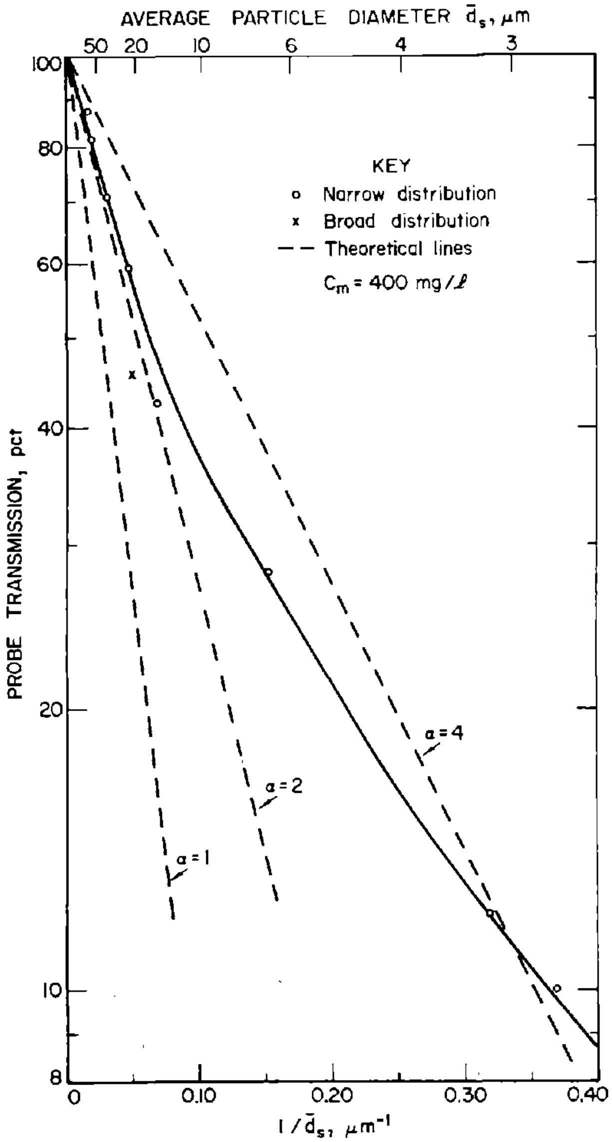

FIGURE 33. - Optical probe transmission as a function of reciprocal of particle diameter for a fixed concentration of 400 mg/l.

Whether this explanation is correct or not, this problem is not significant at limit concentrations because dust loadings are small at concentrations below 200 mg/l. The transmission data, even for the coarser dusts studied, indicate that all the dust is probably airborne at these lower concentrations. The data do indicate somewhat different states of agglomeration at limit concentration ranging from almost no agglomeration for the coarser dust to an agglomeration factor of 2 for the finer dusts. But these differences in agglomeration are not surprising, for the data span nearly 2 orders of magnitude in particle sizes. Yet, the flammability data show virtually no dependence of the lean limit on particle sizes. Hence, it appears unlikely that the small differences in agglomeration can have a significant influence on the flammability behavior near the limits.

Recent measurements of the burning velocities of coal-dust air mixtures had shown a strong dependence of the peak burning velocity on particle size (37). In fact, the peak burning velocities (measured at high dust concentrations) correlated quite well with the surface area per unit volume. If the flammability behavior at the lean limit had also depended on the surface area of the dust, then the optical dust probe would have been valuable as a hazardous dust cloud monitor because it also measures the cross-sectional surface area of the dust (equation 2). However, an inspection of table 2 clearly shows that the lean limit of flammability depends mainly on the mass concentration of dust in the air and not on the surface area of the dust. Figure 31 clearly shows that, at the lean limit, the transmission as measured by the dust probe varies significantly with particle size. This is also shown in table 2 where the optical density per unit length varies greatly with particle size at the lean limit of flammability. Therefore, it is concluded that any hazardous dust cloud monitor should be based on a measurement of the mass concentration of the airborne dust.

Pressure Development

An important factor in determining the explosibility hazard of a dust is the rate of pressure rise during the explosion. The rate of pressure rise controls the time interval available to suppress the explosion or to limit the damage by venting the system. The pressure growth curves for two of the sizes studied are shown in figures 34-35. These data are typical of all the sizes studied. Both figures depict the pressure development in the combustion chamber for eight different concentrations. The lowest concentration depicted, 150 mg/l, is just above the lean limit. The highest concentration depicted, 500 mg/l, is near the maximum concentrations studied. Figure 34 is for the 2.7-μm coal, which is the smallest size fraction studied and figure 35 is for the 22-μm dust, which is an intermediate size fraction. Both peak pressure and the maximum rate of pressure rise increase monotonically with increasing concentration. The maximum values of these parameters appear to be attained at 400 to 500 mg/l. The curves are analyzed in more detail in tables 3-4. The analysis shows that pressure development does not depend too markedly on the particle size, but is a strong function of concentration. However, at high dust concentrations, the peak pressure ratio and the maximum rate of pressure rise are somewhat higher for the finer dust than for the coarser size. This will be discussed in more detail in the next section. Despite these small differences, tables 3-4 clearly show that the pressure development curves and the calculated burning velocities are comparable for these two sizes.

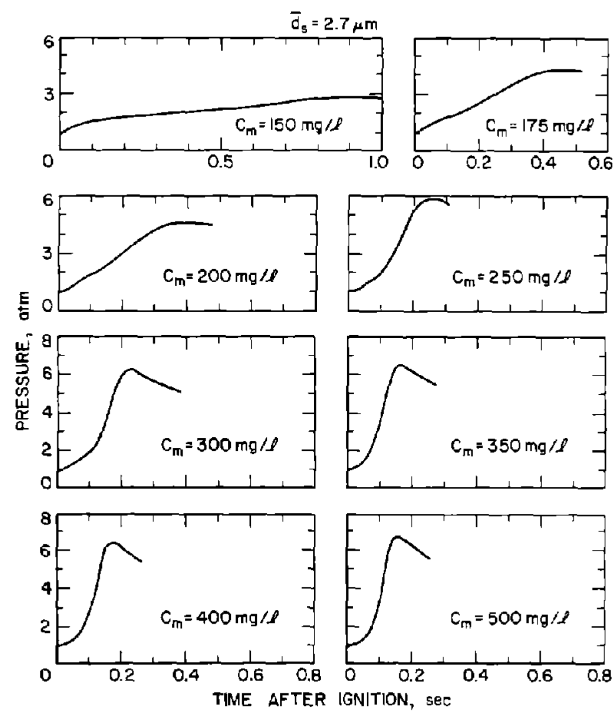

FIGURE 34. - Explosion pressure growth curves for eight different concentrations of Pittsburgh coal with $\bar{d}_s = 2.7$ μm.

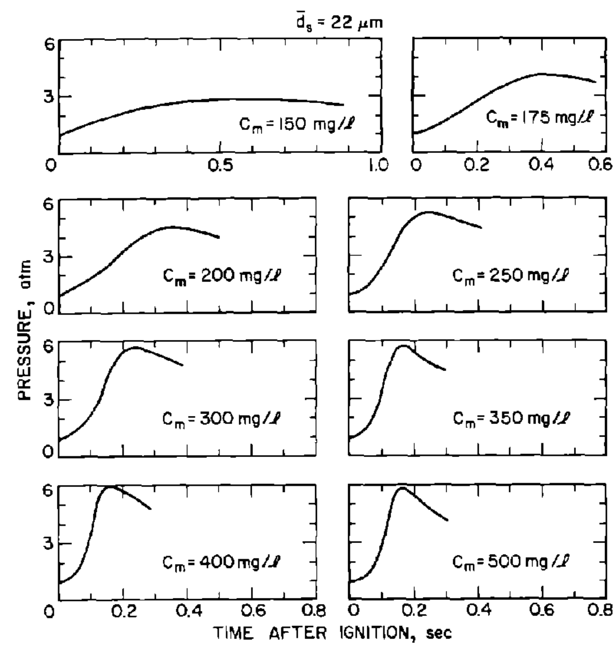

FIGURE 35. - Explosion pressure growth curves for eight different concentrations of Pittsburgh coal with $\bar{d}_s = 22$ μm.

The burning velocities are rough estimates calculated in the following manner. The average flame speed is obtained by dividing the "time to peak pressure" into the maximum travel distance. The average flame speed, divided by a typical expansion ratio, ρ_u/ρ_b, gives the calculated average burning velocity shown in the last column of the table. The expansion ratio is the density of the unburned mixture (ρ_u) divided by the density of the burned gas combustion products (ρ_b). The maximum travel distance was taken as 16.5 cm, which is the distance from the ignitor source to the top plate of the chamber. The burning velocity value shown is thus a crude estimate, uncorrected for the changes in expansion ratio, ambient pressure, buoyancy, and gasflow velocity that occur during the explosion process. However, the range of values are comparable to those observed for methane-air mixtures in an essentially similar apparatus (21).

TABLE 3. - Pressure development, residual O_2, and calculated burning velocities for Pittsburgh coal dust with $\bar{d}_s$ = 2.7 μm

Concentration, C_m, mg/l	Peak pressure ratio	Maximum rate of pressure rise, atm/sec	Residual O_2, percent	Time to peak, sec	Assumed ρ_u/ρ_b	Calculated average burning velocity, cm/sec
150	2.6	2	12.2	0.90	5.0	3.7
175	4.1	10	10.2	.44	5.3	7.1
200	4.3	14	8.1	.39	5.5	7.7
250	5.6	42	5.2	.25	5.6	12
300	6.1	52	3.1	.22	5.7	13
350	6.4	70	2.9	.17	5.8	17
400	6.4	83	3.9	.17	5.9	16
500	6.6	105	.2	.15	6.0	18

TABLE 4. - Pressure development, residual O_2, and calculated burning velocities for Pittsburgh coal dust with $\bar{d}_s$ = 22 μm

Concentration, C_m, mg/l	Peak pressure ratio	Maximum rate of pressure rise, atm/sec	Residual O_2, percent	Time to peak, sec	Assumed ρ_u/ρ_b	Calculated average burning velocity, cm/sec
150	2.6	6	14.0	0.55	5.0	6.0
175	3.8	11	10.1	.40	5.3	7.8
200	4.2	18	8.8	.33	5.5	9.1
250	5.1	34	4.4	.24	5.6	12
300	5.5	54	2.1	.23	5.7	13
350	5.8	70	1.0	.17	5.8	17
400	5.8	75	.3	.16	5.9	17
500	5.9	97	1.0	.16	6.0	17

The measured rates of pressure rise from tables 3-4 are for the approximately spherical propagation in the 8-liter vessel. In other vessels with higher turbulence, the rates of pressure rise are expected to be higher (11).

To obtain reliable and reproducible pressure rise rates, it is, of course, necessary to use adequate ignition energies. For the data indicated in figures 34-35 and tables 3-4, four matches were used for the concentrations between 150 and 250 mg/l, three matches for the concentrations between 300 and 400 mg/l, and two matches at 500 mg/l. As can be seen from figure 12, except for the lowest concentration at 150 mg/l, these ignition energies are well into the propagation domain and thus represent adequate ignition energies. As indicated earlier, four matches were chosen as the standard ignitor for limit measurements, even though this may be a somewhat weaker source than that required to obtain true limit values.

The extent to which marginal ignition can influence the rate of pressure rise is illustrated by the data shown in table 5 which shows the effect of various ignitor energies and match configurations on the peak pressure ratio and the time to peak pressure for the 22-μm dust. If one uses the "soft" condition for four matches or less and the "hard" condition for more than four matches, then all cases in table 5 correspond to a flammable concentration. (As defined previously, the "soft" condition refers to a maximum pressure ratio of 2.0 as a flammability criteria and the "hard" condition refers to a maximum pressure ratio of 3.0.) Nevertheless, there is considerable variability in the peak pressure ratio and the time to peak even though the concentration is fixed at 150 mg/l. This variability tends to disappear as one moves from the marginal ignition conditions of less than four matches to the adequate ignition conditions of five to six matches. The data at four matches seem to indicate that the "facing" configuration is more efficient than the linear array.

TABLE 5. - Effect of ignition energy and match head configuration on pressure development at a fixed concentration of 150 mg/l[1]

Number of matches	Configuration	Peak pressure ratio	Maximum rate of pressure rise, atm/sec	Time to peak, sec
2...............	Facing.......	4.0	19	0.34
2...............	.....do......	2.9	6	.65
3...............	.....do......	3.7	20	.29
3...............	.....do......	3.7	20	.34
4...............	Linear array.	2.4	5	.55
4...............	.....do......	3.4	14	.42
4...............	Facing.......	3.8	22	.33
4...............	.....do......	4.1	32	.24
5...............	.....do......	4.0	45	.20
5...............	.....do......	3.7	28	.27
6...............	.....do......	3.5	32	.24
6...............	.....do......	3.4	23	.26

[1] Pittsburgh coal, $\bar{d}_s$ = 22 μm and initial O_2 = 21.5 percent.

Similar data on the effect of various ignition energies at a somewhat higher concentration of 175 mg/l for the 6.6-μm coal is shown in table 6. As in table 5, the two-match ignition source is marginal and gives a slow pressure rise for the dust explosion. The four- and six-match ignitors are both adequate and produce similar rates of pressure rise.

TABLE 6. - Effect of ignition energy on the pressure development at a fixed concentration of 175 mg/l[1]

Number of matches[2]	Peak pressure ratio	Maximum rate of pressure rise, atm/sec	Time to peak, sec
2.............	2.0	3	0.48
2.............	2.4	5	.49
4.............	4.1	31	.28
4.............	4.1	28	.28
6.............	3.8	36	.23
6.............	4.0	38	.20

[1] Pittsburgh coal, $\overline{d}_s$ = 6.6 μm and initial O_2 = 20.2 or 20.6 percent.
[2] All configurations facing.

Correlation of Peak Pressure Ratios with Residual Oxygen Contents

As indicated earlier, there is very good correlation between the peak pressure ratio generated and the percent of initial O_2 consumed by the explosions in the 8-liter vessel. This is readily apparent from the similarity of the two curves plotted in figures 13, 15, 17, 19, 21, 23, 25, 27, and 29. The correlation between these two parameters for all the particle sizes studied is shown in figure 36. The correlation coefficient between the peak pressure ratio and the fraction of initial oxygen consumed by the explosions for all the points indicated in figure 36 was 0.987. Clearly, this good correlation indicates that either parameter is equally satisfactory in determining the completeness of combustion. The scatter of the points at high pressures is not completely random, but varies systematically with particle size. The dashed lines shown in figure 36 are for dusts with average diameters of about 3 μm ($\overline{d}_s$ = 2.7 and 3.2 μm) and 34 μm, respectively. At the higher dust concentrations, for a given fraction of initial oxygen consumed, the finer dusts attain a higher peak explosion pressure than the coarser dusts.

Although there is no particle size dependence at the lean-limit concentration (for the range of sizes studied here), there is clearly a significant particle size dependence in the flammability behavior at higher concentrations. Indeed, this particle-size dependence would probably have been more marked had it been possible to disperse the 51- and 65-μm dusts at higher concentrations. The data in figure 36 contain points for these two coarsest coals only at lower concentrations (where the fraction of oxygen consumed was generally below 0.60) because it was not possible to disperse the assembled mass of these coarse coals at concentrations in excess of 300 to 350 mg/l (figs. 28, 30). Based on the data trends for the intermediate sizes, it is expected that for

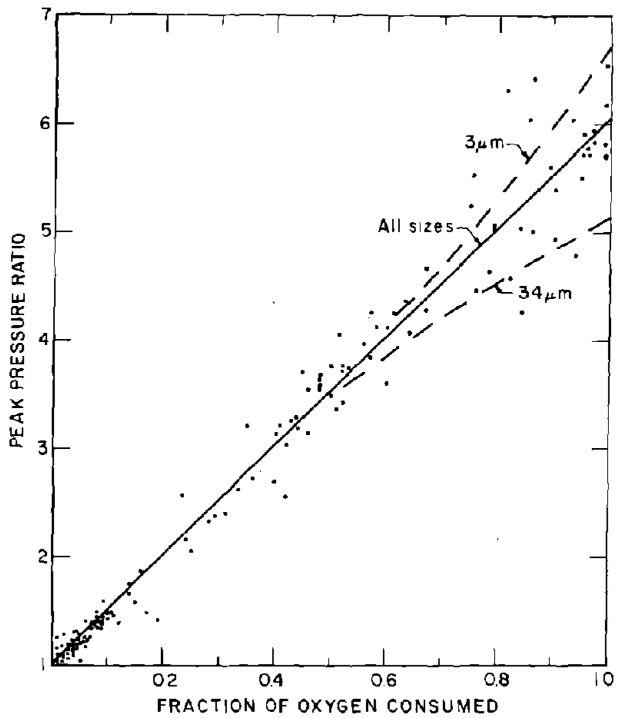

FIGURE 36. - Correlation between peak pressure ratio and oxygen consumption for all the coal dust sizes and concentrations studied.

higher fractions of oxygen consumed, these coarsest coals would have given significantly lower peak pressure ratios than the 34-μm coal curve depicted in figure 36.

The origin of this particle-size dependence at higher pressures is probably related to the higher peak burning velocities of the finer dusts (37) and the fact that those higher burning velocities result in lower heat losses to the surroundings during the development of the explosions. Those measurements of laminar-burning velocities for coal dust-air flames show a strong dependence of the maximum burning velocity with particle size. The finer dusts are characterized by maximum velocities in the range of 30 to 35 cm/sec, whereas the very coarse dusts are characterized by maximum velocities as low as 10 cm/sec. The explosion process for the rapidly propagating flames is more adiabatic simply because there is less time available for heat losses by radiation and convection to the surroundings. In the present study, for the finer dusts at high concentrations, the time to reach peak pressure is in the range of 150 msec; whereas, for the coarser dusts at comparable concentrations, the time to peak pressure is in the range of 300 to 400 msec. Thus, there is more time available for heat losses and these higher heat losses to the surroundings result in lower peak pressures for the coarser dusts.

In addition, the coarse dusts have a lower opacity. More of the energy radiated by the fireball is transmitted through the unburned mixture and can be absorbed by the walls. The finer dispersed dusts are more opaque and therefore the unburned mixture absorbs the radiating energy. This absorbed fraction is retained in the unburned mixture rather than being lost to the walls and is then returned to the fireball as the wave advances.

Flame Temperatures

Dust particle and gas flame temperatures were measured for explosions of 6.6-μm Pittsburgh coal dust in the 8-liter chamber by using the six-channel infrared pyrometer described earlier in this report. Four of the wavelengths are used to characterize the continuum radiation from the hot dust particles. These four wavelengths (1.57, 2.30, 3.46, and 5.19 μm) were chosen to avoid the emission bands of gases that would be present in the flame. Figure 37 shows typical gas band emission from a methane-air flame (21). Note that the four dust wavelengths correspond to minima in the gas flame radiation. The

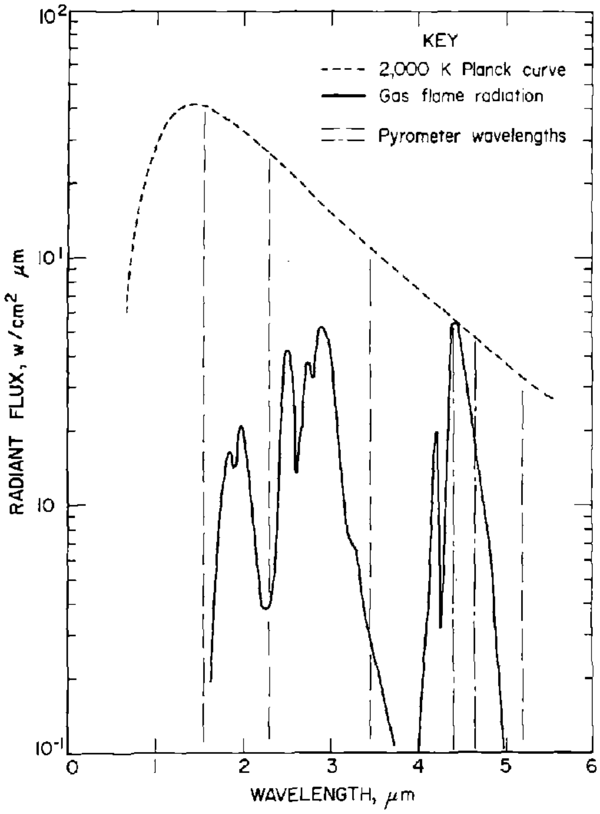

FIGURE 37. - Infrared spectrum of a 2,000 K methane-air flame at 2 atm pressure (adapted from fig. 1, BuMines RI 7779, p. 5). Vertical dashed lines show the wavelengths of the six-channel pyrometer for comparison

remaining two wavelengths (4.40 and 4.67 µm) of the pyrometer are used to characterize the gas flame temperature by measuring radiation from the hot CO_2 product gas. Note the strong gas emission band at these later two wavelengths in figure 37.

A cloud of hot dust particles emits continuum radiation similar to the dashed line Planck curve in figure 37. An individual dust particle emits continuum radiation but with an emissivity less than unity. However, the combined emitted and scattered radiation from an optically thick cloud of dust particles has an emissivity close to unity at all four of the dust wavelengths of the pyrometer. Similarly, an optically thick cloud of gas molecules will have an integrated emissivity of close to 1 at the two gas wavelengths. The gas flame shown in figure 37 is optically thick at the 4.40-µm wavelength but not at the 4.67-µm wavelength. An optically thick flame that includes both hot particles and gases will show a Planck continuum from the dust particles and either emission or absorption bands from the gases depending on whether the gases are hotter or cooler than the dust particles (21).

The data from the optical dust probe can be used to determine the optical thickness of the dust explosions if we assume that the emissivity of the hot dust is related to the transmission by the equation $\varepsilon = 1 - T$, where T is the measured transmission. The dust probe has a path length, $\ell = 3.8$ cm, and an effective extinction coefficient, $Q = 1.5$. In calculating the emissivity of the dust, the extinction coefficient is closer to 1.0 because both emitted and scattered radiation contribute to the integrated emissivity. Using the data from figure 18 and equation 2, the optical path length necessary to give an emissivity $\varepsilon = 0.95$ can be calculated for the 6.6-µm coal dust. At a dust concentration of 150 mg/l, an optical path length of about 23 cm would give $\varepsilon = 0.95$. At 400 mg/l, an optical path length of about 13 cm would give $\varepsilon = 0.95$. Although these calculations are based on the transmission of the dust probe at a wavelength of 0.95 µm, they are also approximately correct for the four dust wavelengths of the pyrometer. The reason is that the dust particle size is larger than the wavelength of light so that the extinction coefficient Q is relatively constant with wavelength. Since the actual optical path length through the dust cloud in the explosion chamber is 33.5 cm, the emissive cloud is optically thick and its emissivity is near unity for flames that fill at least the top half of the chamber.

For the carbon dioxide gas, the path length necessary to obtain an emissivity of 0.95 can also be calculated from the extinction values of Ferriso (13) at 2,000° K and an estimated CO_2 gas content of about 10 percent. For the 4.40-μm wavelength, a total optical path length of about 15 cm at 1 atm would give $\epsilon = 0.95$. For the 4.67-μm wavelength, an optical path length of about 100 cm at 1 atm would give $\epsilon = 0.95$. For the dimensions of the 8-liter apparatus, and the peak pressures observed, the total optical depth of the explosion fireballs are in the range of 70 to 200 cm-atm. Therefore, the 4.40-μm wavelength should always be optically thick, whereas the 4.67-μm wavelength should be thick only at the higher peak pressure ratios.

Since the previous discussion shows that the dust flames are optically thick, the dust temperatures can be calculated in the following manner. The relative radiation at each of the six wavelengths of the pyrometer is obtained by multiplying the measured voltage, V_λ, by the sensitivity factor, b_λ, at each wavelength. As described earlier in the apparatus section of this paper, the wavelength sensitivity factor, b_λ, is determined for each wavelength by a calibration of the pyrometer with the blackbody radiation standard. Equation 7 can be rewritten for the dust wavelengths as

$$b_\lambda V_\lambda = \frac{2a\epsilon\pi hc^2}{\lambda^5}\left[\exp(hc/\lambda kT)-1\right]^{-1}. \quad (8)$$

The only unknowns are a, ϵ, and T. Since observations are restricted to optically thick clouds, the emissivity, ϵ, is close to unity and is independent of wavelength. The value, a, is also independent of wavelength and therefore the two can be combined into one scale factor, $a\epsilon$. The dust temperature and scale factor are calculated by a nonlinear least squares fit to the above equation using the four experimental data points (relative radiation at each of the four dust wavelengths). An approximate calculation can be made with a small, portable, programmable calculator, or a more exact calculation with a large FORTRAN computer program. An example of a computer plot of the data is shown in figure 38. The radiation at the four dust particle continuum wavelengths is shown along with the best fit Planck curve through these points.

After the scale factor, $a\epsilon$, has been calculated using the radiation at the four dust wavelengths, the gas temperatures can be calculated at 4.40 and 4.67 μm by assuming the same scale factor to be applicable to those wavelengths. This assumption is generally valid for optically thick flames. However, the flame may be optically thin in the gas at 4.67 μm for some of the explosions. Therefore, that wavelength may see more radiation from the dust than from the gas and the temperature calculated would then be closer to the dust temperature than to the gas temperature. The radiation values at 4.40 and 4.67 μm are also shown in figure 38. The fact that these points lie above the best fit Planck curve for the dust particles means that the gas is at a higher temperature than the dust. For this explosion, both of the gas wavelengths appear to be optically thick.

The six-channel, infrared pyrometer was used to measure infrared radiation from explosions at several concentrations of 6.6-μm coal dust. The chamber pressure during the explosion was recorded continuously along with the

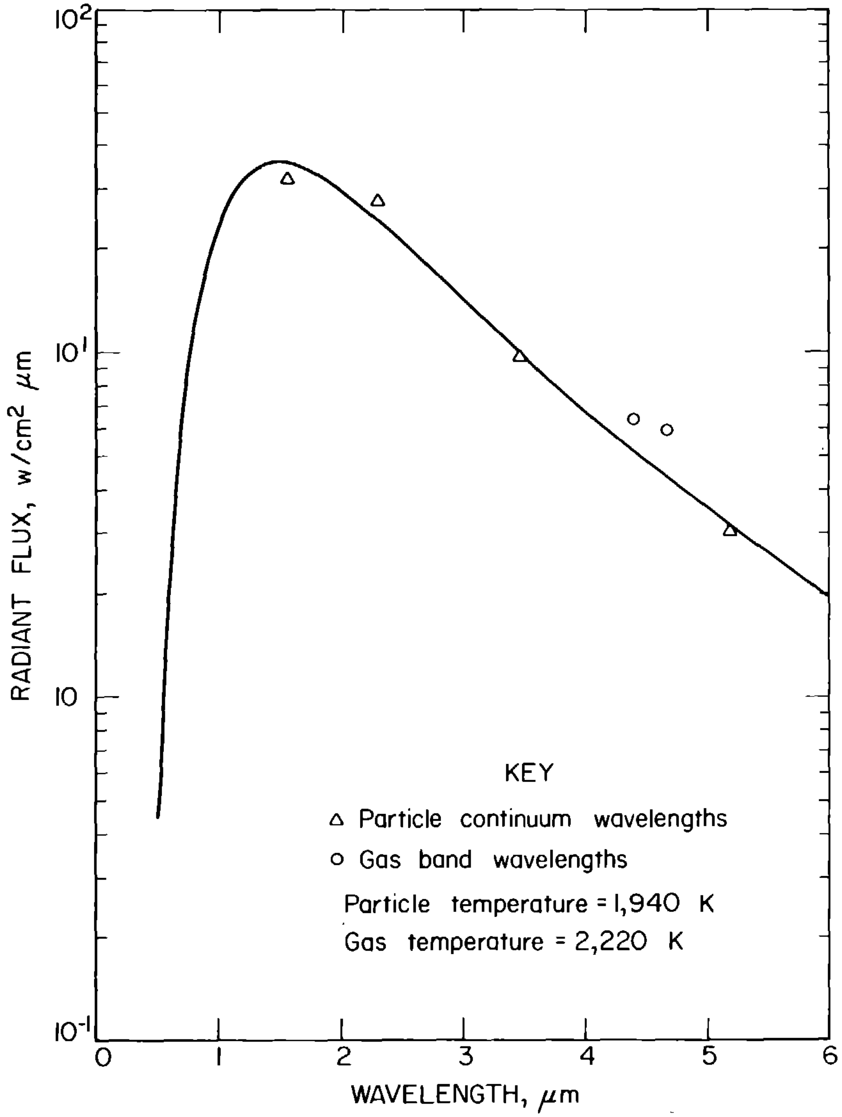

FIGURE 38. - Infrared radiation from a $d_s = 6.6$ μm Pittsburgh coal dust explosion measured at six wave lengths by the infrared pyrometer. The solid line shows the best fit Planck curve to the particle continuum radiation.

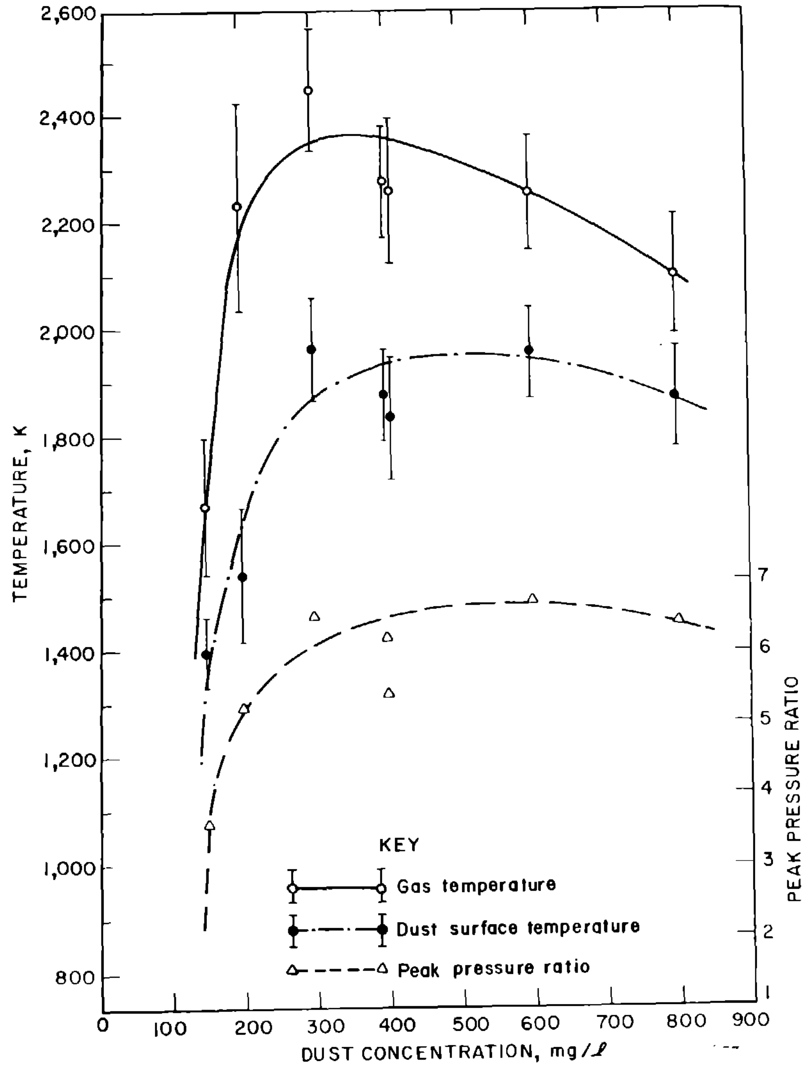

FIGURE 39. - Peak gas and dust-surface explosion temperatures as a function of dust concentration for 6.6-μm coal dust, obtained with the six-channel, infrared pyrometer. Comparison with peak pressure ratios shows the effects of adiabatic compression at constant volume.

radiance at the six wavelengths. The maximum radiance occurred at approximately the same time for all six wavelengths. This would correspond to the time the flame reached the window on the top of the 8-liter chamber, with the peak pressure occurring slightly later. Due to buoyancy, the flame front would reach the top flange before reaching the bottom of the chamber. The additional, later burning in the bottom part of the chamber causes the peak in the pressure trace to occur later than the peak radiance.

Figure 39 shows preliminary infrared temperature data obtained with the six-channel pyrometer for the 6.6-μm coal dust. For each explosion, the dust particle and gas flame temperatures were calculated from the measured radiance data at the time of maximum radiance. As described earlier, the dust temperature was calculated by the best fit to a Planck curve of the measured radiation at the four dust wavelengths. The gas temperature for each test is an average of the gas temperatures at the two gas wavelengths except for the 150 mg/l temperature which was based on the 4.4-μm wavelength only. The pressure ratios plotted in figure 39 are for the peak pressure that occurred slightly later than the time of maximum radiation which is when the temperatures were calculated.

The maximum measured value for the gas temperature in these dust-air explosions is about 2,400° K at a concentration of 300 mg/l, when the peak pressure ratio was 6.5. This temperature value is quite consistent with recent explosion temperatures of CH_4-air mixtures obtained from absolute radiance measurements in the 4.4- to 4.6-μm band (20) at comparable peak pressures. These maximum measured temperatures for both experiments are quite close to the calculated adiabatic values for the constant-volume combustion of stoichiometric hydrocarbon-air mixtures. For the 6.6-μm coal dust, the maximum in gas temperature occurs at C_m = 300 mg/l and this concentration is quite close to the value at which the burning velocity is a maximum for dust in this size range (37). It is also close to the concentration at which the ratio of combustible volatiles to air is effectively stoichiometric.

The dust surface temperatures are some 250 to 500° K cooler than the gas or flame temperatures. The largest difference occurs near this same concentration of 300 mg/l. These data tend to confirm a combustion mechanism which involves the devolatilization of coal particles to generate hydrocarbon gases which then combust in the gas phase. Gas phase temperatures are comparable to those obtained in premixed hydrocarbon gas combustion. The dust particles remain substantially cooler because of their larger density, their continuing pyrolysis, and the fact that the seat of the exothermic reaction is in the gas phase at a significant distance from the particle.

There are two effects reflected in the shapes of the temperature curves shown in figure 39; one is the effect of adiabatic compression, the other is the effect of dust concentration. The comparison of the temperature curves with the peak pressure ratio curve shows how adiabatic compression increases the temperature of both gas and dust. But it is difficult to ascribe the temperature variations to this effect alone without an independent measurement of how the temperature would vary as a function of concentration if the pressure were held constant. Both effects are superimposed in the data and it is difficult to separate them in these experiments. At the lowest concentrations studied (150 mg/l), the effect of adiabatic compression is at its minimum, and the flame temperature measured at that concentration was 1,600 to 1,700° K while the dust particle temperature was about 1,400° K. These values are only slightly higher than the values obtained with the six-channel pyrometer in recent mine experiments (33). In these full-scale mine explosion tests, flame zone pressures did not exceed 2 atm absolute and conditions were near the flammability limits. If the gas temperature curve in figure 39 is extrapolated to the lean-limit concentration of 135 mg/l, a value of 1,500° K is obtained for the limit flame temperature of a coal-dust air mixture. This value is nearly identical to the generally recognized limit flame temperature for premixed hydrocarbon gas combustion (6, 19). This is additional evidence to support the gas-phase hydrocarbon combustion mechanism as the driving force in coal dust explosions. The temperature data in figure 39 are preliminary data, and more detailed measurements for different sizes of dusts are in progress.

Inerting Requirements

Preliminary studies were made of the inerting requirements for coal dust with several additives: Purple K ($KHCO_3$), rock dust ($CaCO_3$), and salt (NaCl). The Purple K and salt have additives to make them free-flowing and nonhygroscopic. The coal dust used for these tests was the broad distribution with $\bar{d}_s$ = 21 μm. Some typical results are shown in figures 40-41 where the peak

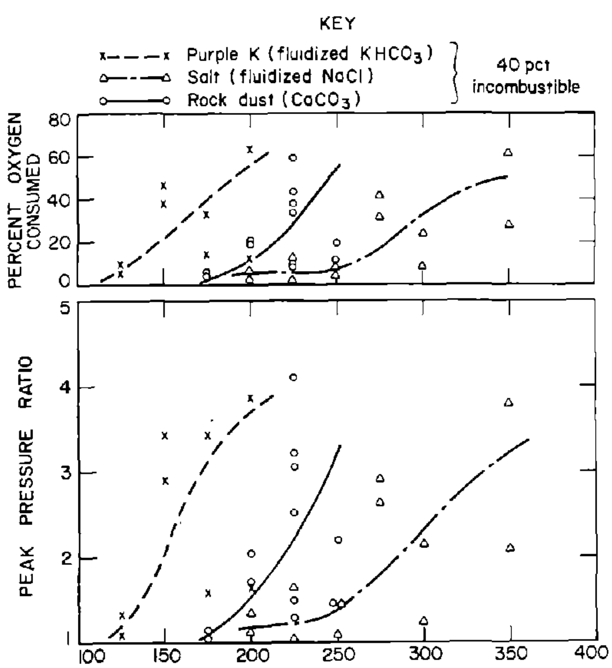

FIGURE 40. - Flammability data for Pittsburgh coal dust inerted to a 40 percent incombustible content with rock dust, $KHCO_3$, or NaCl. Percent of initial oxygen consumed and peak pressure ratio as a function of the coal dust concentration in the mixture.

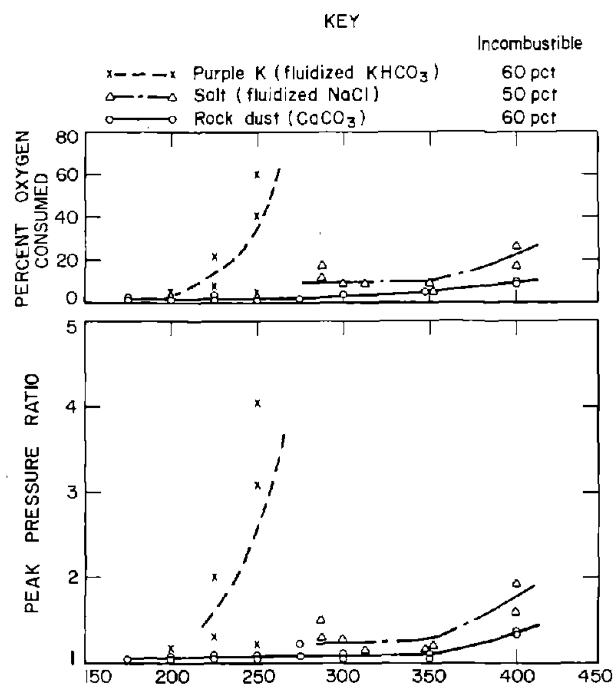

FIGURE 41. - Flammability data for Pittsburgh coal dust inerted to a 50 or 60 percent incombustible content with rock dust, $KHCO_3$, or NaCl. Percent of initial oxygen consumed and peak pressure ratio as a function of the coal dust concentration in the mixture.

pressure ratios and the percent oxygen consumed are plotted as a function of the coal dust concentration of the various coal-inert mixtures studied. The listed percent incombustible includes the 8 percent ash content of the coal in addition to the percent inert. For example, a coal dust concentration of 200 mg/l with 40 percent incombustible would include the 200 mg/l of coal and 106 mg/l of inert giving a total dust concentration of 306 mg/l. The incombustible fraction includes the 106 mg/l of inert and 16 mg/l of ash from the coal giving a total of 122 mg/l, or 40 percent of the total.

Figure 40 shows the results for 40 percent incombustible mixtures of the three coal-inert combinations studied. In figure 41, a coal-salt mixture with 50 percent incombustible is compared with coal-rock dust and coal-Purple K mixtures with 60 percent incombustible. Note that the horizontal axis includes only the coal dust portion of the total dust dispersed. Figure 40 shows that a 40 percent incombustible mixture of coal-Purple K has a lean limit of about 150 mg/l, only slightly above the lean limit (123 mg/l) for pure coal dust. Rock dust is somewhat more effective and raises the lean limit to about 220 mg/l. The NaCl salt is most effective and raises the limit to about 280 mg/l. Figure 41 shows that a 50 percent incombustible mixture of coal-salt or a 60 percent incombustible mixture of coal-rock dust were effective in inerting the mixture up to the highest concentrations studied (400 mg/l coal dust). However, a 60 percent incombustible mixture of Purple K-coal dust is only effective in inerting the mixture up to 240 mg/l coal dust. It should be noted that, at the highest coal dust concentration (400 mg/l), the total dust would be 920 mg/l; and it is quite possible that the disperser air jet is not able to lift and disperse this amount of dust. Therefore, the data for the highest coal dust concentrations in figure 41 should be viewed with caution.

Table 7 is a summary of the results for the three coal-inert mixtures. The listed lean limits are based on the criteria of a pressure rise ratio of 2 (from equation 6). As on figures 40-41, the lean-limit values include only the coal dust concentration fraction of the total coal dust-inert mixture. Table 7 includes the data from figures 40-41 along with additional data for 20 percent incombustible mixtures.

TABLE 7. - Lean-limit coal dust concentrations for three inerting agents

	Lean-limit coal dust concentrations, mg/l[1]			
Incombustible in mixture..percent..	20	40	50	60
Purple K........................	180	150	-	240
Rock dust.......................	150	220	-	>400
Salt............................	180	280	>400	-

[1] Milligrams per liter of coal dust in mixture.

Comparison of these lean-limit values for the three inerting agents clearly shows the following order of effectiveness:

NaCl Salt > Rock Dust > Purple K.

The NaCl salt performed the best, rock dust was intermediate, and Purple K was least effective. However, at the lowest inerting level (20 percent incombustible) studied, Purple K seemed to be about as effective as the salt.

Both the NaCl and $KHCO_3$ contained free-flowing agents whereas the rock dust did not. The probe transmission data showed clearly that the mixtures containing these two additives were dispersed more effectively than the rock dust mixtures. Accordingly, the rock-dust's better effectiveness than Purple K may be partly related to the reduced dispersibility of the rock-dust mixtures. The NaCl mixtures were dispersed as readily as the Purple K mixtures, and therefore its markedly superior effectiveness is probably related to its superiority as a chemical inhibiting agent in coal-dust explosions.

The data reported here corroborate results obtained in the Bruceton Experimental Mine and in a 6-ft-diam gallery (33). Such full-scale experiments require larger amounts of Purple K than rock dust to suppress explosions. The laboratory-scale results in this report and the full-scale studies are in marked contrast to some laboratory studies in ducts and burners that have reported effective inerting with Purple K concentrations as low as 10 percent (14, 36). The free-flowing salt was also tested in the 6-ft-diam gallery and its effectiveness was comparable to the laboratory-scale results reported here in figures 40-41 and in table 7. This is believed to be one of the first instances where laboratory-scale test data on inerting requirements gave comparable results to full-scale explosion tests.

Sampling Data and Photomicrographs

Post-explosion, dust-residue samples were taken after several of the experimental runs. These were studied by proximate analysis, ultimate analysis, and electron microscopy. Comparison of these dust residues with the original coal samples provided additional insight into the nature of the combustion process. The results of the proximate and ultimate analysis data for the 6.6-μm coal at several initial concentrations are shown in table 8. The original coal sample is compared with the post-explosion dust residues for the three concentrations. In the explosion runs, peak pressures were in the range of 6.0 to 6.5 atm, and maximum particle temperatures were 1,800 to 2,000° K. The data in table 8 are used only to show general trends and may not be exact representations of the entire dust residue from each test. The small size of the initial dust loadings, especially for the lower concentrations, made it difficult to collect enough residual dust for accurate analysis.

TABLE 8. - Proximate and ultimate analyses of post-explosion dust residues compared with the original coal $\bar{d}_s$ = 6.6 μm

Sample	As received				Moisture, ash free		
	Moisture, percent	Volatile matter, percent	Fixed carbon, percent	Ash, percent	Volatile matter, percent	Fixed carbon, percent	C:H ratio
Original coal....	2	33	56	9	37	63	1.3
Dust residue from 300 mg/l run....	5	-	-	22	-	-	1.8
Dust residue from 400 mg/l run....	3	20	60	16	25	75	-
Dust residue from 800 mg/l run....	4	17	66	13	21	79	2.0

The data in table 8 show a significant reduction in the volatile content of the dust residues remaining after the explosions. The C:H ratio of the dust residues is significantly higher than its initial value in the unburned coal. This indicates that the volatiles that are consumed by the explosion are richer in hydrogen than the original coal from which they were generated. These data are consistent with probe data obtained from laminar flame studies (29, 36). They tend to confirm the general picture of dust explosions as involving the generation of hydrocarbon volatiles from coal and their subsequent gas-phase combustion. It is difficult to judge whether the remaining volatile matter in the dust residues represents volatiles that were never vaporized or volatiles that were vaporized and then recondensed on the dust after cooling.

The residue samples were also photomicrographed with a scanning electron microscope. The results are shown in figure 42. Although the particles chosen for the figure are larger than the average (7 μm) for the dust used in the tests, their appearance is fairly representative of all the burned particles observed. The post-explosion dust particles show the characteristic blowhole appearance that is associated with the rapid evolution of volatiles. Their appearance is somewhat similar to that of coal particles that have traversed through laminar flames (37); however, there are some differences. For particles traversing through laminar flames, it appears that the entire particle becomes plastic and more spherical as pyrolysis occurs. The small difference in appearance between the two cases may be a reflection of the higher heating rate, higher final temperature, and shorter exposure time for the confined explosions studied in this report. Nonisothermal behavior for the larger particles is probably more likely under the conditions of these studies than in the laminar flame studies.

High-Speed Motion Pictures

Photographic observations of the shape and continuity of the combustion waves propagating in the 8-liter chamber were made with a high-speed motion picture camera. As described earlier in the paper, high-speed motion pictures were also taken of the dust dispersion process without ignition and of the electric match luminosity in the absence of dust. The movies of flame propagation were taken at 300 frames per second and the explosion was viewed from the top through a 2.5-cm-thick plastic cover plate. Some typical frames from two separate experiments at two different dust concentrations are shown in figures 43-44. Figure 43A is a still photograph showing a top view of the chamber with the cover plate removed. The dust probe, electric match array, and pile of dust in the dispersion cup are clearly visible. Frames B-L of figure 43 show the luminosity pattern generated during the course of a dust explosion of the 6.6-μm coal at a concentration of 150 mg/l. The time after ignition is indicated for each frame as well as the corresponding pressure at that time. Zero time corresponds to the instant of electrical initiation of the electric match ignitor array. Since the perspective is a top view of the chamber, any information on the shape and speed of the combustion wave applies only to the horizontal component of flame propagation. Information on the vertical component can be obtained only indirectly.

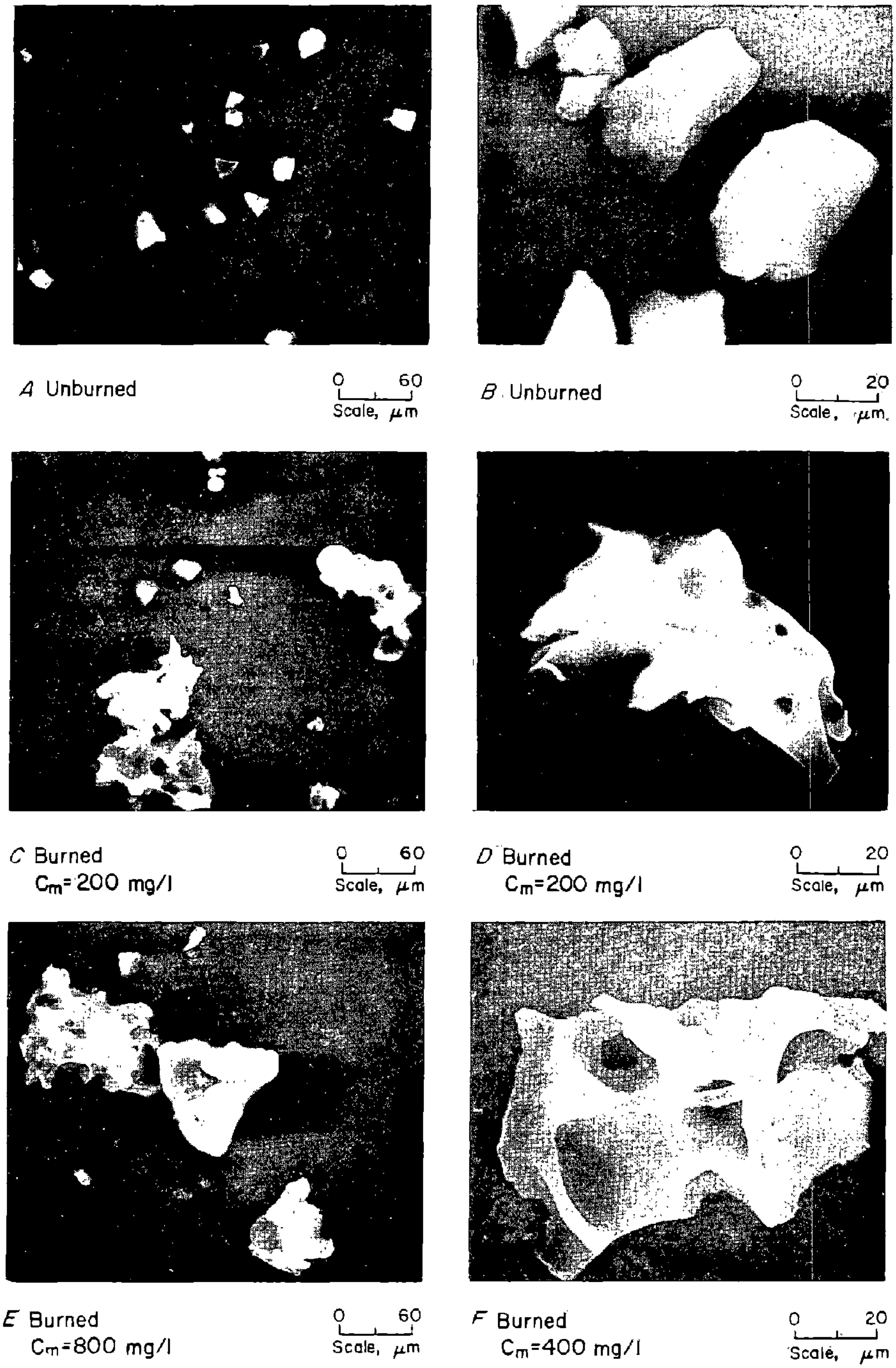

FIGURE 42. - Scanning electron microscope photographs of unburned and burned Pittsburgh coal dust.

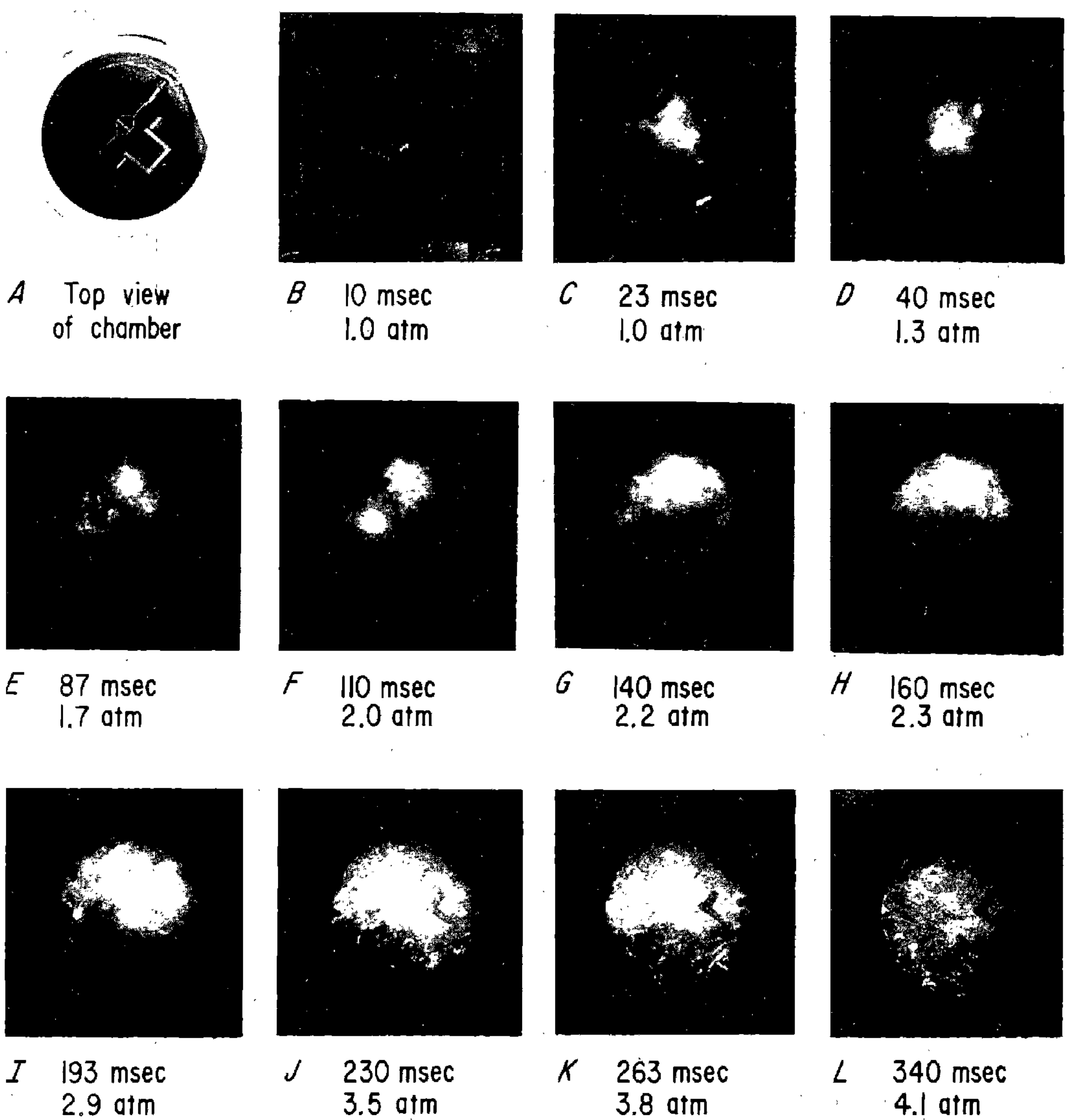

FIGURE 43. - Frames from a high-speed motion picture of a coal dust explosion at a dust concentration of 150 mg/l in the 8-liter flammability chamber. Note: The relative brightness on individual frames of the original movie film was not maintained on these prints of the frames.

In frame B of figure 43, 10 msec after the electric current energizes the ignitor, the match luminosity has just begun to appear. By frame C, the ignitor luminosity has increased markedly, and there may even be some localized coal dust combustion, but the pressure is still essentially atmospheric. This luminosity is no doubt partially obscured and diffused by the unburned dust between the match and the camera. By frame D, the overall ignitor luminosity appears to be decreasing, although a very bright fragment which was probably ejected upward is clearly visible. These ignitor fragments appear much brighter than the dust flame luminosity because of their higher temperature and because fragments thrown upward are seen without attenuation from the intervening dust cloud. By frame E, the ignitor luminosity is nearly gone, and a contiguous zone of dust combustion appears in the northern quadrant of the view field (north being defined as the top of the page). At this time, the chamber pressure is 1.7 atm. By frame F, the contiguous zone of coal dust combustion appears to have grown somewhat in size and another very bright ignitor fragment appears again temporarily. By frame G, the contiguous zone of dust combustion is the only feature left. It has grown in size so that it occupies most of the northern hemisphere in this top view of the chamber, and the pressure has risen to 2.2 atm. Frames G-K show the outward propagation of this contiguous zone until the flame front either reaches the chamber walls or spreads into the opposite side of the chamber. By frame K, the wave appears to have reached the wall nearly everywhere within the top view field of the chamber. The pressure at frame K is 3.8 atm and is nearly at its maximum value. Again, since the view is from the top, only horizontal components of the fireball motion are directly observable. However, note that from frame K to frame L, even though the luminosity has decayed significantly because of cooling of the fireball by contact with the walls, the pressure continued to increase until it reached the peak value of 4.1 atm at frame L. This is consistent with the six-channel pyrometer observations of the infrared radiation. When viewed from the top of the chamber, the maximum of the infrared radiation occurs before maximum pressure. Maximum radiation occurs when the fireball reaches the top window, and buoyancy causes the fireball to reach the top window before reaching the bottom of the chamber (20). The additional burning in the bottom parts of the chamber causes the additional pressure rise that occurs after the maximum in top-viewed radiation.

Note the patchy or streaked appearance of the luminosity from the surfaces of the dust particles in the outer regions of the fireball. The patchy appearance is most marked as the fireball approaches the top of the chamber so that it is unobscured by an intervening, unburned, dust cloud. This patchy or streaked appearance suggests localized variations in dust concentration and/or localized eddies in the residual turbulence from the dispersion pulse. These variations are most significant at the lower concentration. For example, if the spatial uniformity of the cloud is characterized as ±15 percent of its average value, then, although the average concentration is 150 mg/l, there would be regions where the concentration can be as low as 128 mg/l or as high as 172 mg/l. Propagation is not possible in the lower concentration regions since they are below the lean limit. Hence, flame propagation would be restricted to those regions where the concentrations were above about 130 mg/l, leading to the observed patchiness or streaked appearance. Similarly, residual velocity gradients from the dispersion pulse can either aid or quench the propagation of a near-limit wave depending upon the sign of the gradient relative to the propagation direction. This would again lead to a patchy or streaked appearance of the fireball.

Despite this uncertainty, there is a distinguishable leading edge of the fireball which, from frames H-K is propagating from the northern to the southern hemisphere of the view field. Its average horizontal component of flame speed is about 60 cm/sec which, for an expansion ratio of 5.0, would correspond to a horizontal burning velocity of 12 cm/sec. This value of burning velocity is consistent with measured values in a laminar flame at near-limit concentrations of 150 mg/l (37). These photographic burning velocity values are probably much more accurate than the crude calculations in tables 3-4 which were based on the time to reach peak pressure.

The data shown in figure 44 are for a much more rapidly propagating flame, at a dust concentration of 300 mg/l, which reaches a peak explosion pressure of 5.5 atm. Frame A of figure 44 is a view some 20 msec after the ignitor is energized. It shows the ignitor luminosity somewhat obscured and diffused by the dense, suspended dust cloud between the ignitor and the observer. Some bright fragments, that were probably ejected upward and toward the chamber walls, are also seen. In frame B a more general combustion luminosity appears in several regions, but is most intense in the central region of the chamber at the initial position of the ignitor. By frame C, two main, small fireballs appear to dominate in the center of the view field near the ignition point and the pressure has risen to 1.3 atm. Some of the ignitor fragments that were ejected away from the main ignition zone appear to be generating separate, localized zones of dust combustion. By frame D, the two central fireballs have merged into a single oval-shaped fireball. From frame D through frame J, this central, contiguous fireball propagates outward preserving its initial shape, until its extremities actually contact the chamber wall. By frame J, the fireball has enveloped the entire view field and the chamber pressure is rising at a very rapid rate. Some upward propagation into the corner regions of the chamber, and downward propagation toward the dust cup at the bottom, probably continues until frame K, where the pressure peaks at 5.5 atm. Some wall-cooling of the outer regions of the fireball is apparent even at the peak pressure in frame K. This cooling is more pronounced in frame L, where it has caused the pressure to drop to 4.8 atm.

In frames D-G of figure 44, the central fireball expands outward at a propagation rate of 250 to 350 cm/sec. This horizontal component of flame speed, if divided by an expected expansion ratio of about 6.5, corresponds to a burning velocity of 40 to 50 cm/sec. This value is somewhat higher than the maximum values of 30 to 40 cm/sec measured for laminar burner flames at comparable concentrations (37). It is uncertain whether this difference is due to residual turbulence in the 8-liter vessel or could be accounted for by the inherent errors in both experimental measurements.

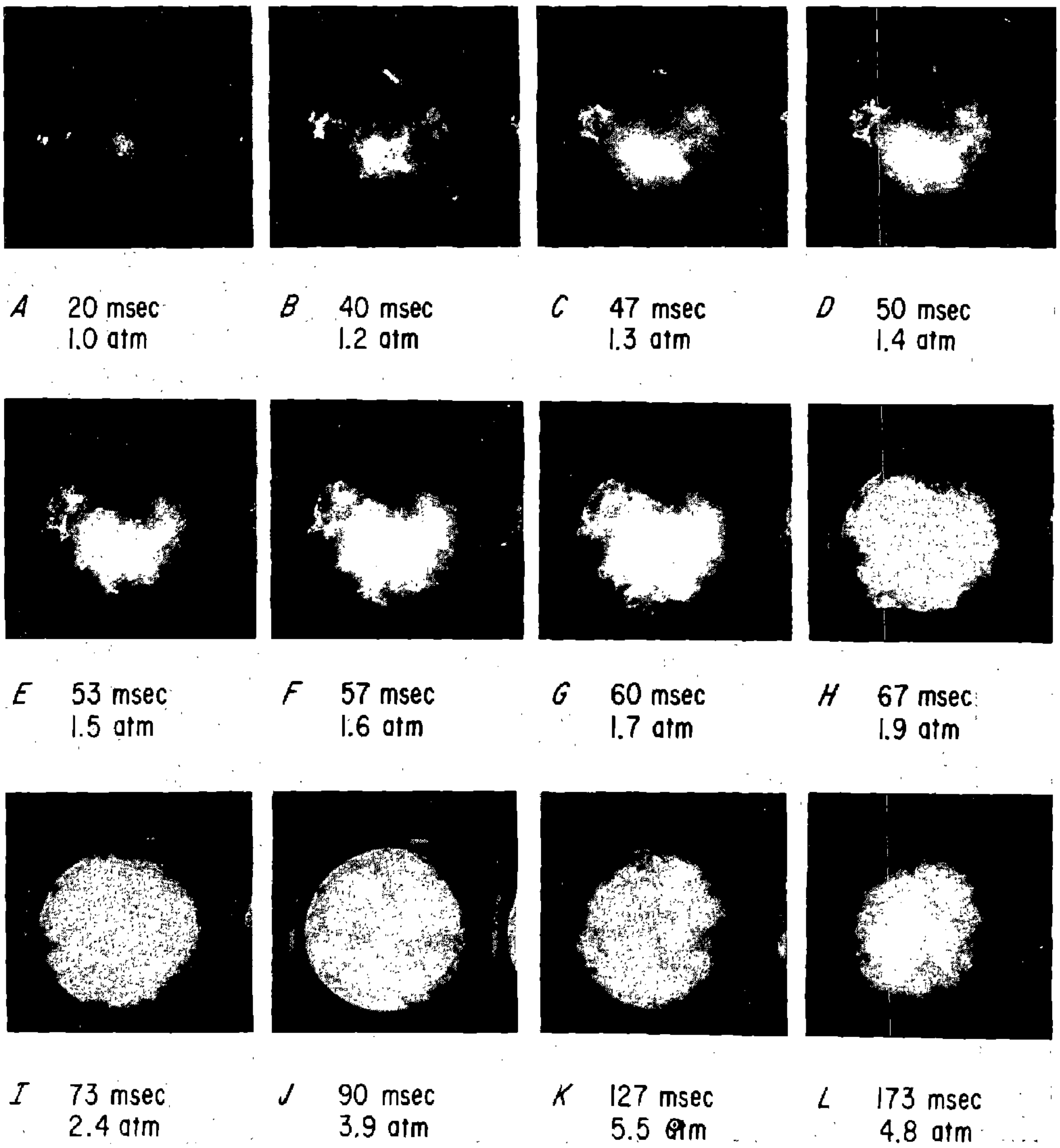

FIGURE 44. - Frames from a high-speed motion picture of a coal dust explosion at a dust concentration of 300 mg/l in the 8-liter flammability chamber. Note: The relative brightness on individual frames of the original movie film was not maintained on these prints of the frames.

DISCUSSION AND INTERPRETATION

The measured lean limit for near horizontal propagation of Pittsburgh seam coal dust is here reported to be 135 mg/l and to be size invariant for the nine size distributions studied (table 2). The values reported in the literature vary almost continuously from below 30 mg/l to above 300 mg/l, and therefore many of the reported values differ significantly from the values in table 2. For example, the "accepted" or Handbook value (31) is 55 mg/l. An attempt will be made here to compare these various reported values of lean limits and to evaluate the dispersion methods, ignition energies, and limit criteria of the various researchers. Clearly, if the different experimental methods are described in sufficient detail, a judgment can be made as to which data are more accurate and reliable.

The variously reported values for Pittsburgh seam coal dust (or coal of similar rank and volatility) are tabulated and categorized in table 9. The lean-limit value from this report and 14 previously reported values are listed. The tabulation is not meant to be comprehensive, but it does cover the range of reported data. In most instances, the tabulated lean-limit values are those recommended by the authors, although in a few instances they are estimates, inferred from the data or read from the published graphs.

TABLE 9. - Evaluation of previous lean-limit measurements

Lean limit, mg/l	Reference	Dispersion method	Ignition energy	Propagation criteria	Concentration measurement
123-145	Present	V	a	$\dot{p}_v$, h	N, T, g
5	(15)	V	m	p_v, s	N, p
35	(15)	V	i	p_v, s	N, p
30-50	(34)	F	a	l, s	M_f, g
40	(24)	T	a	?, ?	M, T, g
50-60	(10, 17, 30, 31)	V	i	p_v, s	N, p
50	(16)	M	a	l, h	L, p
50-60	(9)	M	a	l, h	L, p
60	(32)	M	a	l, h	L, p
60-100	(3-4)	V	m-a	p_v, h	N, ?
50-150	(18)	V	a	$\dot{p}_v$, h	N, ?
85-125	(39)	F	a	l, m	M, g
100-140	(36-37)	F	a	b, m	M_f, g
140-180	(2)	F	m	l, h	M_f ?, T, ?
240-310	(27)	F	m-a	l, m	M, T, ?

Each listed value in table 9 is categorized in terms of the method of dust dispersion, the strength and adequacy of the ignition energy, the chosen criteria for flame propagation, the method of measuring dust concentration, and the uniformity of dust dispersion.

For the first category, there are four basic methods of dust dispersion as follows.

V = air jet, impulse dispersion of a known mass of dust in a fixed volume (Hartmann or similar type apparatus).

F = gravity and/or airflow dispersion in an open tube.

M = open, large-scale mine gallery with flow induced, self-dispersion by an expanding turbulent flame.

T = gravity-tumbler dispersion of some fraction of the dust in a fixed volume.

For the second category, the strength or adequacy of the ignition energy used by the various researchers is evaluated as

a = adequate.

m = marginal.

i = inadequate.

The tabulated data are so categorized according to the type of source used and whether the available energy from the various ignition sources could be expected to satisfy the measured ignition energy requirements shown in figures 11-12. An "adequate" ignition source would correspond to the energy of at least several electric matches. An "inadequate" ignition source would correspond to the energy of the transformer spark discharge of figure 11.

The third category relates to the flame propagation criteria chosen by the various investigators; that is, the extent or quality of flame propagation that was considered necessary to have exceeded the limit condition. There are two elements in this category: The observational method itself and a rating of the criteria chosen. The observational methods include the following:

p_v = pressure attained at constant volume.

$\dot{p}_v$ = rate of pressure rise at constant volume.

l = length of flame travel.

b = ability to stabilize a burner flame in steady-state.

? = unknown, not specified.

The rating of these methods and criteria are as follows:

h = hard.

m = moderate.

s = soft.

The methods are rated according to whether the criteria chosen is realistic in relation to the normally accepted criteria for premixed gases (6, 8, 19, 40). A "hard" criteria would be at least as strict as that chosen to characterize the limit for horizontal flame propagation in a premixed gas. A "moderate" criteria would be comparable to the normal upward limit criteria. A "soft" criteria would be one that would not normally be acceptable in the conventional apparatus even as an upward limit.

The final category relates to the method of measuring or inferring the dust concentration. There are two elements in this category, a description of the method of measurement and an estimate of the uniformity of the dust dispersion. The measuring methods are as follows:

N = nominal concentration (known mass dispersed in a known constant volume).

L = nominal loading (known mass per unit volume desposited along a fixed linear dimension in an open-ended gallery or mine entry of constant cross section).

M_f = measured mass collected in a known airflow during a known time.

M = measured mass collected in a known volume independent of velocity or travel time.

T = relative concentration and/or uniformity monitored by light transmission.

The estimates of dust cloud uniformity (based mainly on the investigators' published evaluations) are

g = good,

p = poor,

? = unknown,

where "good" refers to a fairly uniform dust dispersion and "poor" refers to dispersions where the concentration varies by a factor of 2 or more in various regions of the dust cloud.

These evaluations relating to the adequacy of ignition energy, stringency of the propagation criteria, and uniformity of dust dispersion require a detailed justification. The following discussion contains the justification for the judgments made in the last three columns of table 9. Included is an overall evaluation of the experimental and observational methods used by the various researchers and a discussion of the causes for the apparent differences in the reported lean-limit values. Also included is a discussion of the value reported here (135 mg/l) and an estimate of the uncertainties and systematic errors in the data.

First, consider the large-scale mine gallery results listed as method M. The three reports (9, 16, 32) list a lean limit of 50 to 60 mg/l. In these studies the concentration refers to a nominal dust loading on the walls and floor of the mine. The listed nominal concentration assumes that the dust, when dispersed, is distributed uniformly throughout the cross section and is confined to the length of dusted zone. In such experiments the strength of the ignition source is usually quite adequate, a large explosive charge or a large, premixed methane-air volume. The propagation criteria involves propagation to a length at least equal to the length of the zone dusted, or in the Bureau studies, the criteria is that the pressure at or behind the flame front be maintained or continue to rise as the wave advances through the length of zone dusted. These are considered "hard" conditions for any zone whose length is a reasonable multiple of the diameter (a factor of 10 or so larger). In these studies, the dust is lifted off the confining surfaces (or shelves) by the turbulent airflows that develop ahead of an expanding flame front, which is also turbulent. Thus, the dust dispersion and flame propagation processes are mutually coupled and are occurring simultaneously. Most observations indicate that the dust is not homogeneously distributed throughout the entry, and this is certainly true during the early stages of flame development. Recent studies with the optical dust probe in the Bruceton Experimental Mine also show clearly that actual dust concentrations at the time of flame arrival increase continuously as the explosion propagates down the mine gallery (26, 32). Such a result is quite consistent with a flame front whose speed is continuously accelerated by turbulence. Dust near the flame front advances at an increasing velocity and overtakes the dust ahead of it, causing an effective increase in concentration as the wave moves down the entry. The actual concentration levels attained may be far in excess of the nominal dust loadings. Those data, together with our current concepts of the mechanism by which the dust is lifted (35), clearly indicate that the nominal dust loading is not a realistic measure of the actual dust concentration in the mine gallery. Actual concentrations immediately ahead of the flame front vary markedly both spatially and temporally.

Because of this complexity, it is difficult to relate the minimum nominal mine loading of 50 to 60 mg/l with our lean-limit value of 135 mg/l. The former is a nominal dust loading, the latter is a concentration of uniformly dispersed, airborne dust. It is important to recognize the difference between these two quantities. For the practical application of determining whether the dust loading in a mine is hazardous, the 50- to 60-mg/l value is appropriate. For the practical situation where an airborne cloud of dust already exists, and its concentration can be measured, the higher value of 135 mg/l is applicable. In any case, it is this latter value which is more fundamental. It corresponds to a real limit concentration for the conventional premixed system.

Now, consider the previous work with the 1.2-liter Hartmann apparatus (10, 15, 17, 30, 31). Although the dispersion method is the same as that used in the present study, there are differences in the uniformity of the dust cloud at the time of ignition, the adequacy of the ignition source, and the stringency of the propagation criteria. The lean-limit values for Pittsburgh coal reported by earlier researchers using the Hartmann apparatus are 5, 35, and 50 to 60 mg/l. The apparatus and method are described in reference 10. A continuous electrical discharge is activated before the dust is dispersed by an air jet. The dust cloud is ignited as it is rising between the electrodes. The flame propagation or limit criteria is the rupture of a paper diaphragm on the top of the chamber at an overpressure of 0.1 to 0.2 atm. In the notation of the present report, this would correspond to a pressure ratio of 1.1 to 1.2. This is a much softer criteria than the pressure ratio of 2.0 used in the present report.

The concentrations quoted in the previous Hartmann work are nominal, although it is indicated that the actual concentrations in the chamber were not uniform (10). Photographic evidence from independent investigators (12) shows that less than half of the chamber volume is filled with dust when the cloud is ignited. The optical dust probe data in figures 4-5 also show that the dust is initially lifted en masse by the airblast dispersion impulse and that about 0.2 sec is required for a relatively uniform dust cloud to be established. Therefore, if the ignition source is activated before the dispersion pulse is turned on, then a very high dust concentration passes momentarily through the continuous spark discharge. Even though this continuous transformer discharge is inadequate for ignition of low concentrations of uniformly dispersed dust (fig. 11), it is adequate for igniting the momentarily high concentrations that are present as the dust is initially lifted. The inadequacy of the ignition source is compensated for by supplying a high dust concentration during the dispersion transient. In the previous Hartmann work, the ignition, dispersion, and flame propagation events are overlapping in time. Also, the propagation criteria of a pressure ratio of 1.1 to 1.2 is a very soft criteria. The previous investigators realized these problems, but had designed the experimental method of the 1.2-liter Hartmann chamber so that the lean-limit values would correspond to the results obtained in the Experimental Mine (10, 31). Therefore, it is not surprising that the reported lean-limit value of 50 to 60 mg/l from the previous Hartmann chamber reports (10, 30-31) agrees with the 50 mg/l minimum nominal loading for the mine (16). The lowest reported values with the 1.2-liter Hartmann vessel were 35 mg/l for an electric spark discharge and 5 mg/l for an ignition with guncotton. The latter value probably represents an extreme case. A nonuniform dust concentration of momentarily high concentration is ignited as it passes through the ignition volume and the slight overpressure created is sufficient to rupture the paper diaphragm.

The above argument may be presented in a more concrete form as follows. Consider a 1-liter explosion chamber into which a charge of 50 mg of dust has been placed to give a nominal concentration of 50 mg/l. Dispersion causes the dust to be lifted en masse, and let us assume that during its initial traverse through the ignition electrodes, the cloud occupies only one-eighth of the chamber volume. Thus, its momentary concentration is 400 mg/l. If the continuous transformer discharge is on, this high concentration is readily ignited (fig. 11). Since the propagation rate is relatively rapid at this high concentration, it can be assumed that the dust cloud is consumed rapidly by the flame. It is plausibly assumed that it would have dispersed to occupy one-fourth of the chamber volume during the time of flame propagation. For an expansion ratio (ratio of unburned to burned gas density) of six, a peak explosion pressure of (3/4) 1 + (1/4) 6 = 2.2 atm would be obtained. This would certainly be sufficient to rupture the paper diaphragm and it would thus erroneously be concluded that the mixture containing 50 mg/l was flammable. The above calculation, however, shows that the propagation process could actually have occurred in a dust cloud whose concentration was 400 mg/l at ignition, and was decreasing to 200 mg/l during propagation. The above calculation is only meant as a plausibility argument for the 50-mg/l value in the 1.2-liter Hartmann chamber. It is not meant to be an exact analysis of those experiments.

Clearly, the apparent lean limit that would be obtained in a system in which the ignition discharge is activated before the dust is effectively dispersed would depend on many uncontrollable factors. It would be sensitive to the strength of the ignition source and the extent to which an inadequate ignition energy could be compensated for by a momentarily high dust concentration. It would therefore also be highly sensitive to the transitory nature of the dust dispersion process and to the stringency of the propagation criteria.

Ishihama and Enomoto (24) report a 40-mg/l lean-limit value for a gravity-tumbler type dispersion system. The experimental method (23-24) involves the dispersion of some fraction (about 1/3) of the dust in a fixed volume by rotating a cylindrical combustion chamber about its axis. Dust, falling from the top, collects at the bottom and is redispersed when the bottom rotates upward to become the top. It is difficult to evaluate the 40-mg/l value because the propagation criteria is not given. However, by comparison with the peak pressure data obtained by the same investigators, it would appear that an extremely soft propagation criteria must have been used. The reported pressure rise values for a coal of volatility comparable to Pittsburgh seam show that concentrations of approximately 250 mg/l are required to obtain a peak explosion pressure of 3 atm. The extrapolation of these pressure curves, to find a lean limit at a peak explosion pressure of 2 atm, appears to be inconsistent with the 40-mg/l value mentioned in the discussion section of the report.

The ignition source for this system was 100 mg of guncotton plus an electric detonator fusehead. The ignition energy is probably equivalent to the energy of several electric matches and therefore is considered adequate. Concentrations were measured by the rapid insertion of a dust-collecting cylinder of known volume into the center of the tumbling chamber and then weighing the mass of dust collected. The uniformity of the dust dispersion was evaluated through light transmission measurements and it was reported to be relatively uniform near the center of the vessel (23). The actual quantity of dust that is airborne at any instant of time is only about 1/3 of the dust initially charged into the tumbler. The remaining 2/3 is collecting on the "teeth" of the chamber wall, or is in various stages of dispersion and collection.

Extrapolation of the pressure curves for this gravity-tumbler system (23-24) appears to give a lean-limit value of 150 to 200 mg/l based on the propagation criteria of a pressure rise of 1 atm or equivalently, a pressure ratio of 2. Based on the large uncertainty in the extrapolation, these data do not seem to be inconsistent with the lean-limit values of the present report. The gravity-tumbler data do agree with the present report regarding the lack of particle-size dependence near the lean limit. For the more volatile coals studied in references 23-24, explosion pressures tend to converge to the same values at lower concentrations independent of particle size.

In the gravity-tumbler, the maximum pressures at higher concentrations are lower than the values reported in this report. For a coal of similar volatility to Pittsburgh coal, the maximum pressure rise is about 3.7 atm (or a pressure ratio of 4.7) at a concentration of about 1,000 mg/l. In the present report, pressure ratios greater than 6 were measured at much lower concentrations (400 to 600 mg/l).

Bartknecht (3-4) has studied dust explosions in several large closed vessels. He does not specifically list lean-limit values, but approximate limits can be determined from the graphs of explosion pressure versus concentration. The lowest concentrations for which there are significant pressure rises are 60 to 100 mg/l. The volatility of the coal dust used was not reported. The vessels used are 10 and 1,000 liters and the dust is dispersed by air jets. Ignition occurs after dispersion and the ignition source is a chemical igniter, perhaps similar to the electric matches used in the present report. The reported concentrations are apparently nominal values, a measured mass of dust in the volume of the chamber. The uniformity of the dispersion was not reported. Due to the lack of details regarding the uniformity of the dispersion, the volatility of the coal, and the strength of the ignition source, it is difficult to evaluate the data. The lean limit is perhaps lower than those of the present report due to a less uniform dust cloud; however, this is only speculation. It is also possible that there are effects due to the size of the explosion chamber and that these lower values for the lean limit are real. The maximum explosion pressure rise for coal dust in the 1,000-liter vessel was about 7.8 atm, significantly larger than the pressures attained in the 8-liter vessel of the present report. The maximum rates of pressure rise are also considerably larger than those of the present report, probably due to a higher turbulence in the dust cloud at the time of ignition (11).

Helwig (18) has also studied coal dust explosions in large closed vessels. The dust dispersion method involves the use of very high air flows (high Froude numbers) in a 115-liter chamber. Dust is fed into a turbulence chamber and is then dispersed throughout the main chamber by an array of internal nozzles. Dispersion is accomplished apparently by a very intense air jet impulse, a "whirling up air shock." Although detailed measurements of spatial or temporal dust concentration distributions are not reported in reference 18, it is probable that concentrations were reasonably homogeneous. The concentrations reported are presumably nominal. Ignition was achieved when 1.2 g of a pyrotechnic mixture of zirconium-barium nitrate, triggered by a primer, was propelled into the explosion chamber. This ignition system is categorized as adequate.

The coal dust used had a volatility of 28 percent. Helwig lists two lean-limit values: a "lower ignition limit" of 50 mg/l and a "lower limit of explosion propagation" of 150 mg/l. The criteria for the "lower ignition limit" are not specifically reported. The "lower limit of explosion propagation" is based on an explosion index, which is the product of the mean and maximum pressure rise rates. Using the pressure versus concentration graphs of reference 18 and a pressure ratio of 2 to 3 as the limit criteria, a lean limit of 100 to 120 mg/l is obtained. Considering the lower volatility of the coal used, this limit value would have to be considered significantly lower than the limit values of the present report. A possible reason for this lower value for the lean limit is the unknown spatial distribution of the dust in the vessel. Another possibility, as with Bartknecht's results, is that the lean limit is actually lower in the very large vessels than in the 8-liter vessel of this report.

The rates of pressure rise are larger in Helwig's 115-liter chamber, probably due to the higher turbulence. The general shape of the pressure versus concentration curve is similar to those of figures 13, 15, 17, 19, 21, 23, 25, 27, and 29, in that there is a rather steep rise to a maximum pressure of 6 to 7 atm at about double the lean-limit concentration and then the curve remains relatively constant for higher concentrations.

Finally, we consider the lean limits obtained in flowing systems. There are two main types of methods. In one a steady-state burner flame is stabilized at one position in space, whereas in the other the flame propagates through the length of a duct.

Smoot and others (36-37) studied coal dust propagation by maintaining a laminar burner flame in steady-state. Predispersed coal is fed into a laminar flow burner and a steady-state flame front is maintained by balancing the inlet flow velocity of the coal-air mixture against its burning velocity. The values listed in table 7, 100 to 140 mg/l, are inferred to be the lean-limit values because they were the leanest concentrations that could be maintained as stable flames on the 10-cm-diam burner. Since the coal-air feed is downward, the flame is propagating upward and hence the inferred values are for a moderate propagation criteria. The range of values may reflect the experimental errors in the burning velocity measurements and the difficulty in maintaining uniform and controllable dust concentrations at low dust and air feed rates. For a steady-state flame front, there is no distinction necessary between the static and dynamic concentrations. The actual concentration is given by the ratio of the dust feed rate to the air feed rate regardless of the dust's sedimentation velocity. This is true whether the flow is upward or downward as long as all the flowing dust and air pass through the stationary flame front. These coal dust burner flames are initiated with methane added to the air to guarantee ignition, then the methane is reduced to zero. Therefore, the ignition energy for this burner is adequate. The limits obtained by this burner flame method agree fairly well with the values (123 to 145 mg/l) in the present report. The slight differences may be due to experimental errors in both methods and the fact that the propagation in the burner was upward while the propagation criteria used in the present report would correspond to horizontal propagation. Also in agreement with the present report, the burner flame data show a lean limit that is relatively independent of particle size.

The lowest lean-limit value for a flowing system is 30 to 50 mg/l by Singer, Cook and Grumer (34). In their experiment, dust was suspended in an airstream flowing upward through an open tube. Dust concentrations were measured by collecting the entire flow on a filter at various heights and by using a 1-cm-diam sampling probe. Concentrations were reported to be uniform within ±20 percent. The main reason for the low values of the lean limit was the "overdriven" ignition. The ignition source was a 76-cm^3 bomb of stoichiometric methane-oxygen mixture that shot a 13-cm-long jet into the coal dust-air mixture. The criteria of propagation were flame luminosity observed throughout the chamber and the rupture of a paper diaphragm at about 15 to 20 cm from the ignition jet. When using this ignition source and propagation criteria to study the ignition of methane-air mixtures, Singer and others (34) found that a 4.3 percent methane concentration was ignited. Since the accepted lean limit for methane is 5 percent, they considered the ignition to be "overdriven." The ignition would presumably be "overdriven" for the coal dust-air mixtures also, leading to the rather low reported lean limits of 30 to 50 mg/l. Using weaker ignition sources, they obtained lean-limit values for coal dust-air that were more than double the above values. Their reason for studying the "overdriven" ignition condition was the practical hazard of a strong ignition source communicating a flame for a short distance through a dust cloud of low concentration to a dust cloud of higher concentration that would then be able to sustain the flame by itself.

There are several additional problems regarding the measurement of dust concentrations in flowing systems where the flame propagates through a duct or tube. These problems are discussed in detail by Beachey, O'Donnell, and Milne (5). Concentrations are usually inferred by collecting the dust on a filter for a fixed time and then dividing the measured mass flow rate by the measured volumetric airflow rate. However, if the particle velocities differ from the gas velocity, the above method will not give the true concentration. In calculating the true concentration, the settling velocities of the dust particles relative to the air must be considered. In a downward flowing system, the actual (static) concentrations are lower than the value obtained from the ratio of the dust flow rate to the gas flow rate. In an upward flowing system, the opposite is true. The flame velocity provides an additional complication since the dust concentration that a propagating flame will see in a flowing system depends on both the settling velocity and the flame velocity. When both the particle settling velocity and the flame velocity relative to the air velocity are considered, the true concentration observed by the flame front can differ considerably (either higher or lower) from the value inferred from the ratio of the dust flow rate to the gas flow rate. This complication relates to the important distinction between the static dust concentration and its dynamic value with respect to a moving flame front (5, 27). For dusts (or droplets) dispersed in ducts, gravitational sedimentation causes dust velocities to differ from air velocities. For aggregate masses of dusts, settling velocities (relative to the airstream) can far exceed Stokes' velocities for the individual particles (27). The simplest cases to consider are those in which the flame propagation process does not significantly alter the initial flow conditions. Consider, for example, upward propagation through an open tube in which the upward propagating flame front moves into a stationary gas containing a sedimenting dust cloud. The moving flame front thus encounters a higher input mass flow of dust per unit time than of air, and accordingly, the dust concentration relative to the moving flame front can be substantially higher than the static or volume concentration in the laboratory reference frame. Similarly, a flame front moving in the direction of sedimentation would encounter a lower input mass flux of dust than of air, and hence its dynamic (or kinetic) concentration is less than its static value.

In any real case of flame propagation, it is exceedingly difficult to apply this correction factor because the propagation process itself can markedly alter the preexisting velocity distributions of both dust and air. Nevertheless, any process which is capable of inducing a difference between dust and air velocities, in combination with any observation method which is nonsteady-state and directional, will cause dynamic concentrations with respect to the flame to differ from their static values.

This complication would appear to apply mainly to dispersion method F, which involves gravitational dispersion in ducts, where sedimentation velocities and flame front velocities are both vertical. In the flow-induced, self-dispersal process in horizontal mine galleries (method M), sedimentation velocities would be orthogonal to flame velocities and are trivial in magnitude relative to flame speeds. Thus, correction factors due to sedimentation velocities are probably insignificant. Sedimentation velocities in the Hartmann-type method (V) are usually insignificant, but for the tumbler method (T), they are in fact used to effect dispersion. However, in both of these methods, if the harder propagation criteria are used, the propagation is omnidirectional. For omnidirectional propagation, the correction factors with respect to sedimentation velocities are either zero (for horizontal propagation) or tend to cancel (for the upward and downward cases). In addition, radial accelerations are small for central ignition in a constant-volume chamber, especially as limit conditions are approached. Accordingly, dust particle lags in the accelerating flows are probably not significant for methods V or T. Thus, this complication of distinguishing between static and dynamic concentrations is probably insignificant for methods V and T. For the stationary (burner) flame front (37), static and dynamic concentrations are identical, and the complication does not exist.

In flowing systems, the problem is even more complex. Detailed studies of the dispersion pattern of falling dust clouds in a duct containing initially static air, show that a complex recirculation pattern is induced by the falling dust (28). These induced airflows cause marked inhomogeneities in the dust-dispersion pattern and particle size segregation effects. The recirculation pattern consists first of an upper cell in which air flows downward in the axial regions and upward next to the tube wall. Below this is a lower cell in which air flows upward near the axis and downward near the walls. In the upper cell region of the tube, dust tends to congregate near the axis as it falls, and in the lower regions dust tends to deflect towards the walls. The air recirculation pattern in the lower part of the duct actually carries the finer dust particles upward against gravity. This complex recirculation pattern persists even in the presence of substantial superimposed downward airflows. In addition, the measured settling velocities for the aggregated mass of dust will, in general, far exceed the Stokes' free-fall velocity for the individual particles by more than an order of magnitude (27).

Yu and Chao (39) reported a lean limit of 85 to 125 mg/l for coal with 34 to 37 percent volatile matter (on a moisture-free basis) and about 7 to 8 percent ash. The dust was dispersed by gravitational settling in 60-cm-long by 7.5-cm-diam open tube. Ignition was with a platinum wire ignitor, preheated to about 1,400° K, which was plunged into the tube after a steady-state cloud was established. The ignitor shown would appear to extend the full width of the tube when inserted, In terms of energy available and rate of energy input, such an ignitor is certainly adequate. If the source were of small dimensions, the temperature might be considered marginal; however, for the size of ignitor indicated, 1,400° K would certainly exceed any conceivable autoignition temperature for the hydrocarbon constituents of volatilizing coal. The ignitor used is thus considered adequate. The limit criteria was upward flame travel from the ignitor to the top of the tube, a distance of 46 cm. This is a moderate limit condition. The concentrations reported were the static concentrations, measured by collecting and weighing all the coal dust instantaneously suspended in the tube volume, and therefore there is no correction due to the settling velocity. The uniformity or homogeneity of the dust cloud is uncertain. There is a reported deviation in density of 10 to 20 percent, but it is uncertain whether this refers to the accuracy with which the average concentration is known or to the variations in concentration at different spatial positions. The dispersion method is similar to one in which complex recirculation patterns were induced by falling dust (28). However, the length and diameter of the tubes are different. With a tube length of only 60 cm, it is uncertain whether a significant recirculation would exist in this case. If an upper recirculation cell (similar to that in reference 28) did exist, the dust concentration would tend to be higher along the axis than at the walls. Also, since the flame is propagating up the tube, the concentration that the flame sees would be higher than the measured static concentration. Considering the possible corrections to the measured dust concentration and the softer limit criteria of upward rather than horizontal propagation, the listed limit values of 85 to 125 mg/l do not seem inconsistent with the results of the present report.

The 140- to 180-mg/l values reported by Araki (2) were obtained by upward flow dispersion in a 60-cm-long by 3-cm-diam vertical tube. Settling velocities were first measured and only fines (<10 μm) were used so that they could be floated in air velocities between 1 and 10 cm/sec. Dust clouds were generated by balancing the settling velocities against the average flow velocity. The method of measuring the absolute dust cloud concentration is not reported, but the relative concentration is monitored by measuring the transmission of light through the cloud. The coal dusts studied had a volatility of 35 to 38 percent. The ignition source was a 24-watt transformer spark discharge. This type of source is certainly inadequate as shown by figure 11. However, the spark was apparently on continuously and the ignition delay period was about 60 sec. During this time, it is possible that the continuous spark energy was sufficient to volatilize a significant amount of the coal dust near the electrodes thus making it easier to ignite. For this reason, the ignition energy is rated as marginal rather than inadequate. The propagation criteria is not specifically indicated, but the criteria appears to be upward flame travel for a distance of 50 cm. This would normally be considered a moderate criteria since it is upward flame propagation, but the minimum methane concentration that would propagate in the tube was 6.5 percent. For this reason the propagation criteria is rated as hard. In comparison with the data of the present report, Araki's value of 140 to 180 mg/l is perhaps higher due to the marginal energy of the ignition source. Other possibilities for the difference are the uncertain dust concentration uniformity and the corrections to the listed concentrations due to flame propagation upward in a flowing system.

Maguire, Slack, and Williams (27) reported a lean-limit value of 230 to 310 mg/l for dust dispersed by gravitational settling in 4.7-meter-long by 14-cm-diam open tube. The concentrations reported are static concentrations, but the details of the dust cloud mass concentration measurement are not given. The relative concentration is monitored by light transmission measurements near the bottom of the tube. The coal dust used had a volatility of 36 percent on an ash-free dry basis. Ignition was by a known (but unspecified) volume of methane which was ignited by a spark and presumably burned as a diffusion flame that was 5 cm long. This may be a marginal ignition source because of the relatively low temperature of such a diffusion flame or it may be adequate because of its size. As indicated earlier, detailed studies (28) of the dispersion pattern of falling dust clouds in a duct of similar dimensions showed inhomogeneities in dust concentration and complex recirculation patterns. This recirculation pattern consisted of two well-defined cells: an upper cell extending downward from the top about 0.75 meter and a lower cell about 3 meters long. Dust sample profiles showed that the falling dust concentrated along the axis in the upper cell and along the walls in the lower cell. If these recirculation patterns existed in the experiment by Maguire (27), the ignition flame at the bottom of the duct would be in a region of lower-than-average concentration. This may help to explain the high values that they report for the lean limit. Their data showed a large variability from run to run and a statistical analysis was used to determine the limit. The marked variability may be a reflection of marginal ignition conditions or axial concentration variations or both. The limit condition for the 230-mg/l value was a 50 percent probability of flame traveling 0.4 meter up the tube and the limit condition for the 310-mg/l value was a 50 percent probability of flame traveling 1.5 meters up the tube. These values for the lean limit are much larger than the values of most other investigators. They are probably too high because of the marginal ignition energy and/or the large spatial variations in the dust concentration.

Finally, the lean-limit values of the present report and the uncertainties and possible errors in the data are considered. For the nine size distributions (tables 1-2), the mean value of the lean limit was 135 mg/l and the standard deviation was 8 mg/l. This standard deviation for the different dust sizes is comparable to the error in reading the lean limit from the pressure ratio versus concentration graphs of figures 13, 15, 17, 19, 21, 23, 25, 27, and 29. Also, there was no systematic variation of the limit value with the size of the dust. For these two reasons, it is concluded that there is essentially no variation of the lean limit of flammability with dust particle size over the range studied. At some larger dust sizes, it is expected that the lean limit will eventually start to increase with particle size as shown by previous investigators (1, 17, 22). The range of lean-limit values (123 to 145 mg/l) from table 2 may be due to slight differences in the volatility or dispersibility of the various dust size distributions or some other unknown experimental variable. Even if other variables were controlled, there would probably remain some intrinsic scatter in the value of the lean limit for Pittsburgh seam coal due to the slight variation in volatility and moisture content from sample to sample.

In the 8-liter flammability chamber, the spatial and temporal uniformity of the coal dust cloud was measured using optical dust probes. At the time of ignition the dust cloud concentration varied by only about 15 percent at the various positions of the optical dust probes. As mentioned earlier in this report, these measurements showed that the dust clouds studied were rather uniform. However, this does not prove that the actual average dust concentration was equal to the nominal values based on total mass of dust dispersed in the known volume of the vessel. The additional information needed is the fraction of the dust in the disperser cup that contributes to the dust cloud. It is possible that some fraction is lost as a coating on the walls of the vessel. Because of the short time between dispersion and ignition, this coating should be only a small fraction of the total mass of dust. By using the transmission data at the lean limit (figures 14, 16, 18, 20, 22, 24, 26, 28, and 30 and table 2), an estimate of the maximum possible dust coating on the walls can be made. If it is assumed that there is no agglomeration to particle sizes greater than the Coulter diameters, then the only reason for the high measured transmission values would have to be incomplete dispersion or dust coating on the walls. The maximum amount of dust that is not airborne would be one minus the inverse of the "agglomeration factor," $1 - \frac{1}{\alpha}$, with α taken from table 2. For five of the size distributions ($\bar{d}_s$ = 15, 21, 34, 51, and 65 μm), the calculated maximum amount of dust lost to the walls would range from 10 to 30 percent. However, it is unreasonable to assume that there is absolutely no agglomeration and therefore the amount of dust lost to the walls should be considerably lower than these maximum estimates. Based on the measured transmission values for the smaller size distributions, the calculated maximum possible amount of dust lost to the walls is higher, but the agglomeration should also be larger for the smaller particles due to the higher number density for the same mass concentration. Therefore, a reasonable estimate of the dust coating would be about 10 percent or less of the total mass of dust.

Another possibility for error in the lean-limit values derived using the 8-liter vessel is the question of ignition energy and apparatus size. As mentioned earlier in this report during the discussion of figure 12, the flammability criteria (a pressure ratio of 2.0 for an ignition source of four electric matches) was a compromise. Ideally, a stronger ignition source should be used, but in the 8-liter vessel the pressure rise due to the ignition source alone would then become significant and a pressure ratio of 3.0 would have to be used as the limit criteria. Therefore, it is possible that using a stronger ignition source in a larger vessel might give slightly lower values for the limit. Also, slightly lower values for the lean limit than those in table 2 were measured in some recent flammability experiments using desiccator-stored coal dusts and using the four matches in a facing configuration instead of a linear array.

Based on the above possible errors in the measured value for the lean limit, it is estimated that the range of lean-limit values from 123 to 145 mg/l should have an uncertainty of +10 and -30 percent. These percentages are only meant to give a general idea of the uncertainty in the reported values and should not be considered as actual measured experimental errors.

CONCLUSIONS AND RECOMMENDATIONS

What conclusions can be drawn from the data presented in this report and what recommendations are to be made from the analysis and critique just presented? Of paramount importance is the question of consensus; not so much as it relates to the true limit concentration for coal dust, but rather as it relates the standardization of the test apparatus and methods for evaluating the explosibility of dusts in general. The 1.2-liter Hartmann apparatus and test procedure described by Dorsett and others (10) appears to have been adopted as a kind of "standard." Minimum explosive (lean-limit) concentrations, pressure rise rates, and explosibility indices measured with that apparatus and test method, appear to be the "accepted" methods (31). Yet, the data presented here, as well as many of the other independent measurements listed in table 7, seriously question the validity of those "accepted" values. For example, the "accepted" minimum explosive concentration of 55 mg/l appears to be too low by about a factor of 2. The argument has been made that the acceptance of this low value for the minimum explosive concentration is a "good" error in the sense that it errs in the conservative direction. It makes one more cautious than necessary, and hence its adoption as a standard provides an even larger measure of safety in evaluating the explosibility hazard of a dust. The logic of that argument has serious flaws. First, determining the truth of a matter has its own intrinsic value apart from any current or practical concerns relating to hazard evaluation. Second, even in terms of hazard evaluation, there is no assurance that an error involved in adopting the method as a "standard" will always be a "good" error that leads to a conservative overestimate of the hazard. On the contrary, as shown below, for other dusts, the error can be a "bad" error that grossly underestimates the hazard and can thus have disastrous consequences.

As indicated by the evaluation in table 7, and the discussion of previous limit data from references (10, 15, 17, 30-31), the standard Hartmann method has serious deficiencies. The ignition source is clearly inadequate for Pittsburgh seam coal dust at uniform concentrations below 400 mg/l. In the adopted experimental procedure, this inadequacy is compensated for by activating the discharge before the dust is dispersed. Ignition actually occurs in a locally high dust concentration as the dust is lifted en masse through the discharge zone, before it has had a chance to disperse uniformly. There is also some partial compensation by adopting a very soft flame propagation criteria. This "standard" experimental procedure is actually a "prescription" for obtaining successful ignitions with an inadequate ignition energy. As indicated by the examples presented, the type of flammability behavior that is actually observed by using this "prescription" is sensitive to too many uncontrollable variables. It depends upon the extent to which an inadequate ignition energy can be compensated for by a momentarily high dust concentration. While such a compensation is possible for Pittsburgh seam coal, it may not be possible for a coal of much lower volatility.

Pocahontas seam coal (standard volatility 16 to 18 percent) is nonflammable at any concentration by this "standard" test method. For a continuous spark ignitor in the 1.2-liter Hartmann vessel, Pocahontas coal dust could only be ignited with difficulty after varying the dispersion pulse from the "standard prescription" (25). Yet, Pocahontas seam coal generates severe dust explosions in the Experimental Mine. Although Pocahontas coal is not ignited by the "standard Hartmann prescription," it is readily ignited by match ignitors in the 8-liter apparatus at concentrations in excess of 250 mg/l. There may be many other examples of highly flammable dusts that are difficult to ignite. While the ignitability of Pittsburgh coal is markedly enhanced by increasing its dust concentration, other dusts need not behave similarly. For such dusts, the "standard Hartmann prescription" would give the erroneous conclusion that they were nonflammable. In reality, they may be highly flammable in the presence of a stronger ignition source. For such dusts, the standard method can grossly underestimate the hazard and lead to disastrous consequences.

If there is a lesson to be learned from the data, it is that the ignitability characteristics of a dust must be separated from the flame propagation characteristics. An independent assessment of the effect of ignition energy must be made before true limit concentrations can accurately be measured. Such an assessment is shown in figures 11-12, and should be required for each new dust that is studied. In addition, in performing any tests the dust should be uniformly dispersed before the ignitor is activated; otherwise, the real concentration in the region of propagation will generally be significantly different from the nominal dust loading. And finally, the propagation criteria should always be realistic. All other things being equal, moderate to soft criteria are probably preferable since they would give a conservative estimate of the hazard. However, soft criteria should never be used to compensate for an inadequate ignition energy or a nonuniform dust dispersion. The compensating factors are generally too complex and uncontrollable, and they are highly sensitive to the specific properties of any given dust.

It is also important to recognize that even when a consensus is reached on the value for the lean limit of flammability for uniformly dispersed coal dust, this value will only be of practical importance when an effective means is found for measuring the mass concentration of an unconfined dust cloud. Optical dust probes, that are based on light transmission, measure the cross sectional area of the dust cloud particles, not the mass concentration. Only if the average particle size of the dust is known can this type of optical probe be used to calculate the airborne mass concentration of dust (26). Therefore, in a practical situation where the size of the dust generated is constant and known, an optical probe could be used as a hazardous dust monitor to measure the mass concentration of airborne dust and warn when the flammability limit was approached. However, in most practical situations, the average particle size is both unknown and varying in time. One possible means of directly measuring the mass concentration of airborne dust is by beta-ray absorption. Since the attenuation of beta particles is dependent only on the mass of material along the path, it might be useful as a basis for a hazardous dust monitor. One of the future experimental studies planned for the 8-liter flammability apparatus is to use beta-ray transmission to determine directly the mass concentration of dust in the air and therefore better determine the accuracy of the nominal concentration values used in the present report.

An important result of the present work was the design of a laboratory flammability apparatus and test method that gave data that correlated well with the large-scale gallery and mine experiments in terms of the relative effectiveness of various inerting agents. In most previous studies the result of laboratory experiments on inerting agents differed greatly from the mine results. In this report, the relative effectiveness of the three inerting agents (rock dust, Purple K, and NaCl salt) studied in the 8-liter vessel agreed well with the large-scale gallery and mine results, although the absolute values of the amount necessary to completely inert coal dust may have differed slightly from the large-scale tests. Because of the overall good correlation with large-scale experiments, future tests with the 8-liter vessel are planned to search for a more effective inhibitor for coal dust explosions. Such tests are simpler to run and less costly than full-scale mine tests. These laboratory tests could then serve as a guide in planning full-scale mine tests with other inhibitors.

Other studies planned or in progress are the measurement of the lean limit of flammability for coals of different volatility and for oil shales. Also in progress are experiments to investigate the flammability of coal dust in atmospheres with different concentrations of oxygen and to determine the minimum oxygen concentration necessary for flammability.

Flame temperature measurements in future studies will be made with the six-channel, infrared pyrometer and a new three-channel, infrared pyrometer which measures continuum radiation from the dust particles at wavelengths of 0.8, 0.9, and 1.0 μm and can therefore be used to obtain the dust particle temperature. Future temperature measurements will be made of both coal dust-air and coal dust-inert-air explosions in order to obtain some insight into the inhibition mechanism.

REFERENCES

1. Agarwal, S. C. Effect of Size of Coal Dust on Its Inflammability. J. Mines, Metals and Fuels, September 1964, pp. 284-289.

2. Araki, S. Experimental Studies on Dust Explosion. Proc. 10th Internat. Conf. of Directors of Safety in Mines Research, Pittsburgh, Pa., Sept. 28-Oct. 2, 1959, 35 pp.

3. Bartknecht, W. Brenngas- und Staubexplosionen in Behältern und Rohrstrecken (Gas and Dust Explosions in Chambers and Galleries). Stahl und Eisen, v. 92, No. 6, 1972, pp. 245-251.

4. _____. Brenngas- und Staubexplosionen (Gas and Dust Explosions). Forschungsbericht F45, Bundesinstitut für Arbeitsschutz, Koblenz, 1971, 195 pp.

5. Beachey, J. E., J. E. O'Donnell, and T. A. Milne. The Quenching Behavior of Coal Dust-Air Mixtures. First Annual Technical Progress Report. Bureau of Mines Contract No. J0166076, June 1977, available from Pittsburgh Mining and Safety Research Center, Bureau of Mines, Pittsburgh, Pa.

6. Burgess, D., and M. Hertzberg. The Flammability Limits of Lean Fuel-Air Mixtures. Thermochemical and Kinetic Criteria for Explosion Hazards. Trans. ISA, v. 14, No. 2, 1975, pp. 129-136.

7. Cashdollar, K. L., M. Hertzberg, and C. D. Litton (assigned to U.S. Department of the Interior). Multichannel Infrared Pyrometer. U.S. Pat. 4,142,417, March 6, 1979.

8. Coward, H. F., and G. W. Jones. Limits of Flammability of Gases and Vapors. BuMines Bull. 503, 1952, 155 pp.

9. Cybulski, W. Coal Dust Explosions and Their Suppression. (Translated from Polish). Published for the Bureau of Mines and National Science Foundation by the National Center for Scientific, Technical, and Economic Information, Warsaw, Poland, 1975, 583 pp. Available from National Technical Information Service, Springfield, Va., TT 73-54001.

10. Dorsett, H. G., Jr., M. Jacobson, J. Nagy, and R. P. Williams. Laboratory Equipment and Test Procedures for Evaluating Explosibility of Dusts. BuMines RI 5624, 1960, 21 pp.

11. Eckhoff, R. K. The Use of the Hartmann Bomb for Determining K_{St} Values of Explosible Dust Clouds. Staub-Reinhalt. Luft, v. 37, No. 3, 1977, pp. 110-112.

12. Eggleston, L. A. and A. J. Pryor. The Limits of Dust Explosibility. Fire Technol., v. 3, 1967, pp. 77-89.

13. Ferriso, C. C. High-Temperature Spectral Absorption of the 4.3 Micron CO_2 Band. J. Chem. Phys., v. 37, No. 9, 1962, pp. 1955-1960.

14. Grumer, J., and A. E. Bruszak. Inhibition of Coal Dust-Air Flames. BuMines RI 7552, 1971, 14 pp.

15. Hartmann, I. Recent Research on the Explosibility of Dust Dispersions. Ind. Eng. Chem., v. 40, No. 4, 1948, pp. 752-758.

16. _____. Studies on the Development and Control of Coal-Dust Explosions in Mines. BuMines IC 7785, 1957, 27 pp.

17. Hartmann, I., M. Jacobson, and R. P. Williams. Laboratory Explosibility of American Coals. BuMines RI 5052, 1954, 8 pp.

18. Helwig, N. The Effect of Precompression and Explosion Volume on the Explosion Indexes of Coal Dust/Air Mixtures. Staub-Reinhalt. Luft, v. 27, No. 8, 1967, pp. 11-17.

19. Hertzberg, M. The Theory of Flammability Limits. Natural Convection. BuMines RI 8127, 1976, 15 pp.

20. Hertzberg, M., A. L. Johnson, J. M. Kuchta, and A. L. Furno. The Spectral Radiance Growth, Flame Temperatures, and Flammability Behavior of Large Scale, Spherical, Combustion Waves. Sixteenth Symposium (International) on Combustion, The Combustion Institute, 1977, pp. 767-776.

21. Hertzberg, M., C. D. Litton, W. F. Donaldson, J. M. Kuchta, and A. L. Furno. The Spectral Growth of Expanding Flames: The Infrared Radiance of Methane-Air Ignition and Coal-Dust-Air Explosions. BuMines RI 7779, 1973, 38 pp.

22. Ishihama, W. Studies on the Critical Explosion Density of Coal Dust Clouds. Proc. 11th Internat. Conf. of Directors of Safety in Mines Research, Warsaw, Poland, Oct. 16-24, 1961, No. 47, 16 pp. Available from Pittsburgh Mining and Safety Research Center.

23. Ishihama, W., and H. Enomoto. New Experimental Method for Studies of Dust Explosions. Combust. Flame, v. 21, No. 2, 1973, pp. 177-186.

24. _____. On the Aftergases of Coal Dust Explosions in an Experimental Chamber. Proc. 16th Internat. Conf. on Coal Mine Safety Research, Washington, D.C., 1975, No. VII-8 and discussion of paper VII-8 on p. 82. Available from Pittsburgh Mining and Safety Research Center, Bureau of Mines, Pittsburgh, Pa.

25. Kubala, T. A. Private communication, 1978; available for consultation at Pittsburgh Mining and Safety Research Center, Bureau of Mines, Pittsburgh, Pa.

26. Liebman, I., R. Conti, and K. L. Cashdollar. Dust Cloud Concentration Probe. Rev. Sci. Instr., v. 48, 1977, pp. 1314-1316.

27. Maguire, B. A., C. Slack, and A. J. Williams. The Concentration Limits for Coal Dust-Air Mixtures for Upward Propagation of Flame in a Vertical Tube. Combust. Flame, v. 6, No. 4, 1962, pp. 287-294.

28. Mason, W. E., and K. V. Saunders. Recirculating Flow in Vertical Columns of Gas-Solid Suspensions. J. Phys. D, v. 8, 1975, pp. 1674-1685.

29. Milne, T. A., and J. E. Beachey. Exploratory Studies of Flame and Explosion Quenching (Research Contract No. H0122127). BuMines Open File Rept. 112-77, June 25, 1976, 254 pp.; available for consultation at Bureau of Mines facilities in Denver, Colo., Twin Cities, Minn., Bruceton and Pittsburgh, Pa., and Spokane, Wash.; Department of Energy facilities in Carbondale, Ill., and Morgantown, W. Va.; National Library of Natural Resources, U.S. Department of the Interior, Washington, D.C.; and National Technical Information Service, Springfield, Va., PB 268 695/AS.

30. Nagy, J., and W. M. Portman. Explosibility of Coal Dust in an Atmosphere Containing a Low Percentage of Methane. BuMines RI 5815, 1961, 16 pp.

31. National Fire Protection Association, Boston, Mass. Dusts. Fire Protection Handbook, 14th ed. sec. 3, ch. 8, 1976, pp. 3-106-3-118.

32. Richmond, J. K., and I. Liebman. On the Propagation and Control of Coal Mine Explosions. Fourth International Symposium on Combustion Processes. Czestochawa, Poland, Sept. 15-18, 1975; pub. in Archiwum Thermodynamiki i Spalania (Poland), v. 8, No. 1, 1977, pp. 27-41.

33. Richmond, J. K., I. Liebman, A. E. Bruszak, and L. F. Miller. A Physical Description of Coal Mine Explosions. Part II. Seventeenth Symposium (International) on Combustion, Leeds, England, August, 1978 (to be published by The Combustion Institute).

34. Singer, J. M., E. B. Cook, and J. Grumer. Equivalences and Lower Ignition Limits of Coal Dust and Methane Mixtures. BuMines RI 6931, 1967, 35 pp.

35. Singer, J. M., M. E. Harris, and J. Grumer. Dust Dispersal by Explosion-Induced Airflow. BuMines RI 8130, 1976, 50 pp.

36. Smoot, L. D., and M. D. Horton. Exploratory Studies of Flame and Explosion Quenching. Quarterly Technical Progress Report No. 1. Bureau of Mines Contract No. G0177034, Mar. 15, 1977. Available from Pittsburgh Mining and Safety Research Center, Bureau of Mines, Pittsburgh, Pa.

37. Smoot, L. D., M. D. Horton, and G. Williams. Propagation of Laminar, Pulverized Coal-Air Flames. Sixteenth Symposium (International) on Combustion, The Combustion Institute, 1977, pp. 375-387.

38. U. S. Congress. Federal Coal Mine Health and Safety Act of 1969. Public Law 91-173, sec. 303, 83 Stat. 742, Dec. 30, 1969.

39. Yu Shen-han and Chao Tzu-chih. Experiment on the Lower Limit of Explosibility of Coal Dust Clouds. Internat. Conf. of Directors of Safety in Mines Research, Sheffield, England, July 12-16, 1965, No. 39, 16 pp. Available from Pittsburgh Mining and Safety Research Center, Bureau of Mines, Pittsburgh, Pa.

40. Zabetakis, M. G. Flammability Characteristics of Combustible Gases and Vapors. BuMines Bull. 627, 1965, 121 pp.

☆U.S. GOVERNMENT PRINTING OFFICE: 1979-603-002/37 INT.-BU.OF MINES,PGH.,PA. 23736